1994

High resolution, high speed, and low cost digitial radiography and computed tomography system

R. Kasiviswanathan
Iowa State University

High resolution, high speed and low cost digital radiography and computed tomography system

by

R Kasiviswanathan

A Thesis submitted to the

Graduate Faculty in Partial Fulfillment of the

Requirements for the Degree of

MASTER OF SCIENCE

Department : Electrical Engineering and Computer Engineering
Major : Computer Engineering

Approved: Members of the Committee:

_____ _____

_____ _____

In Charge of Major work

_____

For the Major Department

_____

For the Graduate College

Iowa State University
Ames, Iowa

1994

DEDICATION

To my grand parents and parents for teaching me the values of life, and to my uncle for his constant encouragement.

TABLE OF CONTENTS

ACKNOWLEDGEMENTS vi

1. INTRODUCTION 01

1.1 Need for NDE 01

1.2 Motivation for this research 02

1.3 Project overview 07

2. X-RAY DETECTOR DESIGN AND DEVELOPMENT 09

2.1 Types of X-ray detectors 09

2.1.1 Physical arrangement 09

2.1.2 Mode of operation 10

2.1.3 Material properties 12

2.2 Current mode X-ray detectors 14

2.2.1 Principle of operation 14

2.2.2 Instrumentation design 15

2.2.3 Instrumentation development 30

2.2.4 Performance of instrumentation 32

2.3 Current mode X-ray detector based on CdZnTe 36

2.3.1 Dark current stability 37

2.3.2 Afterglow 37

2.3.3 X-ray detector system 38

2.3.4 Performance of the detector system 38

2.4 Current mode X-ray detectors based on scintillating crystals 47

2.4.1 Front end of the detector 47

2.4.2 X-ray detector system 49

2.4.3 Performance of detector 49

3. DIGITAL RADIOGRAPHY AND COMPUTED TOMOGRAPHY USING CURRENT MODE DETECTORS 63

3.1 System setup 65

3.1.1 Distributed control for sample positioners 67

3.1.2 Data acquisition card 67

3.2 Scans for digital radiography and computed tomography 69

3.2.1 1D scan 70

3.2.2 2D scan 70

3.2.3 Tomo scan 70

3.3 Results and performance of digital radiography and computed tomography system 72

3.3.1 Spatial resolution 72

3.3.2 Contrast resolution 82

3.3.3 Dynamic range of the system 83

3.3.4 Speed of operation 83

3.3.5 Versatility of the detector 84

4. CONCLUSIONS AND FUTURE WORK 86

4.1 Conclusions 86

4.2 Future work 88

BIBLIOGRAPHY 90

APPENDIX A. DEFINITION OF SPECIFICATIONS AND COMMONLY USED TERMS 93

APPENDIX B. PRINCIPLES AND TECHNIQUES FOLLOWED IN THE DEVELOPMENT OF INSTRUMENTATION 95

APPENDIX C. VME BUS BASED DATA ACQUISITION SYSTEM 108

APPENDIX D. DATA PACKET FORMAT FOR NETWORK TRANSFER AND SOURCE CODE FOR SERVER SOFTWARE 110

APPENDIX E. SOFTWARE FOR 1D, 2D AND TOMO SCAN..... 129

ACKNOWLEDGEMENTS

Words cannot express my thanks to Dr. Terry Jensen, my committee member, without whose guidance and help, this research work would not have been possible. I wish to express my deep and sincere appreciation for all the help and guidance rendered by Dr. Terry Jensen during the course of this research work. I also wish to thank Dr. Joe Gray, my co-major advisor, for his constant suggestions and encouragement. I wish to thank Dr. Doug Jacobson, my major advisor for his valuable time and cooperation. I wish to thank Dr. James Davis, my committee member for his valuable time.

I am also grateful to a number of people at the Center for NDE. To name a few - Dick Wallingford and Vivekanand Kini. I wish to thank Dr. Doug Robinson of Microelectronics Research Center for his useful suggestions and help in this project.

Finally, I would like to thank my family members for their constant support and encouragement.

This work was sponsored by NIST under cooperative agreement #70NANB9H0916 and was performed at the center for NDE, Iowa State University, Ames.

1. INTRODUCTION

1.1 Need for NDE

Non-destructive evaluation is a branch of science that is concerned with all the aspects of uniformity, quality and serviceability of materials and structures. By definition, nondestructive evaluations are the means by which materials and structures may be inspected without disruption or impairment of their serviceability. Using NDE, internal properties of hidden flaws are revealed or inferred by appropriate techniques. Another important application of NDE is in process control monitoring where NDE techniques are used in the development of new materials and their evaluation. NDE is becoming an increasingly vital factor in the effective conduct of research, development, design and manufacturing programs.

Aircraft industry is a prime example of this need for NDE. The fleet of commercial and military aircraft that are in use today is aging and consequently it has become critical to develop economical and fast systems for inspection of turbine blades, wing structures etc. Also, the materials used in the manufacturing industries vary widely from exotic composite materials to conventional materials like aluminum and nickel. So, the inspection systems must be capable of handling such varied materials in addition to speed and cost considerations.

There are three primary inspection methods used at the center for Non Destructive Evaluation. They are 1. X-ray based NDE, 2. Ultrasonics based NDE, and 3. Eddy current based NDE techniques. Eddy current techniques are widely used in the industry for the de-

termination of the existence of surface cracks and their lengths in conducting materials. Ultrasonic techniques are used extensively in the production and in-service inspection of composite panels for problems such as delamination and for detection of cracks in metals. X-ray based NDE techniques are used for detection and quantification of fatigue cracks, determination of porosity and density gradients in ceramics, detection of voids in parts manufactured for automobiles etc. X-ray digital radiography and computed tomography techniques are finding increasing use in the industry today in the detection and analysis of voids, cracks and inclusions in materials and manufactured parts. Although each of these inspection methods has its own merits, it is research into some of the X-ray based methods that will be discussed in this thesis. Reference [1] provides further details on various NDE techniques, their applications and present developments in the field. Reference [2] provides details on radiography and X-ray based techniques.

Traditional radiography uses X-ray film for X-ray detection. With the usage of other forms of X-ray detectors like semiconductor detectors, scintillators, etc., data acquisition and image processing becomes inevitable. NDE techniques require wide spread use of computers for data acquisition, image processing and storing of images. Although NDE is a branch of science in its own respect, implementation of NDE techniques like digital radiography and computed tomography and improvements of these techniques require the application of computer engineering concepts to a great degree.

1.2 Motivation for this research

The motivation for this research stems from the following discussion about some requirements in the field of X-ray based NDE and the state of existing systems in the industry.

There are two types of X-ray based NDE techniques. One is by transmitted X-ray measurements and the other is by measuring the scattered X-rays. We will consider the first method, where X-rays are shone through the sample or object which is to be evaluated. X-rays when passing through the sample are attenuated by a certain amount depending upon the elemental composition, density, and thickness of the sample material. Those X-rays that pass through the sample without being absorbed are measured using a radiographic film or some kind of a X-ray detector. This measured value gives information about the sample. Figure 1.1 shows the bremsstrahlung spectrum of X-rays from a X-ray generator with a tungsten target for a maximum energy of 90 kVp. Different materials attenuate the X-ray energy spectrum in different ways. Figure 1.2 shows the linear attenuation coefficient of two commonly used materials, aluminum and nickel. The graph in Figure 1.2 shows the attenuation caused per cm of the material to different X-ray energies.

X-ray detectors used can be either of a point type or an array. In point type detectors, a fine collimator is placed in front of the detector so that only a fine pencil beam of X-rays are allowed to be incident on the detector. So, point type detectors give information about the point in the sample through which the pencil beam passes through and is incident on the detector (refer Figure 1.3). So, the smaller the collimator size is, the lower the X-ray flux that will be incident on the detector.

Some of the point detectors used are based on semiconductors like germanium (Ge), and crystals like sodium iodide (NaI) etc. These detectors are used generally in the photon counting mode of operation. In this mode, the total number of photons incident on the detector within a time period is counted, and this photon count gives a measure of the attenuation

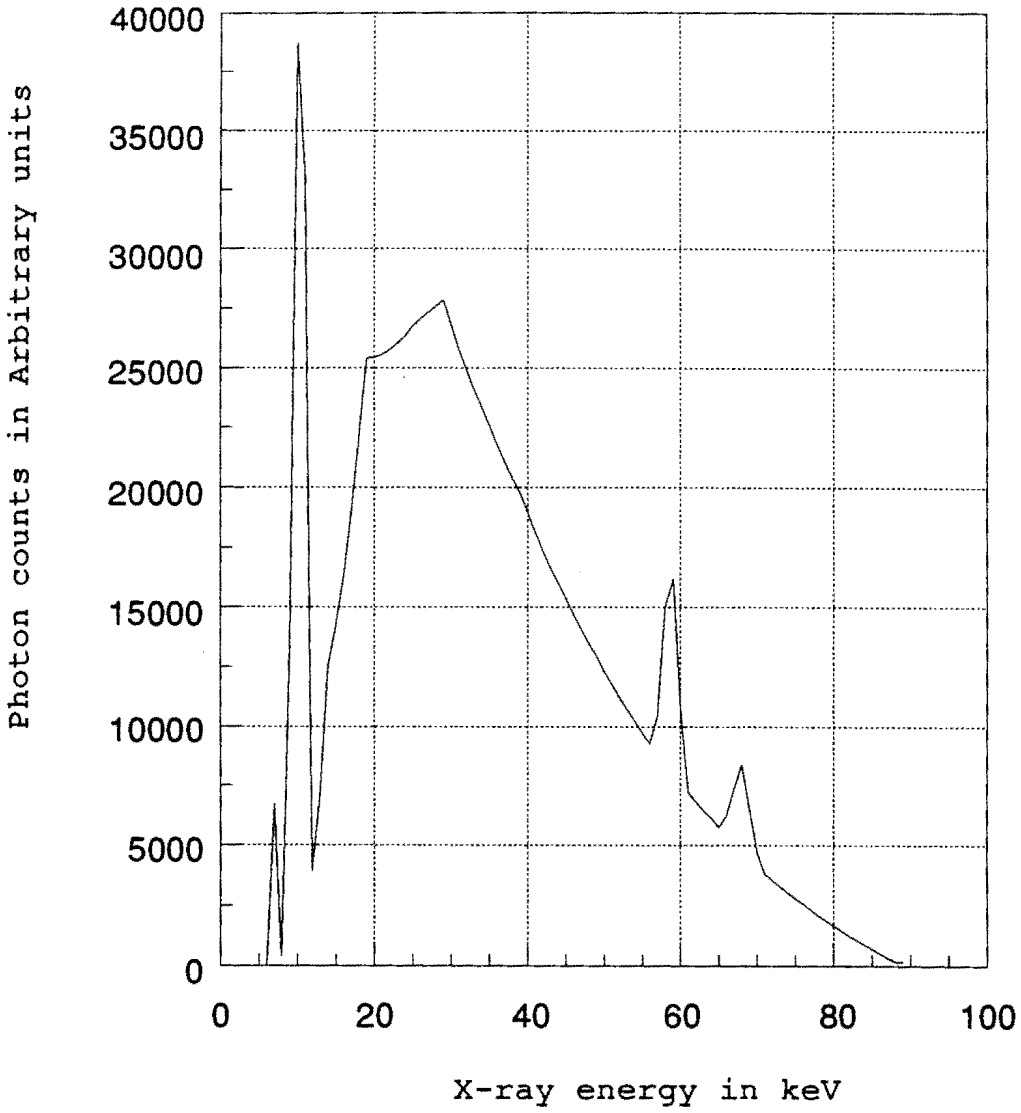

Figure 1.1 Bremsstrahlung spectrum of X-rays

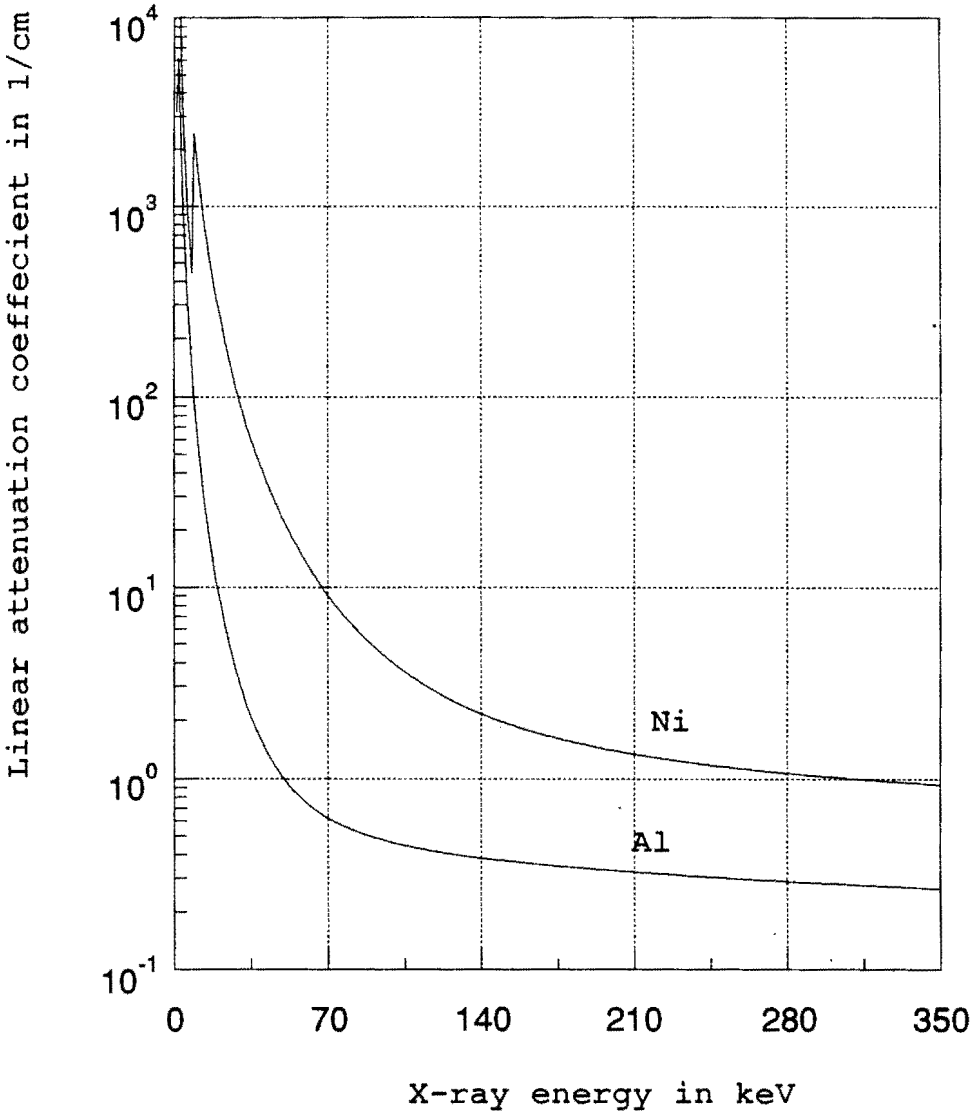

Figure 1.2 Linear attenuation coefficient of Al and Ni

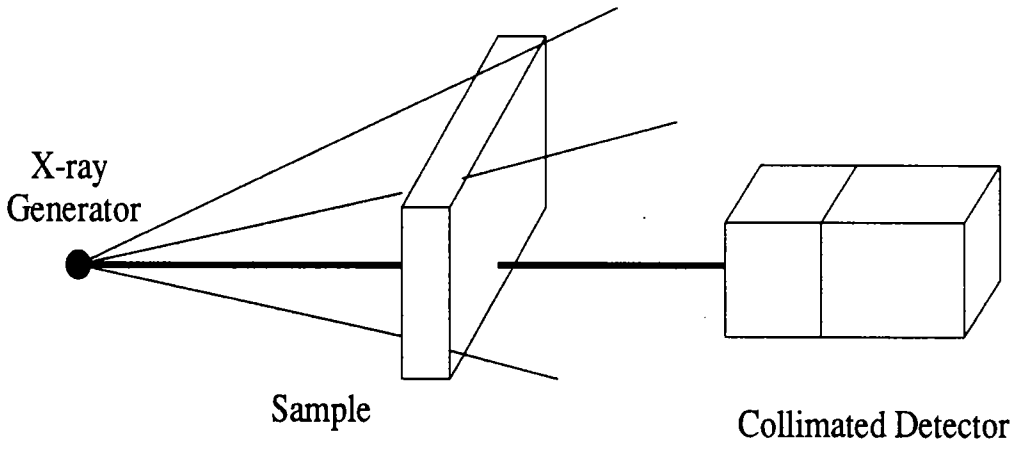

Figure 1.3 Point detector arrangement

by the sample at the point through which the pencil beam of X-rays passed. These systems are very slow. Also, detectors based on Ge have to be cooled to liquid nitrogen temperatures for proper operation. The electronics and data acquisition systems associated with such detectors tend to be costly. But these systems have very good spatial and contrast resolution. To speed up these systems, some of the existing detectors work in the current mode of operation. Although higher speed of operation is achieved in this mode, the existing current mode detector systems tend to have poor spatial resolution. So, in this research, the objective is to design a detector system that will have very high speed of operation compared to the photon counting mode detector systems present today, higher spatial resolution compared to the existing current mode detector systems, smaller size compared to the existing systems for ease of mounting and portability, very low cost, and operation at room temperature. This is followed by the design and development of a digital radiography system and computed tomography system based on the above mentioned detector.

1.3 Project overview

The project discussed in this thesis covers the design and development of a X-ray based, high resolution, high speed and low cost digital radiography and computed tomography system. Chapter two provides an introduction to the various kinds of X-ray detectors. It then continues with a discussion of the design and development of a current mode X-ray detector system. Then the development of prototype detectors based on cadmium zinc telluride (CdZnTe) and sodium iodide (NaI) is discussed. This chapter concludes with the performance of these detector systems developed. Chapter three begins with a discussion of the design and development of a digital radiography system and computed tomography system

based on the detector described in chapter 2. As part of the system setup for implementing these systems, a networking based software solution for distributed control is proposed and implemented. This chapter concludes with results obtained from the system developed and a comparison of its performance with existing systems. Chapter four proceeds with the conclusion of this research work and future directions in which this research could be extended.

2. X-RAY DETECTOR DESIGN AND DEVELOPMENT

There are many types of X-ray detectors used in the industry today for non-destructive evaluation purposes. They are basically classified according to the physical arrangement of detecting materials, materials out of which the detectors are made, and the mode of operation. In this chapter, we will look at some of these classifications of detectors. Then, we will proceed to discuss the principles of a current mode point detector followed by the design and development details of necessary instrumentation. Two specific detector materials, cadmium zinc telluride (CdZnTe) and sodium iodide (NaI) are considered in this research work. This is followed by the development of prototype X-ray detector systems based on these two materials. The chapter concludes with the properties and performance of the developed prototype detector systems.

2.1 Types of X-ray detectors

2.1.1 Physical arrangement

X-ray detectors are classified as array detectors and point detectors based on the way the detecting material is arranged physically.

2.1.1.1 Array detectors Array detectors consist of an array of X-ray detecting material. It can be a one dimensional array or a two dimensional array. In the case of a one dimensional array as shown in Figure 2.1, information about a line of points in the sample can be obtained at a time. The associated instrumentation for processing the signals for one point will be duplicated so that all the points in an array can be processed at a time. Thus a one dimensional array can be considered as a series of point detectors in a line, with the

inter point gaps being very small. In case of a two dimensional array detector, information about an area of the sample can be obtained at a time. This detector can be considered as a set of one dimensional array detectors placed parallel to each other. Figure 2.2 shows a conceptual view of a two dimensional array detector. Typically, instrumentation for signal processing and data acquisition for a two dimensional array detector consists of some kind of a camera which can process the entire image at a time. An image intensifier viewed by a charge coupled device (CCD) camera is an example of a two dimensional array detector.

2.1.1.2 ***Point detectors*** A point X-ray detector consists of some kind of a X-ray detecting material and its related instrumentation with a fine collimator placed in front of the detector. The detector is shielded and X-rays are allowed to be incident on the detector only through the collimator. Figure 1.1 shows this arrangement. This type of detector has good spatial resolution. In a point detector, only one point equal to the area of the collimator can be evaluated at each instant of time. If a one dimensional scan is to be performed using this detector, the sample has to be moved across the detector and data collected at each point.

2.1.2 Mode of operation

A point detector can be operated in two basic modes. In the photon counting mode, each incident X-ray photon produce many electron-hole pairs due to photoelectric effect. This results in small current pulses or light scintillations across the detector material. The resulting current pulse is integrated by a charge sensitive preamplifier producing an output voltage pulse with a height proportional to the incident photon energy. Using specialized electronic counters, the number of pulses are counted. By counting the number of pulses for

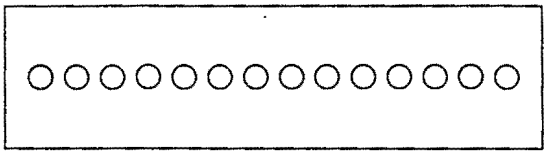

Figure 2.1 Conceptual view of one dimensional array detector

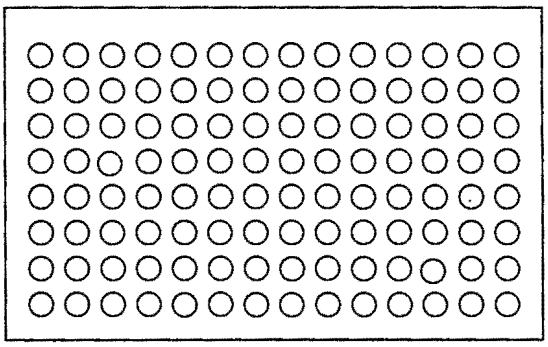

Figure 2.2 Conceptual view of two dimensional array detector

a particular duration, information about the incident radiation beam is obtained. Since shaping of the pulses take longer time, the system is inherently slow. To increase the speed of operation, the detector can be operated in the current mode. Incident photons produce electron-hole pairs due to the photoelectric effect. This constitutes a short circuit current commensurate with the transit time of the charge carriers. The short circuit current is measured using some sensitive instrumentation and this provides a measure of incident flux. Since there will be a short circuit current generated in the detector material within a very short time, (practically, it is instantaneous) this method of detection will be much faster compared to the photon counting mode of operation. The main problem is that the strength of the current signal produced is very weak and so the instrumentation used to measure this has to be very sensitive.

2.1.3 Material properties

This classification is based on the material from which the detector is made of, and its principle of operation. Semiconductor detectors are built from semiconductor materials like germanium(Ge), silicon(Si) and cadmium zinc telluride(CdZnTe), to name a few. When an X-ray photon interacts within a semiconductor, it generates free charge (electron-hole pairs) and therefore a current (I) for a time commensurate with the lifetime or transit time of the carriers.

The electrons and holes move in opposite directions when an external electric field (E) is applied. To achieve full charge collection at both electrical contacts, the semiconductor should have high mobility (μ_{ch}) for both free electrons and holes and long trapping time T_{ch}. Hence a good charge collection efficiency requires an average mean free path length,

(refer [3]) that is longer than the crystal thickness for both electrons and holes. On the other hand, the absorption probability of X-rays increases with increasing thickness of the semiconductor. A reasonable compromise between high X-ray detection and high charge collection efficiencies can be achieved with a thickness of the order of the mean free path (λ) of the incident X-ray in the semiconductor material. As for the choice of the crystals for X-ray detectors, high Z(density) materials are desirable since they have higher radiative stopping powers.

Scintillation detectors are basically inorganic compounds like sodium iodide (NaI) and cesium iodide (CsI). The NaI and CsI detectors make use of the ability of a large group of crystal lattice structures to respond to radiation sources by emitting scintillation light. These crystals, when laced with a small amount of impurity (thallium iodide), produce an exceptionally large scintillation output when exposed to a radiation beam. This scintillation may be converted to an electric signal, which may then be amplified and counted. Photomultiplier tubes are used to convert the relatively weak light output into a usable current pulse without introducing a large amount of random noise. Reference [4] provides a detailed review of various scintillating detector materials, principle of operation, and their applications.

Since both semiconductor and scintillation detectors are generally used in photon counting mode of operation, they have good energy sensitivity. Energy sensitivity is defined as the ability of the detector to resolve energy levels of incident photons. So energy sensitive detectors will give photon counts for each energy range (usually called as energy bin) which can be specified during data acquisition.

2.2 Current mode X-ray detectors

For any application which requires measurement of radiation flux, proper attention must be paid to detector design and mode of operation, particularly if the measurement requires a wide dynamic range using the same detector. This is a direct consequence of the interactions that occur within a detector when a X-ray photon is absorbed. In low intensity flux, each event produces a discrete electric pulse or light scintillation which can be digitally counted (photon counting mode). Because of the large integration times for counting these pulses, these systems are slow. However, if the incident flux is high, the pulses produced will no more be discrete and it becomes impossible to count digitally. Only an increase in the average current or average light output can be measured.

2.2.1 Principle of operation

In a semiconductor detector, when X-ray photons are incident on the detector, electron-hole pairs are produced. These charge carriers are swept across the detector material by applying a high voltage across the detector. Each of these pairs produces a current pulse and all these pulses constitute a current. The current is converted to a voltage signal, amplified and measured.

In a scintillation mode detector, each incident photon produces scintillation. Instead of using a photomultiplier tube and counting individual scintillations, the entire light output of the detector is converted into a current signal using a photodiode. The current signal represents a measure of incident flux.

Since individual pulses are not counted and only the integral current or light output is measured, current mode detectors do not have energy resolving capability.

Measurement of current output from a detector requires a low input impedance current-to-voltage converter. But the current measurement mode introduces three practical problems.

1. The quiescent value of the device current (dark current) can be so high that it masks the small value of photo current generated.

2. In a semiconductor detector, the existence of traps can cause the photo current to continue for an extended period after the radiation flux is removed. In a scintillation detector, due to phospor lifetime, the light output may extend after the radiation flux is removed. This effect is usually known as "afterglow".

3. To get higher spatial resolution from the detector, it has to be collimated to a fine degree. This reduces the incident flux and as a result, the photocurrent produced due to incident flux variations will be very small. To measure such small variations in current, the instrumentation has to be very sensitive.

The main advantage of measuring photo current is the speed that will be gained in this mode of operation.

2.2.2 Instrumentation design

The main parameter that needs to be measured effectively and accurately in a current mode detector is the photo current. Figure 2.3 shows the block diagram of the instru-

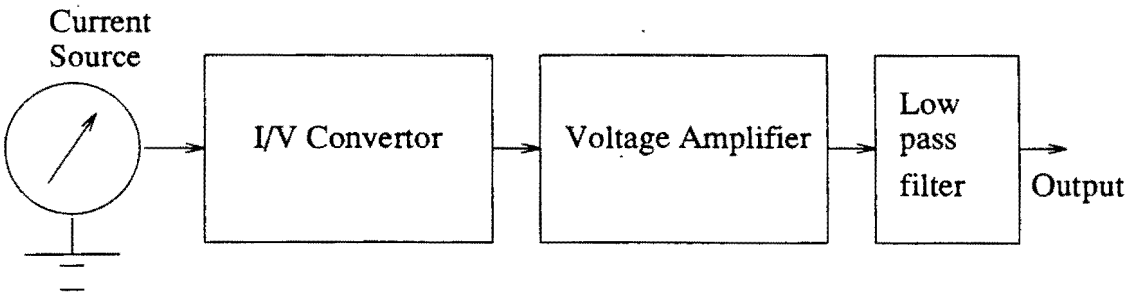

Figure 2.3 Block diagram of instrumentation

mentation that is designed and developed to measure such low current signals. It consists of a very low noise, high gain current-to-voltage converter circuit (I/V converter) that converts the current into a voltage signal with a gain factor. This is followed by a voltage amplifier and a low pass filter.

2.2.2.1 ***Design considerations for instrumentation*** The instrumentation used for measuring the current signal is conceptually very simple. The primary parameter that needs to be determined is the scale factor by which the input current has to be multiplied and converted to a voltage signal. In addition, there are a number of factors that need to be considered in the design of the instrumentation.

As mentioned before, for achieving higher spatial resolution from the detector, finer collimation has to be used. This will in turn reduce the incident flux, and as a result, the current output from the detector will also decrease. So, the current to voltage converter must be capable of measuring current signals of the order of a few hundred femto amperes (10^{-15} amps). This requires the gain of the I/V converter stage to be very high.

For efficient charge collection in semiconductor detectors, a high voltage is usually applied across the semiconductor. This will produce a current(dark current) which will be in the nano ampere range. In order to minimize the output voltage due to dark current, the scale factor of the I/V converter must be as low as possible. Thus, these two conditions provide contrasting design requirements on the part of the instrumentation, and this is the main reason for going into a combination of I/V converter and differential amplifier.

The I/V converter is designed for measuring low currents. As a result, even a small amount of noise will reflect as large errors at the output. So, current to voltage conversion is to be done with as minimum a noise introduced as possible.

One of the research goals is to develop a detector that operates at room temperature. In order to achieve this, the circuit should be stable with respect to room temperature variations.

As this is a point detector, scanning larger objects may take extended periods of time of operation of the detector. During the scan period, the quiescent output of the circuit should be stable. If not, the variations in the quiescent output will reflect as variations in incident flux intensity, which is obviously an error.

The relationship between the input current and output voltage of the circuit is to be linear over the entire range of input that the circuit can handle.

Although all the signals that this circuit will be dealing with are DC, random noise will be introduced into the circuit at various points and all these will get reflected at the output. So, the output will contain frequency components other than DC. These need to be filtered because the maximum frequency component of the output signal from the instrumentation must be less than half the sampling frequency of the A/D converter. Otherwise errors will be introduced in the digitized signal due to an effect called aliasing. Reference [5] provides further details about aliasing effect and its implications.

Another goal of this research work is to develop a compact detector system so that it can be mounted on X-ray generators as beam monitors. This introduces the requirement of simple circuit design and low power consumption.

Since the objective is to develop a low cost detector system, the instrumentation should have few components. This again leads to the requirement of a simple circuit design.

With all these considerations in mind, the design of instrumentation proceeded as follows.

*2.2.2.2 **Current to voltage converter design*** The design of the current to voltage converter is as follows:

1. The minimum output current from the X-ray detector materials that need to be sensed

will be of a few hundred femto amperes direct current (DC).

2. The source resistance of the detector materials or the current signal source will be in the range of a few hundred M(to few tens of GΩ. (Differs between different detectors)

3. A high voltage of the order of a few hundred volts may have to be applied across the detector material.

4. Dark current from some detector materials will be of the order of a few nano amperes.

5. Output of the I/V converter should be suitable for connecting to a voltage amplifier.

6. Output voltage signal must be linear with respect to the input current signal.

Current may be measured in two ways with an operational amplifier. The current may be converted into a voltage with a resistor and then amplified or the current may be injected directly into the summing node of the operational amplifier. Converting into a voltage is undesirable for two reasons: first, an impedance is inserted into the measuring line causing an error; second, amplifier offset voltage is also amplified with a subsequent loss of accuracy. The use of a current to voltage transducer avoids both of these problems. Figure 2.4 shows the circuit of a current to voltage converter. The input current is fed directly into the summing node and the amplifier output voltage changes to extract the same current from the summing node through R_f. The scale factor of this circuit is R_f volts/ampere. The only conversion error in this circuit is I_{bias} which is summed algebraically with I_{IN}.

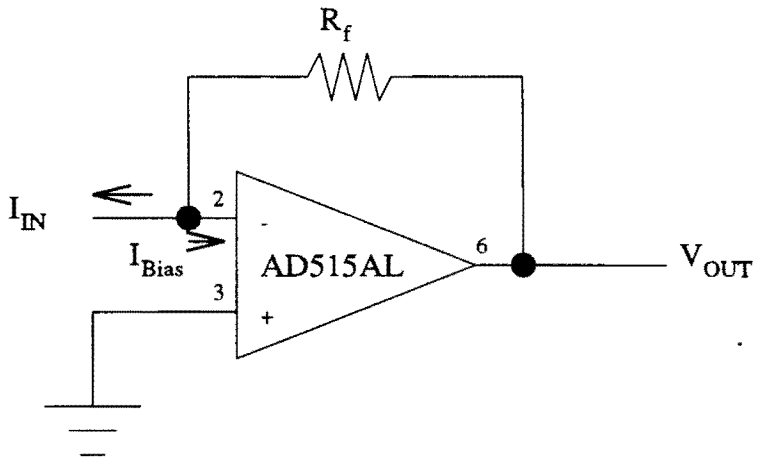

Figure 2.4 Current to voltage converter

Figure 2.4 shows the circuit of a current to voltage converter. It consists of a FET input operational amplifier in inverting configuration. A scale factor resistor is connected in the feedback path to control the gain of the circuit. The reasons for choosing AD515AL are discussed in a subsequent section 2.2.2.2.

In Figure 2.4, once the operational amplifier is chosen, the only other component that needs to be determined is the scale factor resistor. From Figure 2.4, we have,

$V_0 = I_{IN}R_f$ where

V_0 = Output voltage from the current to voltage converter (in volts).

I_{IN} = Input current to be converted (in amperes).

R_f = Scale factor or multiplying resistor (in Ω).

Since the smallest current signal to be measured is of the order of a few hundred femto amperes, let us assume

$$I_{IN(min)} = 200 \times 10^{-15} \text{ amperes.}$$

The output of the instrumentation is to be in the range of -10V to + 10V. This corresponds to a total output voltage swing of 20V. Since we are using a 12 bit A/D converter (reasons for this are discussed in section 3.2.2.1),

One A/D bit corresponds to $20 / 212 = 4.88 \times 10^{-3}$ volts.

For the output of the A/D converter to change by at least one bit for a change of 200×10^{-15} amperes input current, the scale factor or feedback resistor must be equal to

$$4.88 \times 10^{-3} / 200 \times 10^{-15} = 2.44 \times 10^{10} \Omega.$$

This value of scale factor resistor is too high for three reasons:

1. The dark current for some semiconductor detectors like CdZnTe lies in the nano ampere range. Assuming an average dark current of 1 nano ampere, the output will be

   $$1 \times 10^{-9} \times 2.44 \times 10^{10} = 24.4 \text{ V.}$$

   This will saturate the operational amplifier in the current to voltage converter.

2. Johnson noise generated by resistors tends to increase as the resistance value increases.

3. Resistors with higher values tend to cost more than resistances with lower values.

As a compromise, a value of 1 GΩ was chosen as the value for scale factor resistor. The output of the I/V converter corresponding to an input current of 200×10^{-15} amperes will be

$$(200 \times 10^{-15}) \times (1 \times 10^{9}) = 2 \times 10^{-4} \text{ volts.}$$

This signal can be further amplified using differential amplifiers for making it suitable for the A/D converters.

AD515AL is a monolithic FET input operational amplifier with a guaranteed maximum bias current of 75fA. This is the most attractive feature of this selection. As the bias current specification of the operational amplifier decreases, smaller input current signals can be sensed. (Refer to Appendix A for an explanation of bias current). Theoretically, AD515AL with a maximum bias current of 75fA is sufficient to measure currents greater than 75fA.

AD515AL delivers laser trimmed offset voltages, low drift, low noise and low power. Because of the laser trimmed offset voltages, offsetting these signals is easy and the drift of offset voltages with temperature is minimal. Lower drift and noise parameters minimizes the error introduced by the amplifier. Because of low power consumption, heat generation is decreased, and as a result, temperature dependent errors are minimized.

The 10^{15} Ω (common-mode impedance ensures that the input bias current is essentially independent of common-mode voltage. Since the output of the I/V converter is propor-

tional to the algebraic sum of bias current and input current, independence of bias current to common mode voltages improves the linearity of the circuit.

The case of AD515AL is brought out to its own connection (pin 8) so that the case can be independently connected to a point at the same potential as the input, thus minimizing stray leakage to the case. This feature also shields the input circuitry from external noise and supply transients.

Figure 2.5 shows the dependence of peak-peak input noise voltage to source impedance for AD515AL [6]. From this graph, it is seen that in the range of source impedances where this circuit is targeted to operate (100 MΩ to 100 GΩ), Johnson noise of the source easily dominates the noise characteristics of the amplifier. Reference [6] suggests that whenever Johnson noise is greater than amplifier noise, amplifier noise can be considered negligible for application. This makes the design of the circuit straightforward. Reference [6] provides complete details on specifications of AD515AL.

So far, the design of the current-to-voltage converter circuit was discussed. Next we will discuss various factors that were considered in the design of the voltage amplifier stage.

*2.2.2.3 **Voltage amplifier design*** The main purpose of the voltage amplifier stage as shown in Figure 2.3 is to provide voltage amplification with as little noise introduced as possible. There are also many other factors that need to be considered in the design of this stage. Some of the important considerations are:

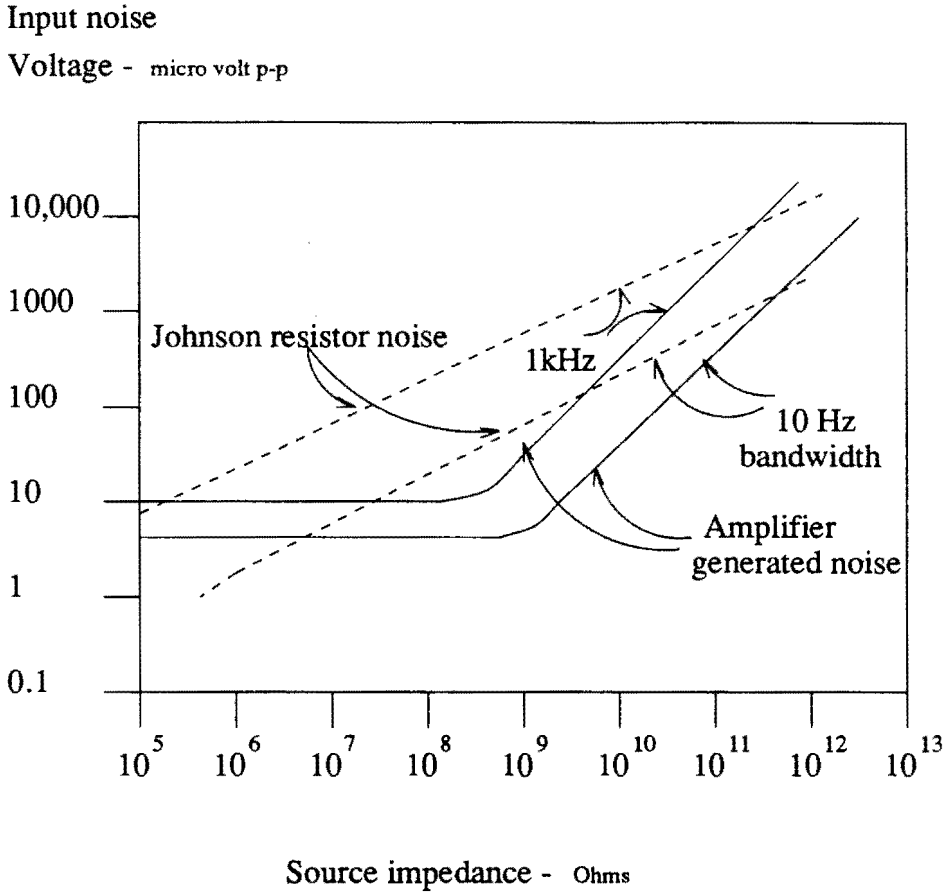

Figure 2.5 Peak-to-Peak input noise voltage vs. Source impedance and bandwidth

1. The input impedance should be as high as possible and as closely matched as possible to decrease the load on the output of the current to voltage converter. The lower the input impedance of this stage, the higher will be the load on the current to voltage converter. This will lead to higher output currents from the I/V converter which will increase the heating of the operational amplifier. This will lead to many other temperature related instabilities and noise in the I/V converter circuit.

2. It should be possible to inject precise voltage signals to the input of this stage, and get this subtracted from the output from the previous stage. This facility is needed for offsetting the dark current of the detector.

3. Output from the voltage amplifier must meet the input specifications of the digitizing circuitry. The circuit should provide good isolation for the instrumentation from the input stage of the digitizing circuitry.

4. The circuit should provide good isolation for the instrumentation from the input stage of the digitizing circuitry.

5. The voltage amplifier must be stable with respect to variations in temperature.

6. The circuit should have a high common mode rejection.

7. Since the detector will be positioned inside the X-ray vault and the data acquisition system outside the vault, it should be capable of driving the output signal over long cables so as to reach the digitizing circuitry.

8. The circuit should be as linear as possible.

9. Offset voltage drifts should be as minimum as possible as these introduce errors at the output.

10. To maintain lower cost and size, the circuit should have few components.

To meet all these considerations, an instrumentation amplifier would be the best choice for the voltage amplifier stage.

An instrumentation amplifier is a closed-loop gain block which has a differential input and an output which is single ended with respect to a reference terminal. The impedances of the two input terminals are balanced and have high values, typically $10^9\ \Omega$ or greater. The output impedance is very low, typically in the order of a few milliohms. Unlike an operational amplifier, which has its closed-loop gain determined by external resistors connected between its inverting input and its output, an instrumentation amplifier employs an internal feedback resistor network which is isolated from its signal input terminals. With the input signal applied across the two differential inputs, gain is either preset internally or is user set by an internal (via pins) or external gain resistor, which is also isolated from the signal inputs.

The most important function an instrumentation amplifier provides is common-mode rejection. This is the property of canceling out common signals (the same potential on both inputs) while amplifying those which are differential (a potential difference between the inputs). Input offset errors and scale factor errors can be corrected by external trimming, if required. Low nonlinearities are designed and built into instrumentation amplifiers by the manufacturers. Gain selection is simple and easy to apply. Gain selection via one external resistor is one common method. Most instrumentation amplifiers provide a choice of inter-

nally preset gains (often pin selectable) which are stable over temperature. Above all, the instrumentation amplifier is very stable and precise in its operation. These are the reasons for choosing an instrumentation amplifier for the voltage amplifier stage.

For the above mentioned design considerations, AD524C from Analog Devices. was the choice for the following reasons. AD524C is a precision monolithic instrumentation amplifier designed for data acquisition applications requiring high accuracy under worst case operating conditions. It has an outstanding combination of high linearity, high common mode rejection, low offset voltage drift, and low noise. It has a high gain bandwidth product and has an output slew rate of 5V/μs and settles in 15μs to .01% for gains of 1 to 100. These parameters makes AD524C suitable for high speed data acquisition. As a complete amplifier, AD524C does not require any external components for fixed gains of 1, 10, 100, 1000. For other gain settings between 1 and 1000, only a single resistor is required. The AD524C input is fully protected for both power on and power off fault conditions. Reference [6] provides complete details on the specifications of AD524C.

The output from the current to voltage converter corresponding to an input current of 200 fA is 2×10^{-4} V. To sense this signal as bit variations in a 12 bit Analog/Digital converter, a gain of 100 was chosen. The gain could have been less than 100 but for reasons of avoiding external resistors for gain selection.

2.2.2.4 ***Output filter design*** The input current signal to the instrumentation is DC. Theoretically, the output of the instrumentation should be a clean DC. This is rarely observed in practice. Random noise gets introduced into the circuit at various points. The predominant noise source in this instrumentation is the Johnson noise of the source resistance

and the feedback resistor in the I/V converter. Since the signal is amplified progressively, noise also gets amplified by the voltage amplifier stage. So the output of the instrumentation contains random noise superimposed on the DC signal. To get rid of this noise, the signal has to be filtered.

The analog output signal from the instrumentation is digitized and stored using a data acquisition system. To digitize the analog signal, an A/D converter is used. There is a fundamental rule called the Nyquist rule being followed in digitization of analog signals. This rule states that the maximum frequency component in the analog signal that is to be digitized must be less than half the sampling rate. Otherwise, errors will be introduced in the digitized signal due to an effect called aliasing. To avoid this error, the output signal must be filtered. Reference [5] provides details on aliasing effect and Nyquist rule.

In addition to filtering the output signal, the circuitry has to be as simple as possible due to reasons of size and cost. So, a simple first order passive low pass filter was chosen for filtering the output. Figure 2.6 shows the circuit diagram for a passive low pass filter.

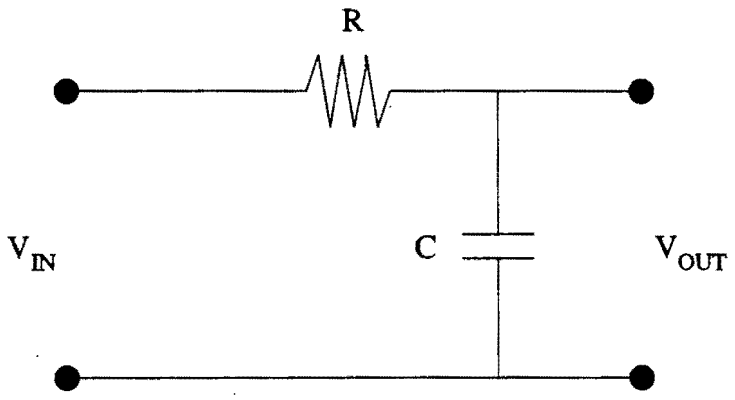

Figure 2.6 Low pass filter

The governing equation for a low pass filter is

$$f_C = \frac{1}{2\pi RC}$$

where

f_c = cutoff frequency (Hz)

R = Value of resistor (in Ω)

C = Value of capacitor (in farads)

Since we are primarily interested in DC signals, a cutoff frequency of 20 Hz was decided upon. So,

$$20 = \frac{1}{2\pi RC}$$

Considering a standard available resistor of 82 kΩ

$$C = \frac{1}{2\pi * 82000 * 20} = .098\ \mu f$$

An industry standard value of 0.1 μf was chosen as the value for the capacitor.

2.2.2.5 Noise Performance of the instrumentation From Figure 2.5, and for source resistances greater than 100 MΩ, we can see that the Johnson noise of the source dominates the noise characteristics of the circuit. The Johnson noise generated in a resistive component R is given by

$$e_n = \sqrt{4kTRB}$$

where, e_n = rms value of the noise voltage

k = Boltzman's constant (1.38×10^{-23} joules/K)

T = Absolute temperature of resistance, K

B = Bandwidth in which noise is measured (Hz)

For a photodiode like the one used as part of this project, the source resistance is 1 GΩ. The Johnson noise generated due to this resistance for a bandwidth of 20 Hz is equal to

$$\sqrt{4 * k * 298 * 1G\Omega * 20} = 1.81 \times 10^{-5} \text{ V rms.}$$

This noise signal is amplified by a factor of 100 by the instrumentation amplifier. So, the noise voltage reflected at the output of the instrumentation is 1.8 mV (rms).

Reference [6] suggests that to convert the rms noise voltage to a peak to peak value, a conversion factor is applied. The factor is 6.6 (V (p-p) / (V (rms), for a criterion of less than .1 % probability of noise peaks exceeding calculated limits. By applying the conversion factor, the calculated peak to peak noise expected at the output of the instrumentation is 12 mV (p-p)

2.2.3 Instrumentation development

Figure 2.7 shows the complete circuit diagram of the instrumentation designed for measurement of very low current signals from X-ray detectors. Section 2.2.2 described the design of the instrumentation for very low current measurements. Although the design

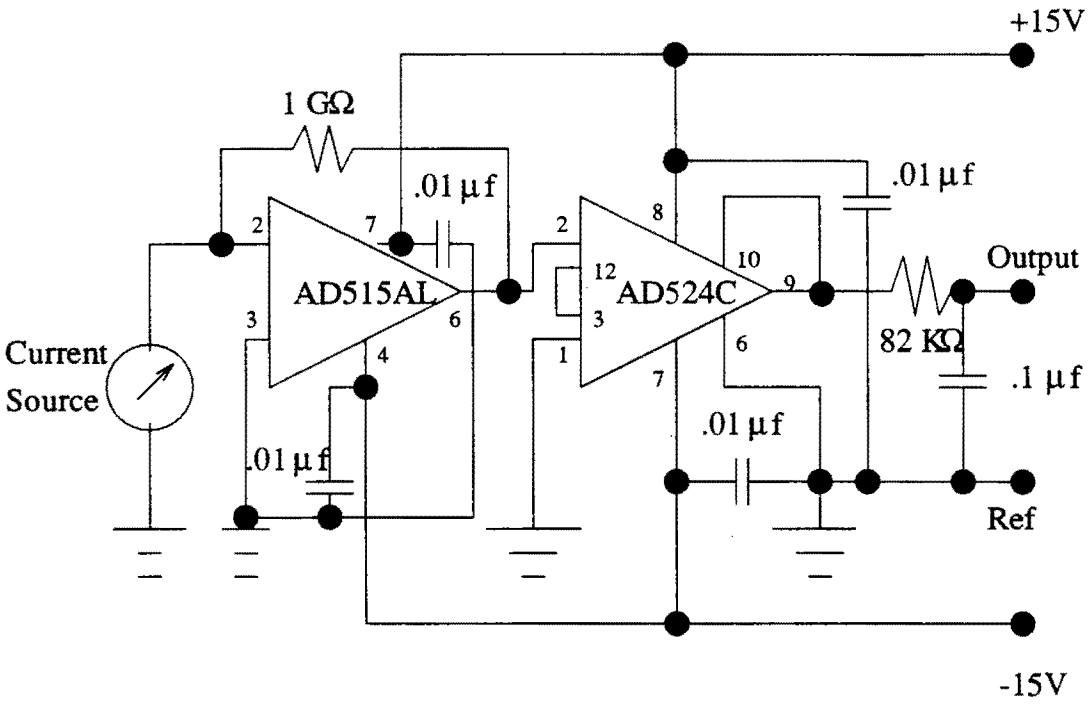

Figure 2.7 Instrumentation for low current measurement

appears deceptively simple, development of the instrumentation and making it operational is very complicated. This is due to the fact that the current signal being measured is very small and as a result, leakage currents, improper grounding, improper shielding etc. will have a drastic effect on the performance of the instrumentation. Appendix B provides a detailed description of the various principles and techniques followed in the development of the instrumentation.

2.2.4 Performance of instrumentation

The prototype detector instrumentation was developed and tested for the following.

- Stability with respect to time
- Linearity of the instrumentation
- Noise performance

To measure the above mentioned performance details of the detector, a VMEbus based data acquisition system was used. The description of this system is discussed in Appendix C.

2.2.4.1 Stability with respect to time Since the instrumentation developed is going to be used with a point detector, the time required to scan larger samples will be long. This leads to the requirement that the circuit be very stable over extended periods of time(few hours to few days). To test this, a current source of 2.82 nA was connected to the input of the instrumentation with a scale factor resistor of 100 MΩ. This was derived by connecting a series resistor of 1 GΩ to a stabilized power supply of 2.8 V. The output voltage of the instrumentation was digitized using the VME bus based data acquisition system and stored.

The output voltage with respect to time is plotted in Figure 2.8. From this graph, it can be seen that the output is quite stable over long periods of time. The initial drop in the output voltage is due to the variations in the input current source as the current source was a series combination of resistor and power supply and the effect of temperature on the series resistor is felt as shown in the graph.

2.2.4.2 Linearity of instrumentation For the instrumentation to be useful, the relationship between the input current and the corresponding output voltage generated must be linear. The minimum current signal generated by X-rays can be on the order of few hundred fA and the dark current of certain detectors can be in the nA range. Since it is not possible to generate very low current signals accurately in a laboratory without the aid of complex electronic circuits, the instrumentation was tested by generating current signals using a combination of a series resistor with a voltage source. Figure 2.9 shows the graph of output voltage of the instrumentation for various input currents. It is evident from the graph that the response of the instrumentation is quite linear with respect to input current changes.

2.2.4.3 Noise performance The output of the instrumentation was observed using a cathode ray oscilloscope with a source resistance of 1 GΩ. A peak-to-peak noise of 12 mV was observed at the output of the instrumentation. This seems to match closely with the theoretical estimate of noise provided in section 2.2.2.5.

We have a sensitive instrumentation that can measure very low current signals while introducing minimum noise. This instrumentation was used to measure the output current from a CdZnTe semiconductor detector, and from NaI which is a scintillation detector. It should be emphasized strongly at this point that no assumptions have been made regarding

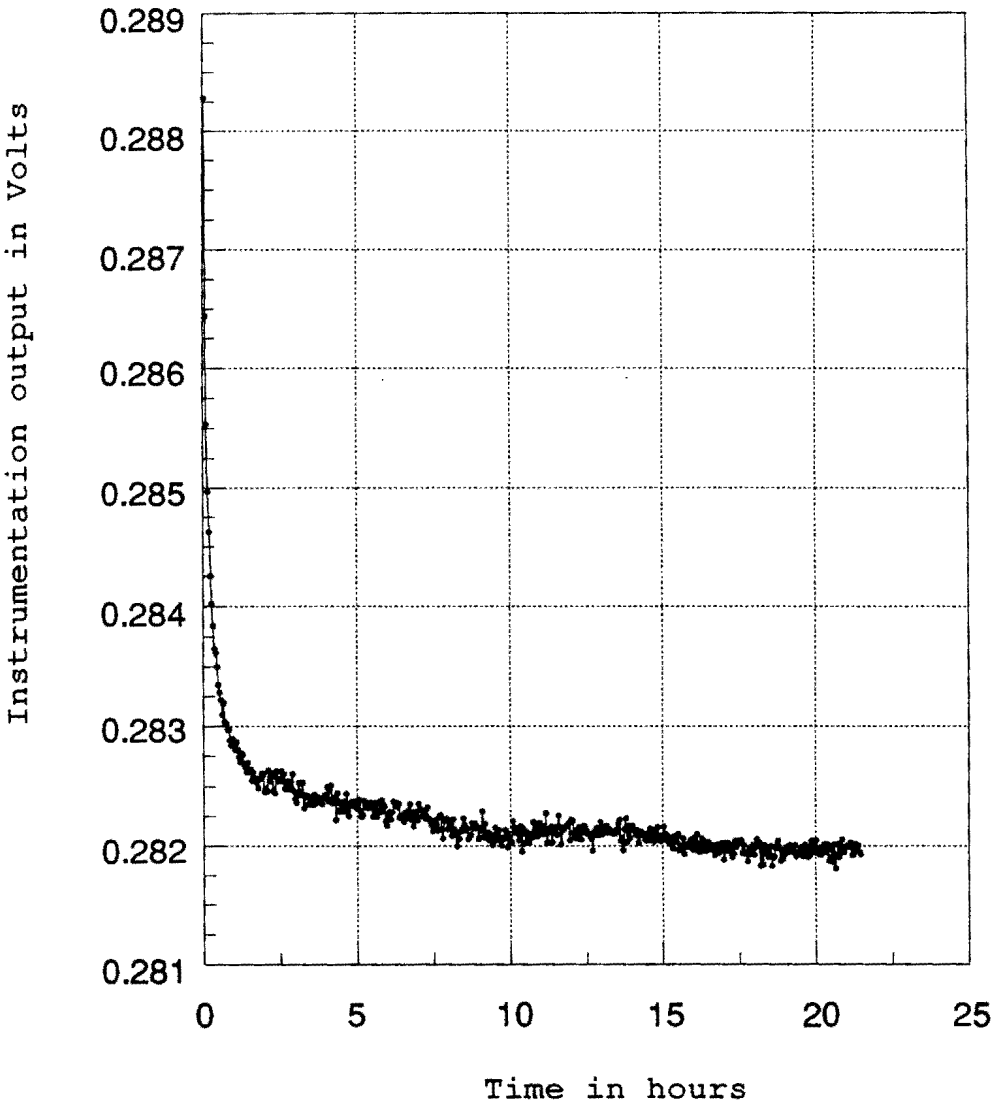

Figure 2.8 Instrumentation output vs. Time

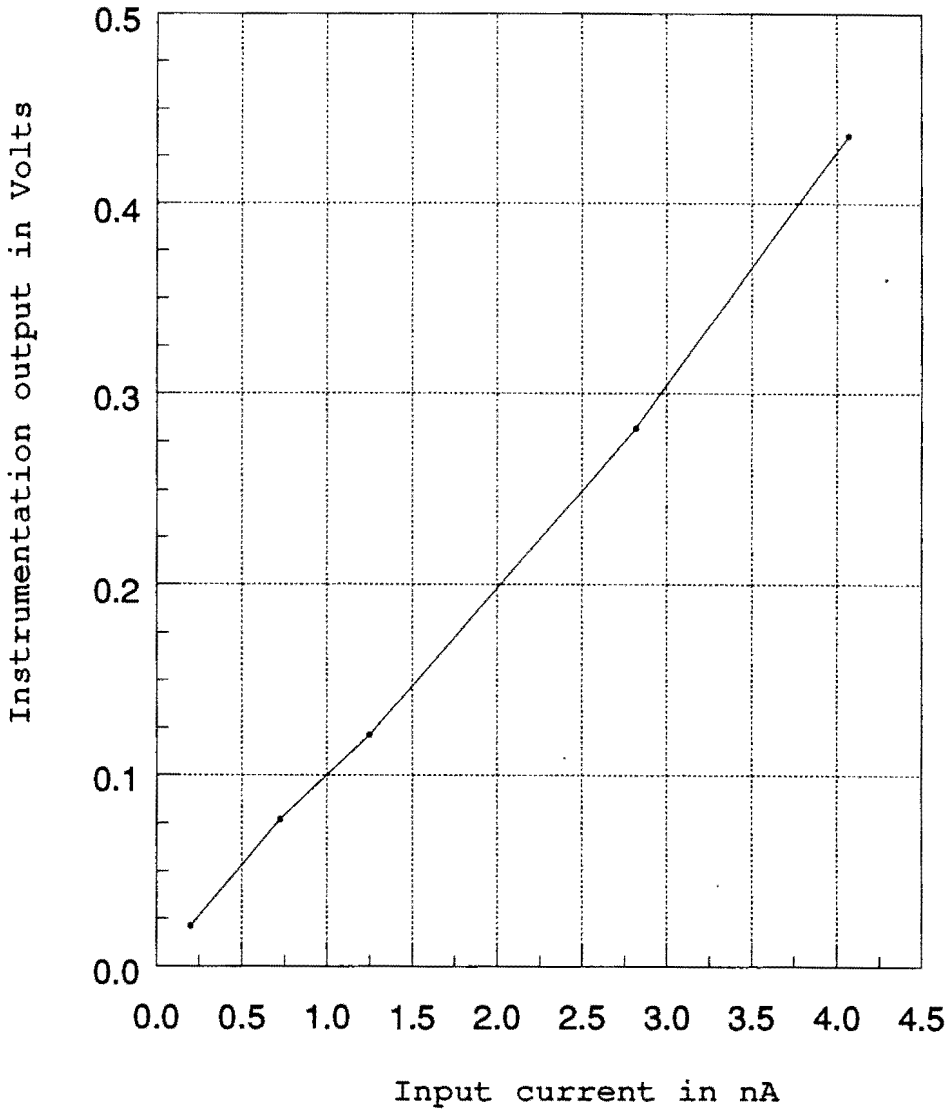

Figure 2.9 Linearity of instrumentation

the current source, except for the fact that the circuit was designed for measuring low currents from X-ray detectors. This is a generic instrumentation and it can be adapted very easily with minor modifications to different kinds of X-ray detectors like semiconductor detectors, scintillation detectors, and fiber optic scintillators.

2.3 Current mode X-ray detector based on CdZnTe

The measurement of absorption of X-ray radiation with good efficiency, high spatial resolution and good speed is the goal of any digital radiography and computed tomography system. The attractiveness of solid state detectors for this purpose is the available technology for semiconductor production and the flexibility in the instrument design that makes it possible to construct a compact detector.

As part of this research work, it was decided to evaluate the feasibility of using cadmium zinc telluride ($Cd_{1-x}Zn_xTe$ where $x = 0.2$ for the crystals that were used in this research work) in current mode of operation. The potential benefits of using CdZnTe are room temperature operation, small size, high radiative stopping power, high stability, solid state reliability, and ruggedness. There is much literature available on the material properties of CdZnTe and its performance as a X-ray detector in photon counting mode of operation [7-12]. Surprisingly, there is very little available about the performance of CdZnTe in current mode of operation [13-17].

The principle of operation of a current mode detector was explained in section 2.2. For a semiconductor material to be suitable for a high speed detector system, two parameters are of paramount importance.

- Dark current stability of the detector material
- Low afterglow

These two factors are discussed further to justify their importance.

2.3.1 Dark current stability

According to the principle of operation of a semiconductor detector as explained in section 2.2.1, charge collection efficiency can be improved by applying a bias voltage across the detector material. As a result of bias voltage and the resistivity of the material, a current flows in the circuit even when there is no incident X-ray radiation. This current is termed as "dark current".

When X-ray radiation is incident on the detector, higher energy level electrons are knocked out of their shells. These in turn dislodge electrons from outer shells creating a number of electron-hole pairs. These charge carriers are swept across the detector material to the electrical contacts by the applied bias voltage. This photon produced current algebraically sums up with the dark current. As long as the dark current value does not change, changes in output current of the detector reflect the changes in photon intensity. If the dark current changes due to some reason, there will be no way of finding out and this will reflect as photon produced current variations at the output. So, for a semiconductor detector to operate in current mode, the dark current has to be extremely stable.

2.3.2 Afterglow

The other important factor is afterglow. Due to semiconductor properties, the photocurrent can continue for an extended period after the radiation flux is removed. This effect is

known as "afterglow". This has a direct consequence on the speed of operation of the detector.

For scanning samples, the sample has to be moved from one point to another and data collected. If the afterglow of the detector material is high, data can be collected at a new point only after the signal from the previous point dies out completely. This would decrease the speed of operation of the system.

2.3.3 X-ray detector system

To evaluate CdZnTe as a X-ray detector in current mode of operation, the instrumentation described in section 2.2.2 and section 2.2.3 was used. The current source that was used to test the instrumentation was replaced by a CdZnTe crystal. Figure 2.10 shows the circuit diagram of the X-ray detector system. One end of the crystal is connected to the I/V converter input. The other end is connected to a negative high voltage power supply. This is an unorthodox way of applying high voltage and measuring current. This was chosen because of the simplicity of the circuit, size and cost. Reference [18] discusses a more usual way of applying high voltage and measuring current. The circuit was enclosed in an aluminum box and shielded according to the techniques described in Appendix B.

2.3.4 Performance of the detector system

The X-ray detector system based on CdZnTe was tested for the following features.

- Dark current stability with respect to temperature
- Afterglow

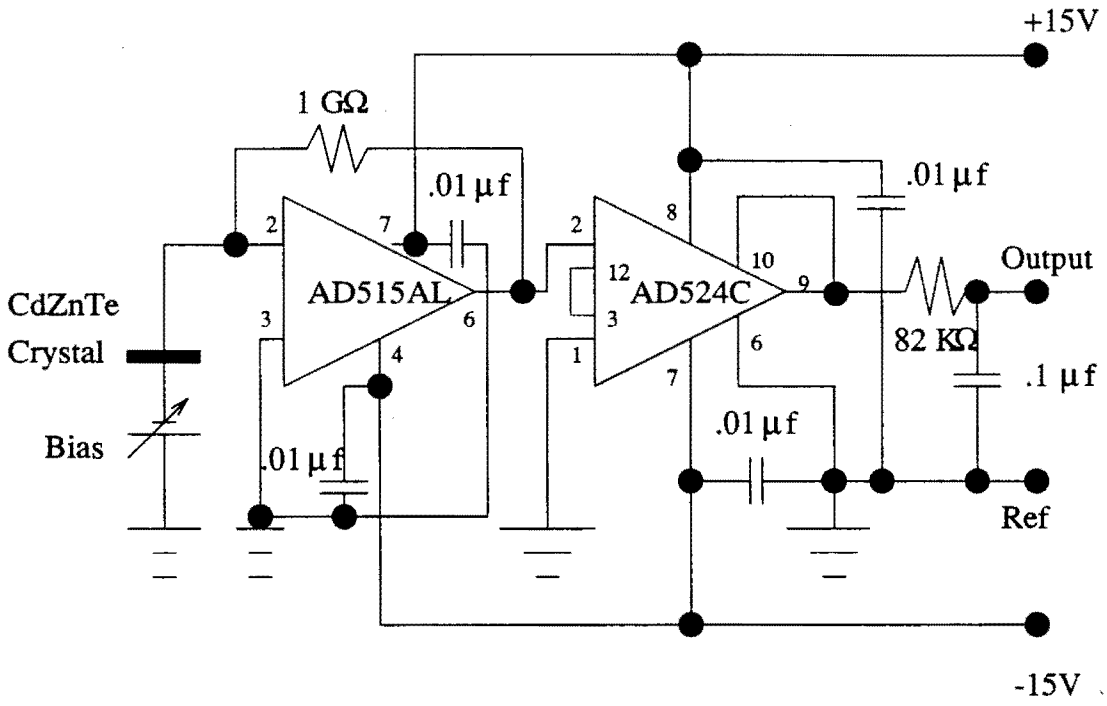

Figure 2.10 CdZnTe based X-ray detector circuit

2.3.4.1 Dark current stability with respect to temperature The stability of dark current was tested in a laboratory environment. To perform this test, some sort of temperature measuring circuitry was needed. The circuit shown in Figure 2.11 was built to measure temperature. This circuit consists of a negative temperature coefficient thermistor in a bridge configuration. Reference [19] provides a detailed design of the circuit. The temperature sensing circuit was also enclosed inside the same box as the detector system in such a way that the thermistor was in close proximity to the CdZnTe crystal. The output of the detector and the temperature sensing circuit were sampled, digitized and stored using a VME bus based data acquisition system explained in appendix C.

Figure 2.12 is a graph depicting the detector output vs. time. Figure 2.13 depicts the temperature sensed by the temperature sensing circuitry vs. time. In fact, every point in Figure 2.12 corresponds in time to every point in Figure 2.13. From the two graphs, remarkable dependence of dark current on temperature is observed at room temperatures.

In order to obtain fine spatial resolution and track minor flux variations, the observed dark current stability may be unacceptable. Some kind of temperature stabilizing mechanism may be required to improve the stability of dark current.

2.3.4.2 Afterglow To check the afterglow, the X-ray detector system was shielded from X-ray radiation using lead shields. A lead collimator of about 250 microns diameter was used. Then the detector was exposed to X-ray radiation through the collimator. The output before and after exposing the detector was noted down. Then the X-ray generator was turned off. The output was noted again. Also, the time that elapsed from the point when the generator was turned off to the point when the output reached the original value was also

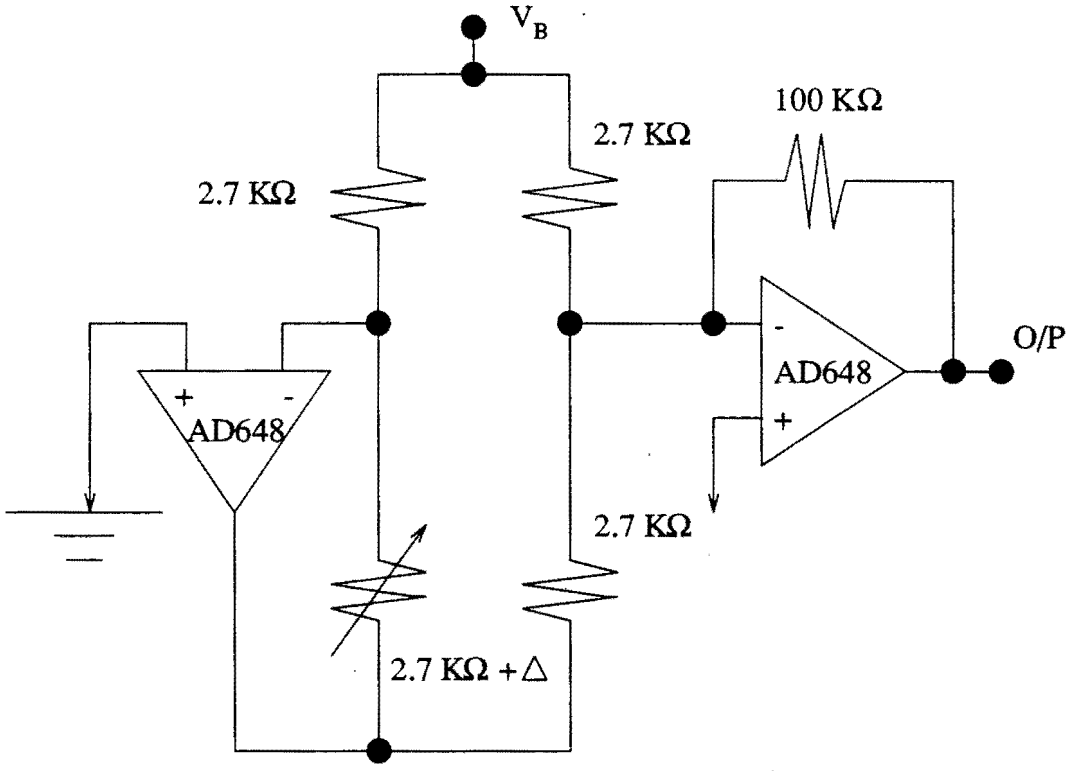

Figure 2.11 Temperature measurement circuit

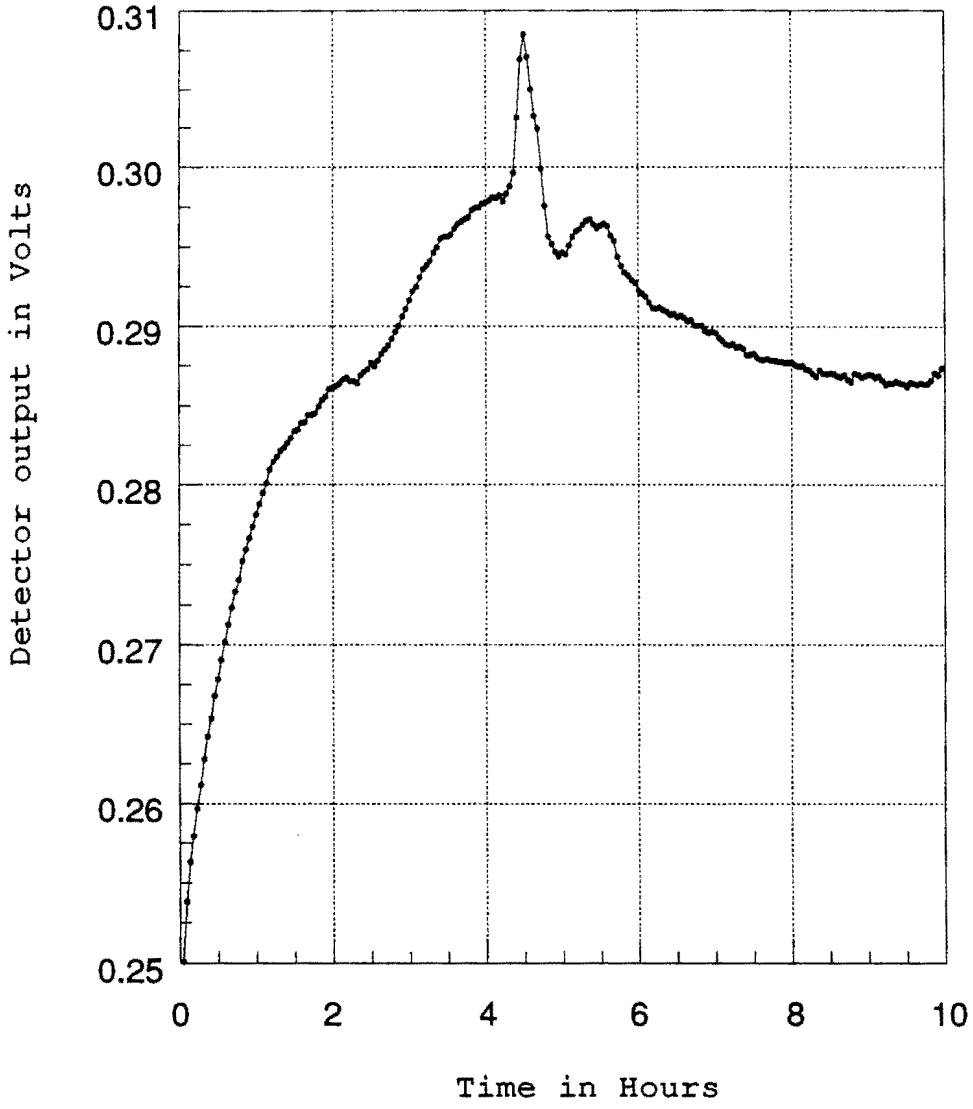

Figure 2.12 Detector output vs . Time

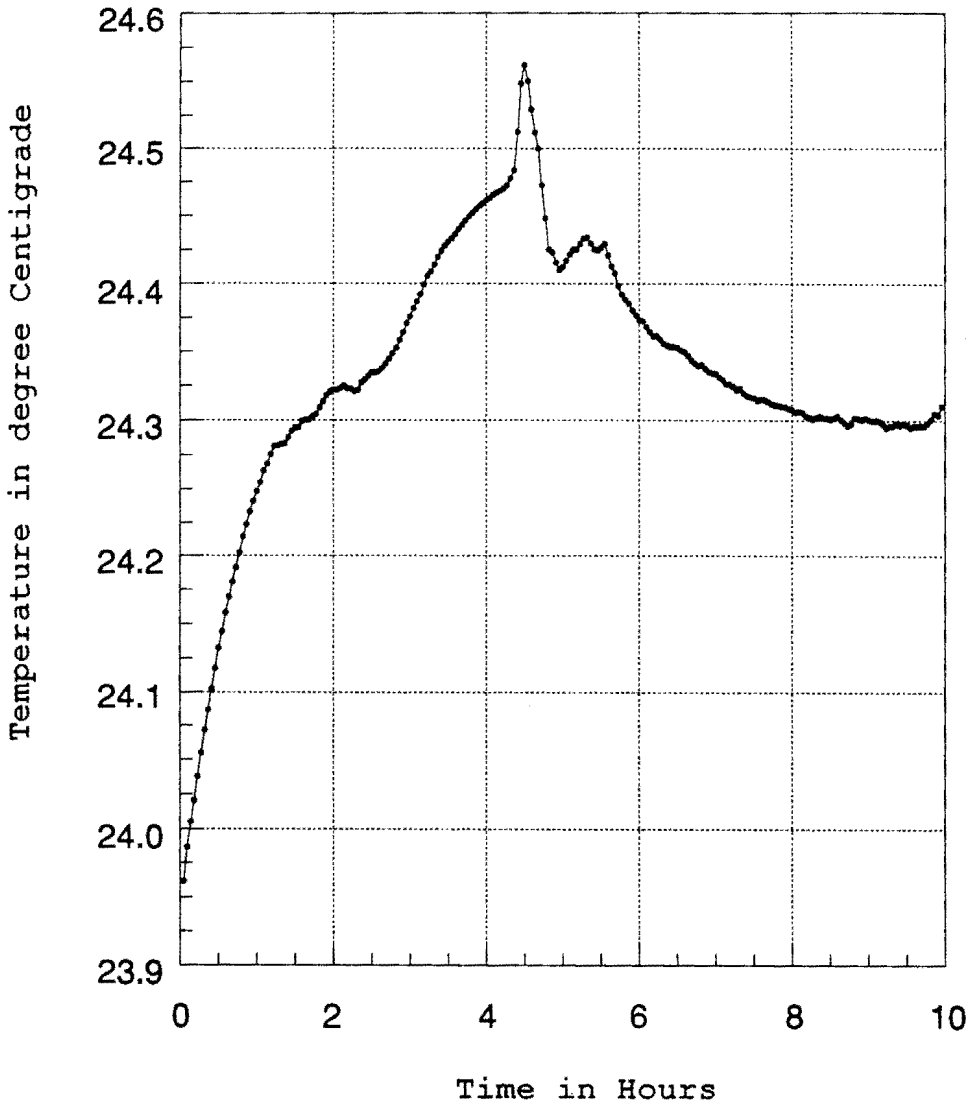

Figure 2.13 Temperature vs. Time

noted. Table 2.1 gives these values for various flux intensities. From this, it can be made out that afterglow runs into seconds and this is totally unacceptable for a current mode detector.

Surprisingly, all the literature ([7-8] and [14]) available on afterglow measurements on CdZnTe provides details on afterglow for flash X-ray experiments and not for continuous exposure to radiations.

*2.3.4.3 **Response of detector to X-ray radiation*** Response of the detector to incident radiation, provides information about the linearity of the detector system to incident radiation. The detector was exposed to X-ray radiation of various intensities and the output was noted . Figure 2.14 provides a graphical view of this data for a bias voltage of -100V and Figure 2.15 for a bias voltage of -225V. From the graph, it can be easily seen that the detector is quite linear in response to incident flux. Although the thermal stability of the detector

Table 2.1 Afterglow measurements for CdZnTe

Generator voltage	Generator current	Initial output	Output after Generator ON	Time to decay
(keV)	(mA)	(V)	(V)	(seconds)
80	2.0	0.222	0.225	5
80	4.0	0.222	0.227	15
130	1.0	0.304	0.314	20

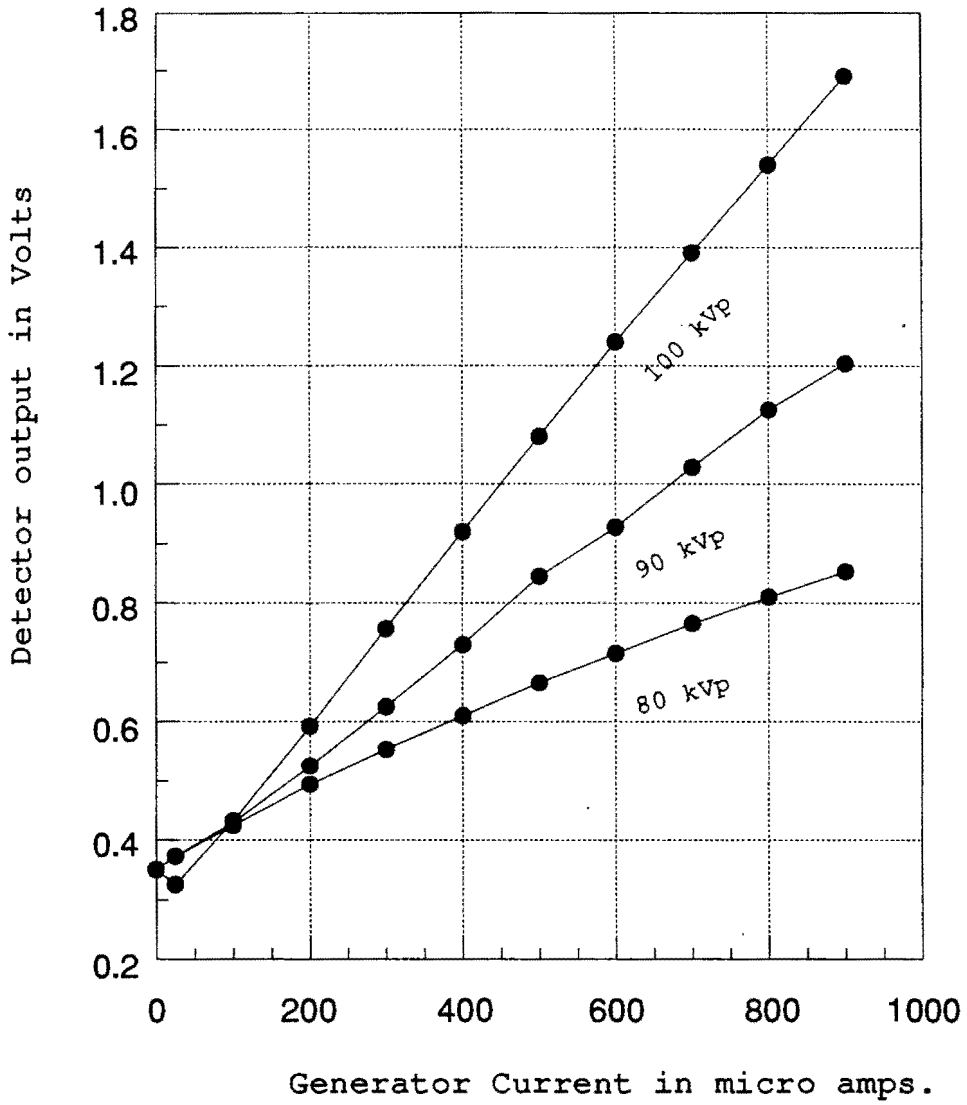

Figure 2.14 Response of CdZnTe detector at -100 V bias

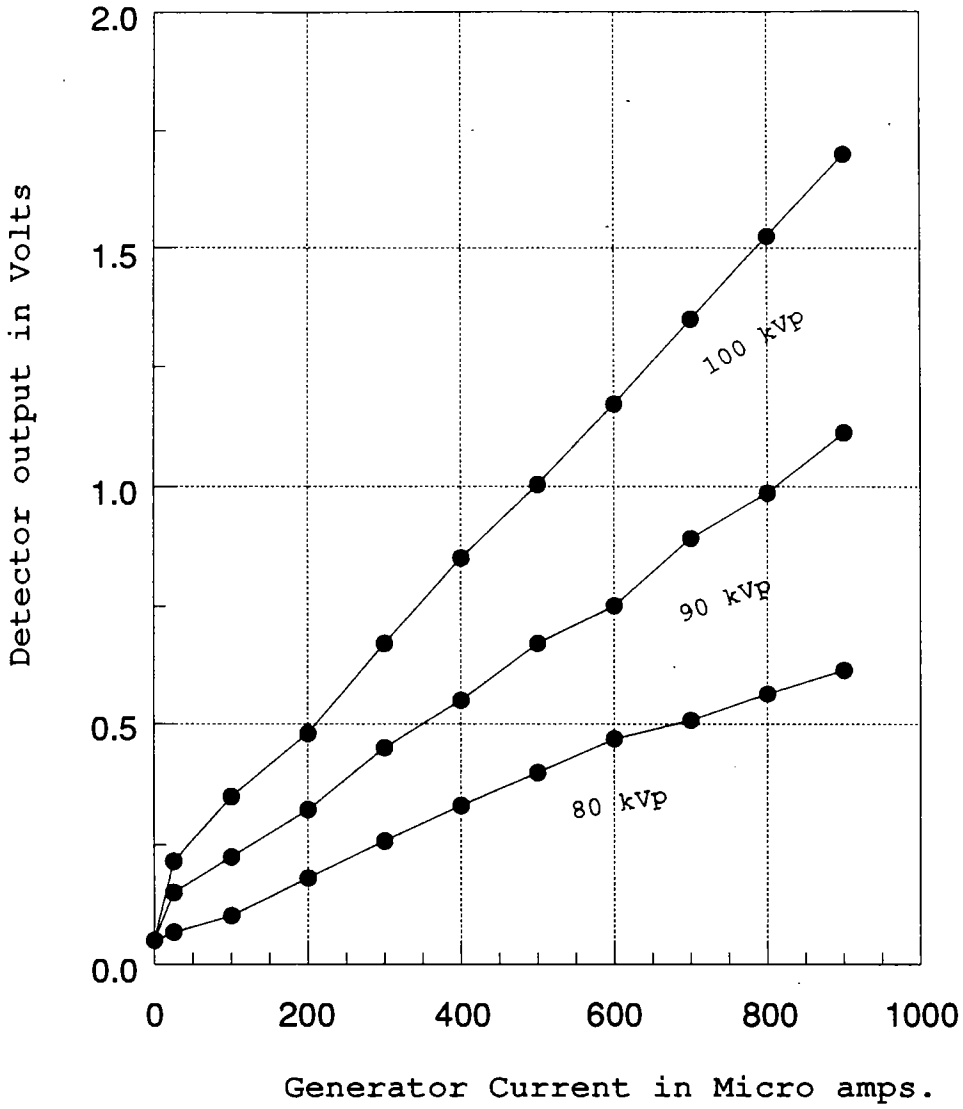

Figure 2.15 Response of CdZnTe detector at -225 V bias

could have been improved by stabilizing the temperature of the detector, the unacceptable amount of after glow for current mode operation forced us into looking for a substitute detector material. This led to selection of scintillation mode crystals which are very popular in the industry as X-ray detectors.

2.4 Current mode X-ray detectors based on scintillating crystals

After finding it infeasible to use CdZnTe in current mode for our purpose, attention was turned towards scintillation mode crystals like NaI and CsI. References [20] and [21] suggest that these crystals have lower conversion efficiency as compared to semiconductor detectors. They give visible light scintillations in response to incident radiation. So the light has to be converted to a current signal before the instrumentation described in section 2.2 can be connected. As a result, a mechanical/electrical front end was designed and developed to convert light scintillations into current with minimum of instability introduced.

2.4.1 Front end of the detector

NaI and CsI crystals give out visible light scintillations in response to X-ray photons. Traditionally, a photomultiplier tube will be used to amplify the signal. Due to reasons of size, cost and simplicity, it was decided to use a photodiode instead. A Hamamatsu photodiode (S1337-33BQ) was chosen to convert the light scintillations into useful current signal. Reference [23] provides details on S1337-33BQ.

2.4.1.1 Reasons for choosing S1337-33BQ At the center for NDE, there were NaI and CsI crytals available in the shape of a cylinder with 10 mm length and 10 mm diameter. When photons are incident on one face of the crystal, visible light can be seen through the

other face. To collect the light efficiently, a photodiode with a photo sensitive area equal to the diameter of the crystal was required.

From a survey of available photodiodes in the industry, it was observed that diodes with larger sensitive areas have higher dark current as compared to ones with smaller areas. From the specification details of these diodes in Reference [23], it was also observed that the absolute variation of dark current with temperature was lower for photodiodes with smaller photo sensitive areas.

The photocurrent produced by a given level of incident light varies with wavelength. This wavelength/response relationship is known as the spectral response characteristics. In order to maximize the output current from a photodiode for a given incident light intensity, the spectral response characteristics of the photodiode must match the output light spectrum of the scintillating crystals. Reference [23] shows the output light spectrum response of NaI and CsI crystals and Reference [20] provides information about the spectral response characteristics of S1337-33BQ. As a compromise between dark current stability, photo sensitive area, and the best match of spectral response characteristics between the scintillators and photodiode, S1337-33BQ was decided upon.

2.4.1.2 Light guide From the specifications of S1337-33BQ photodiode, it can be seen that the effective photo sensitive area is 2.4 x 2.4 mm^2. The size of the face of the available scintillation crystal is 10 mm diameter. For efficient and complete collection of light, the light output from the crystal has to be channelled or guided on to the smaller area of the photodiode.To perform this function, a light guide made of quartz glass was specially manufactured.

2.4.1.3 Mechanical assembly The scintillator crystal, light guide and the photodiode have to be effectively coupled with one another without any light leakage or external light interference. To achieve this, a mechanical assembly as shown in Figure 2.16 was designed and manufactured. The three pieces were mounted inside the mechanical assembly as shown in Figure 2.16. An optical coupling grease was used at the interfaces to provide good light coupling. The light guide was wrapped in a thin sheet of teflon to provide better light channelling capability.

2.4.2 X-ray detector system

The entire front end assembly was mounted inside the same aluminum shield box that holds the instrumentation described in section 2.2.2 and 2.2.3. One output pin of the photodiode was connected to the I/V converter input and the other output pin of the photodiode was grounded. The aluminum box was mounted inside a lead box with a .025" diameter collimator (635 microns). This detector was tested for various performance details which are discussed below. Figure 2.17 shows the circuit diagram of the detector with scintillation crystal as the detector material.

2.4.3 Performance of detector

The detector system was evaluated for the following performance details.

- Long term stability and stability with respect to room temperature variations
- Response of the detector to radiation flux variations
- Noise performance of the detector
- Integration capability of the detector

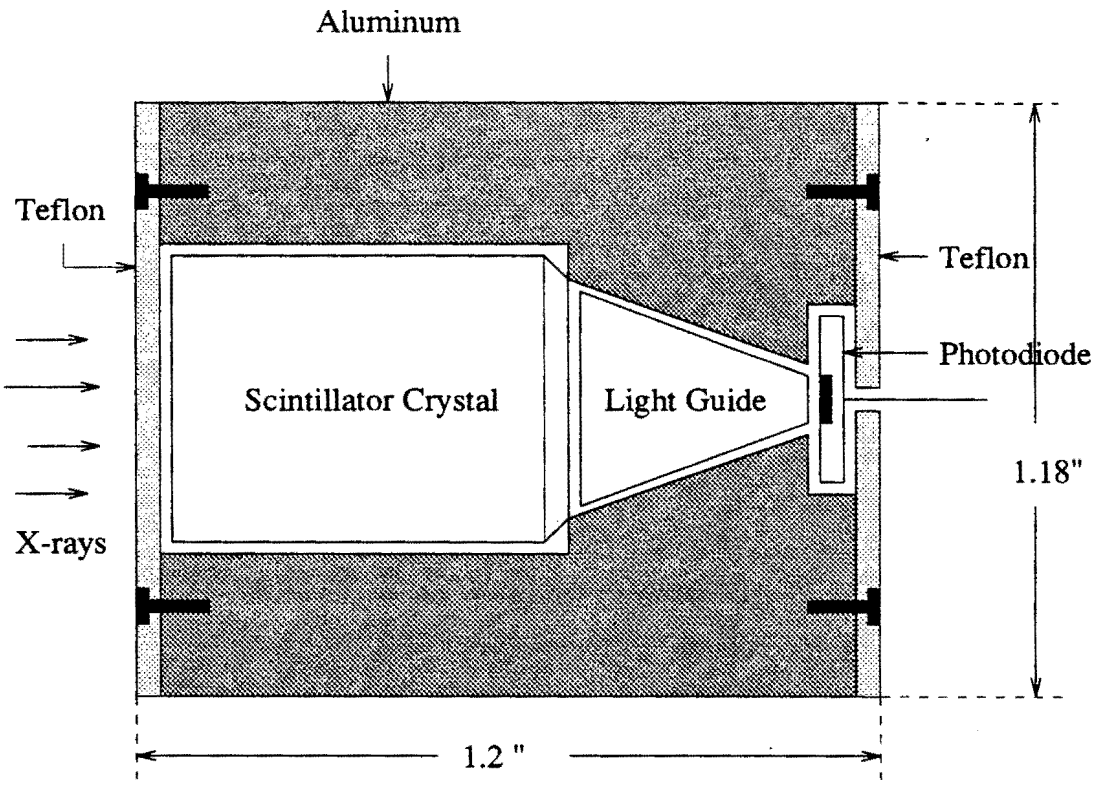

Figure 2.16 Mechanical assembly for front end of detector

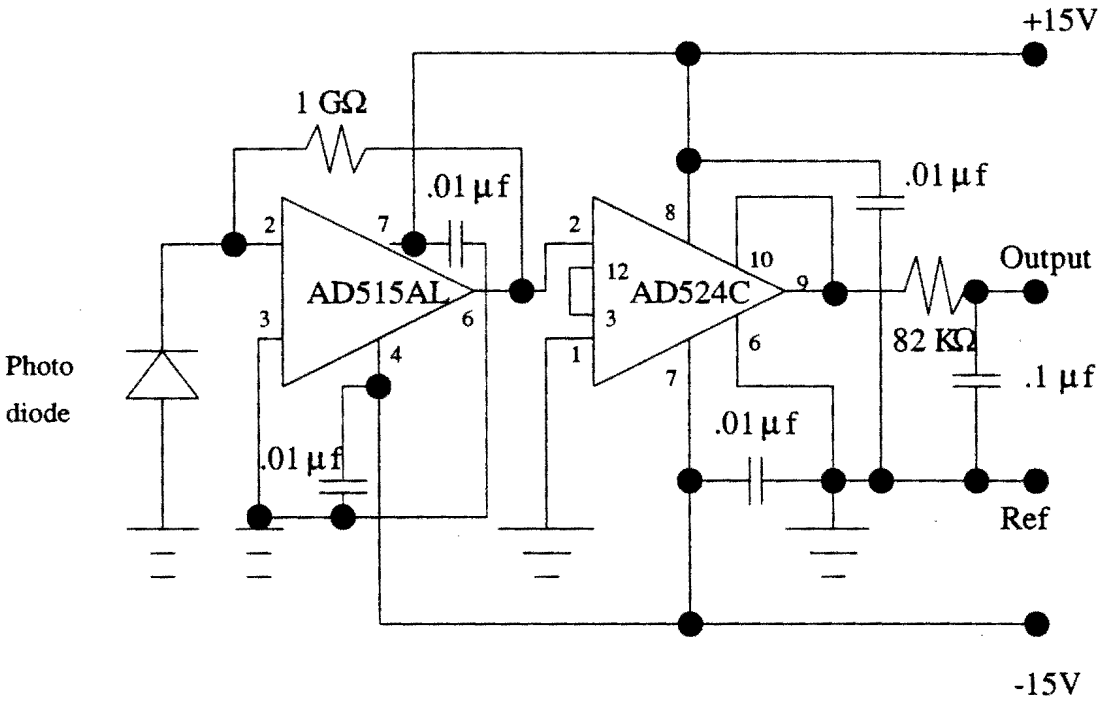

Figure 2.17 Scintillating crystal based X-ray detector circuit

- Speed of Operation
- Dynamic range of the detector

2.4.3.1 Long term stability and stability with respect to temperature variations Long term stability of the detector with respect to temperature variations goes a long way in determining the performance of the detector. The stability was evaluated by measuring the output and temperature at the same time with no incident radiation beam. The same circuit shown in Figure 2.11 was used to measure the temperature of the crystal. The data was collected using the VME bus based data acquisition system described in Appendix C. Figure 2.18 shows the output of the detector over a period of time and Figure 2.19 shows the temperature measured over the same period. Reference [23] specifies that the dark current of the photodiode varies by 1.15 times/ ^{O}C. From the graph in Figure 2.19, for a temperature variation of 0.1(C, the output of the detector should have varied by 0.26 mV. From Figure 2.18, we can see a variation of 0.35 mV.

2.4.3.2 Response of detector to radiation flux variations For proper performance of the detector, its response to flux variations should be linear. To evaluate this, the detector was shielded from radiation using a lead box with a .025" diameter collimator and exposed to X-ray radiations of various intensities. Figure 2.20 shows the response of the detector to various flux intensities. From this graph, it can be seen that the response of the detector system is linear for a very wide range of incident flux intensity.

2.4.3.3 Noise performance of the detector Figure 2.21 shows a plot of output voltage of the detector with respect to time with the X-ray generator turned OFF. The data was collected using a data acquisition system to which the detector was connected using a long

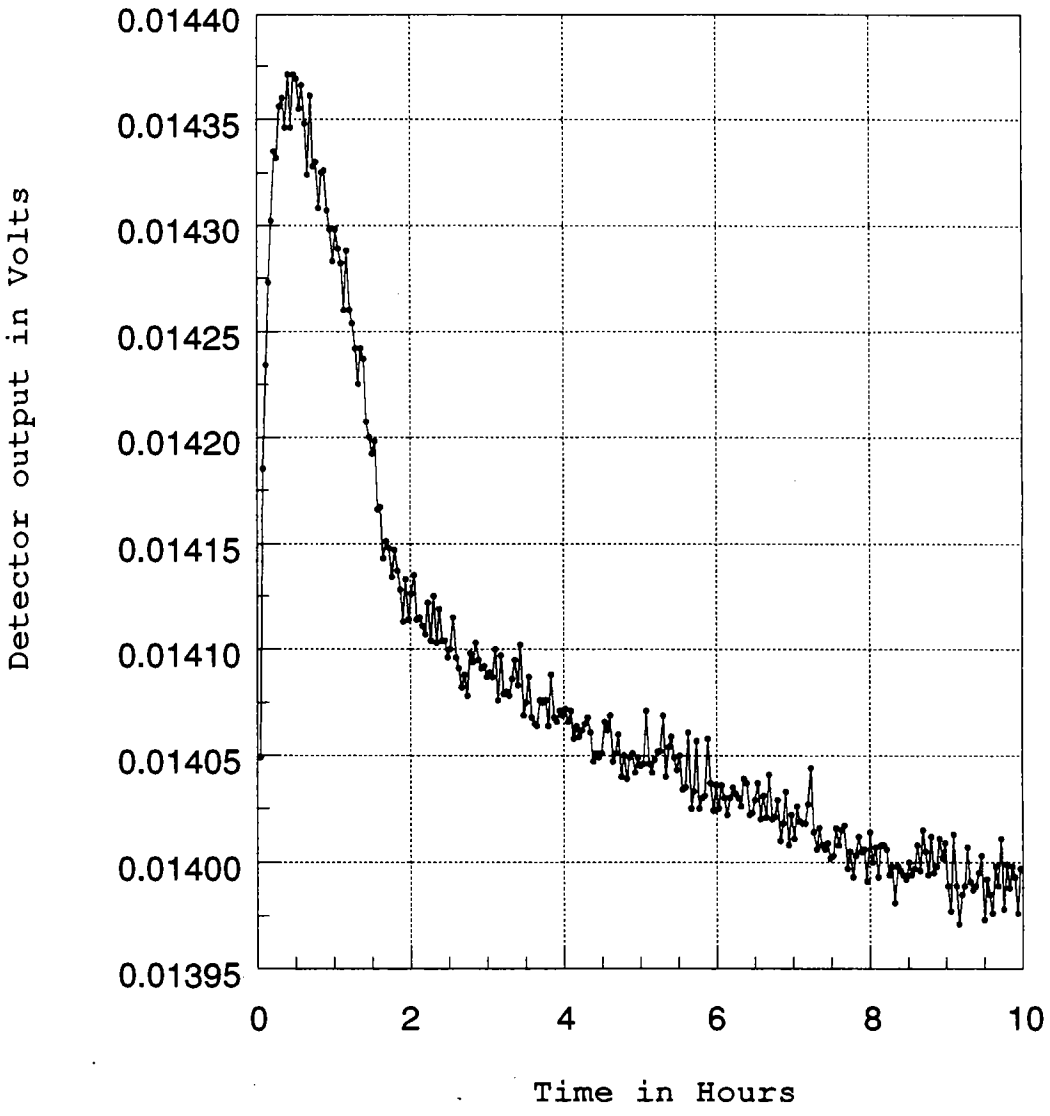

Figure 2.18 Detector output vs. Time

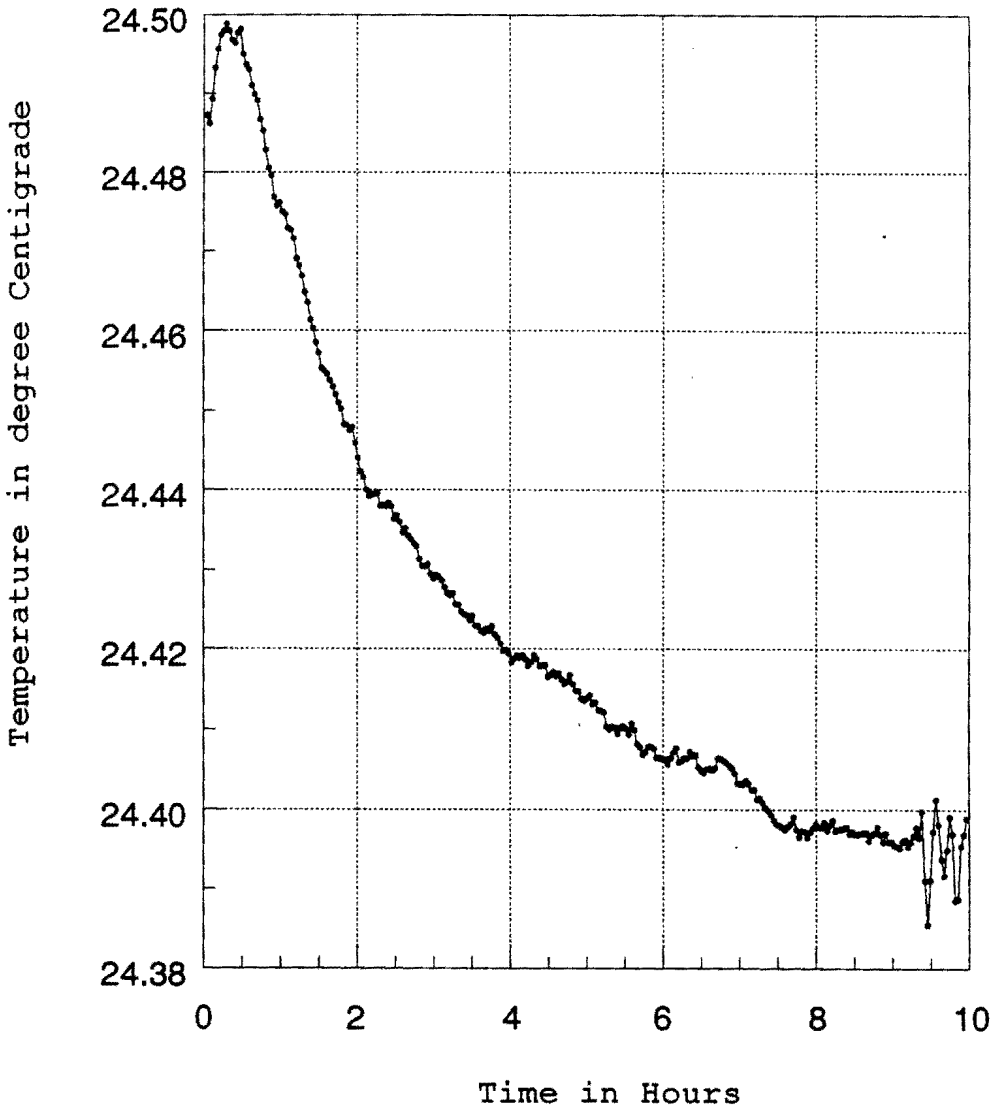

Figure 2.19 Temperature vs. Time

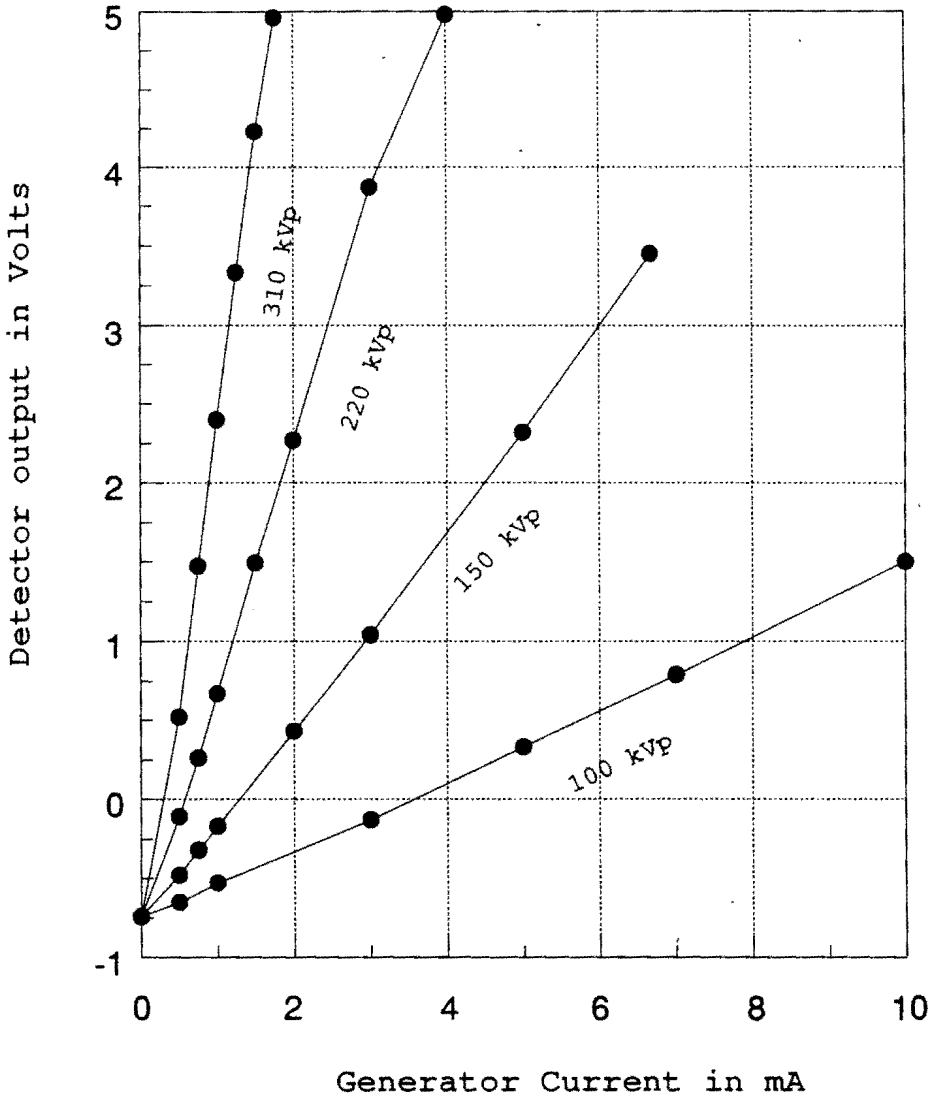

Figure 2.20 Response of NaI based detector to X-ray radiation

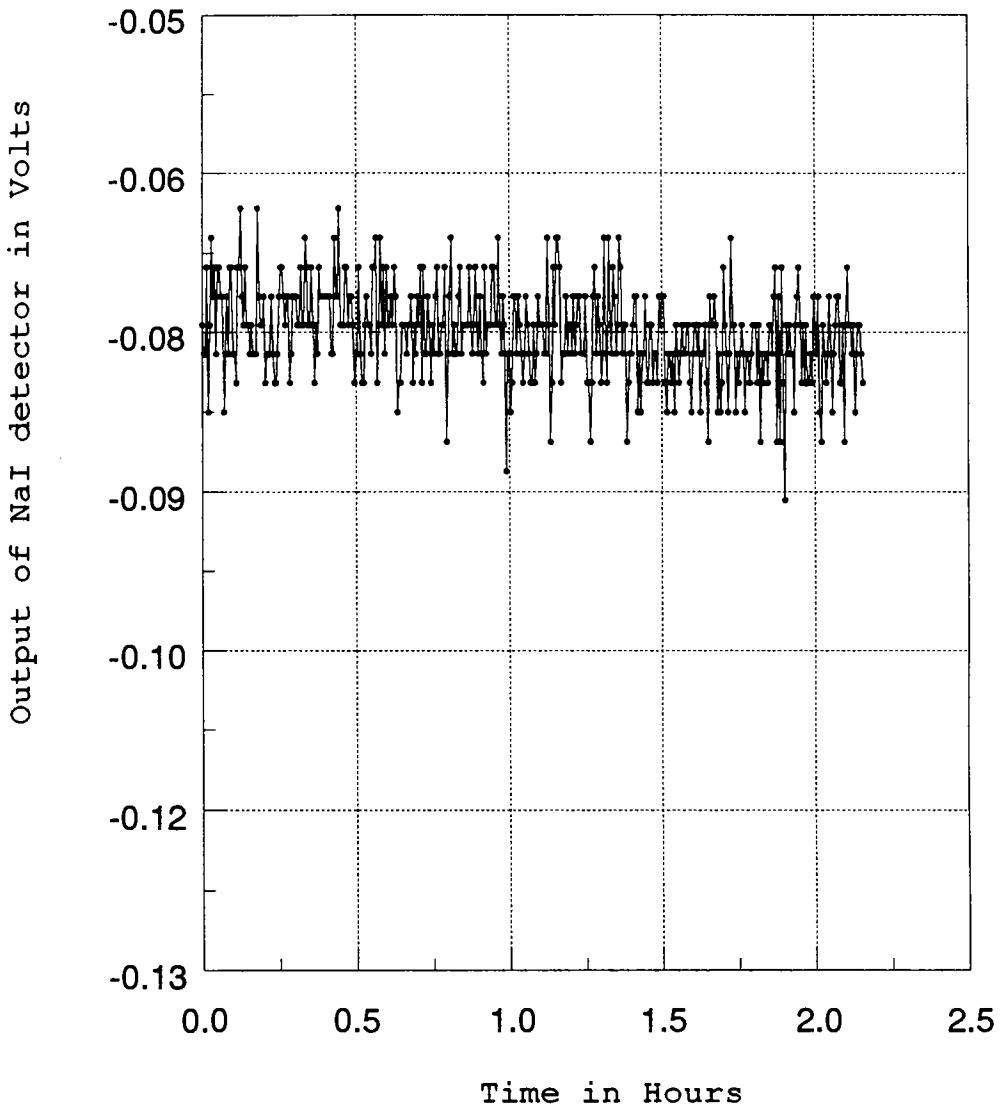

Figure 2.21 NaI detector output vs. Time

shielded cable. The calculated Johnson noise of the photodiode reflected at the output is around 12 millivolts(p-p). A value of 12 mV (p-p) was observed using an oscilloscope at the output of the detector. From the graph of Figure 2.21, a peak-to-peak noise value of 16 mV is observed. The increase from the value of 12 mV is due to the cable connections and noise pickup by the output cable.

2.4.3.4 ***Integration capability*** In photon counting mode of operation of a detector, for obtaining good quality data, photons are counted for long durations of time. There is some such similar capability available in current mode detectors also. The output of the current mode detector is sampled and digitized using an A/D converter. Instead of taking a single sample and digitizing and noting it as the value, a number of samples can be digitized and averaged. By doing so, the random noise content in the output is minimized. Figure 2.22 shows a series of histograms with the X-ray generator turned off and Figure 2.23 shows a set a of histograms with the X-ray generator turned on. A software programmable gain of 8 was used in the data acquisition card while collecting the data for these histograms. As a result, the total peak-to-peak noise at the output of the detector will also get multiplied by a factor of 8. From these two figures, it can be seen that as the number of samples averaged is increased, the width of the histogram narrows demonstrating that the effect of noise is decreasing.

2.4.3.5 ***Speed of operation*** Speed of operation of a detector system is controlled by two factors.

- Afterglow
- Noise performance of the detector

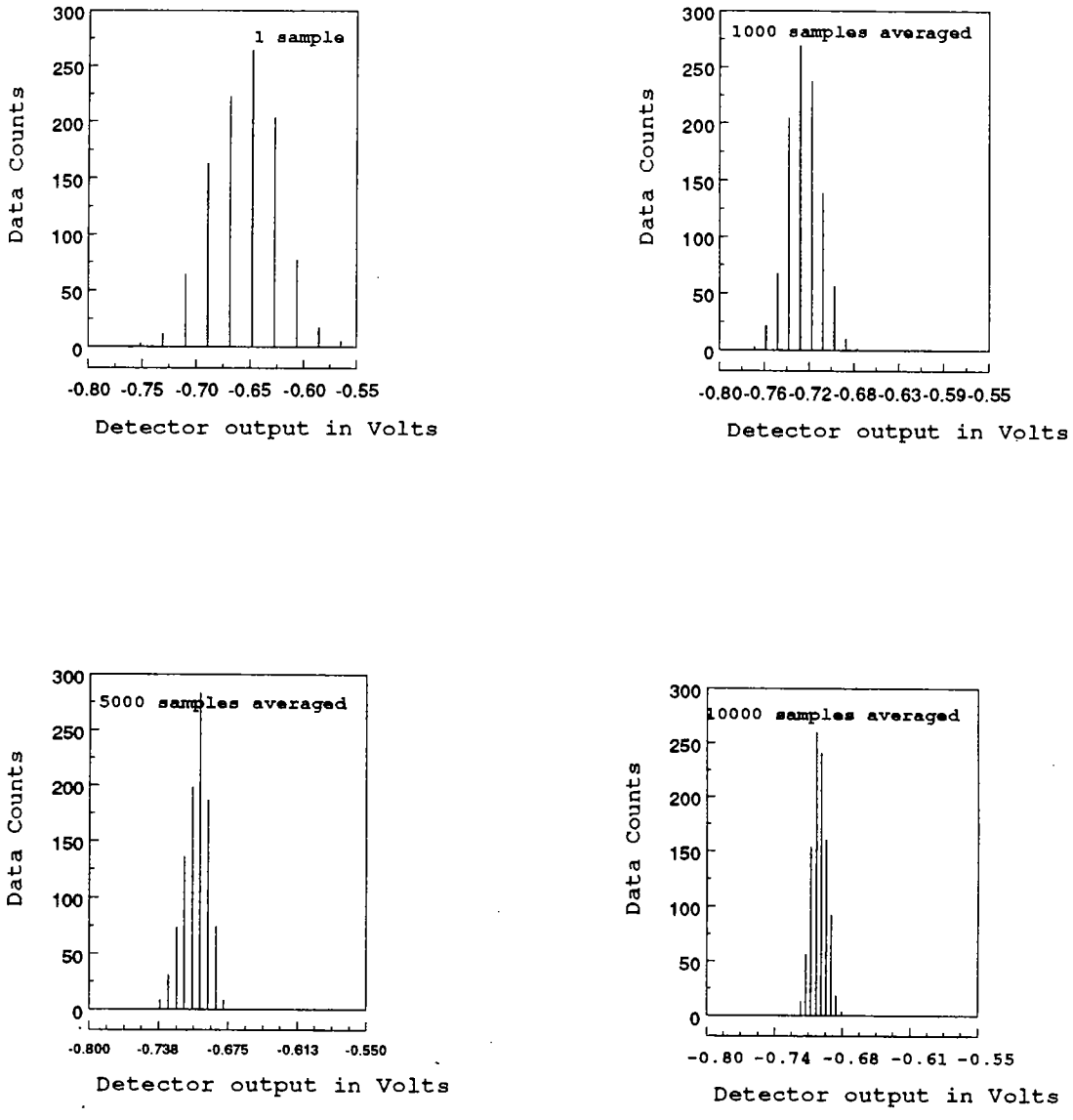

Figure 2.22 Histograms of NaI detector output (X-ray generator OFF)

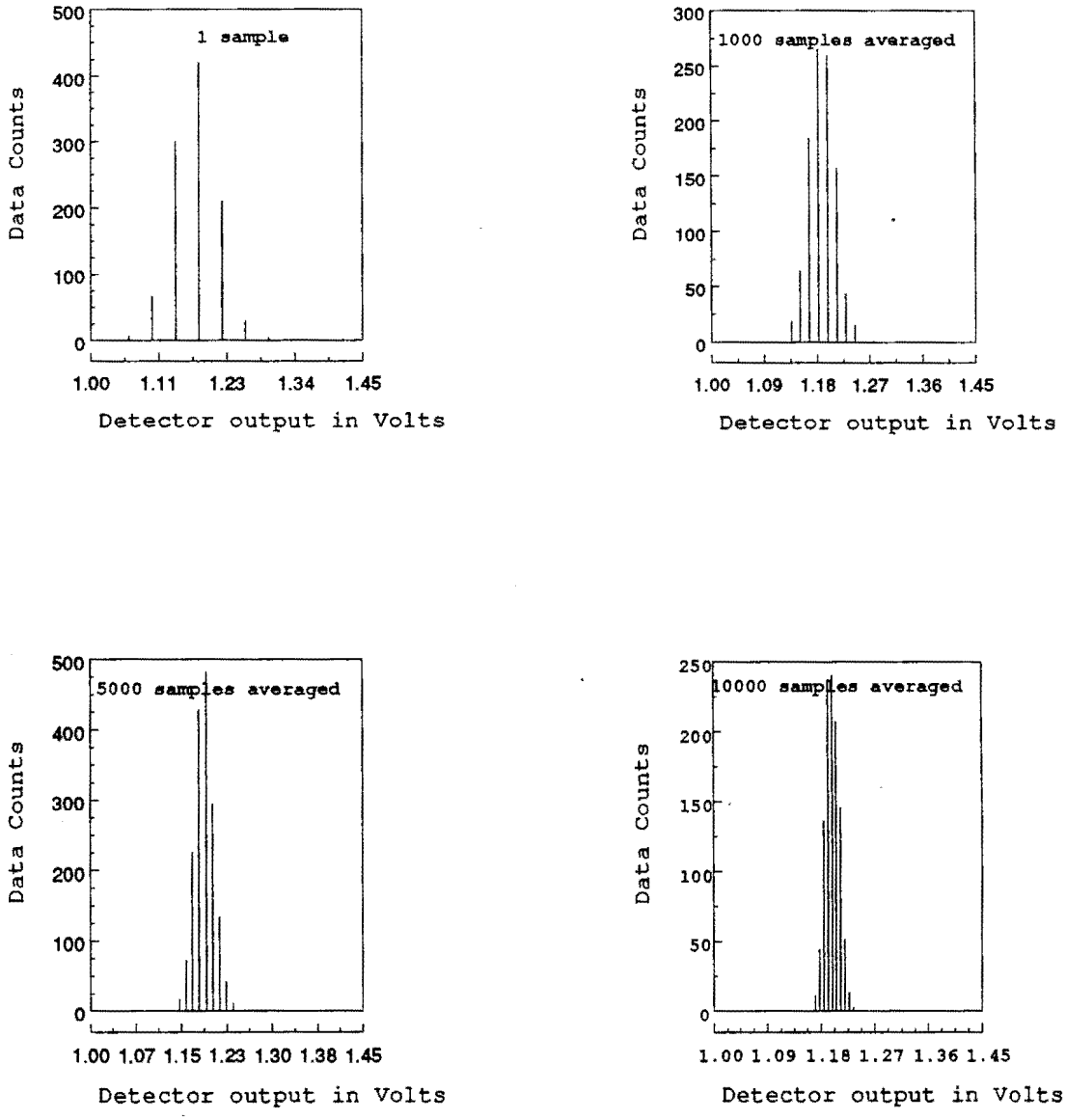

Figure 2.23 Histograms of NaI detector output (X-ray generator ON)

If the afterglow is high, the detector cannot be used at high speeds due to reasons explained in section 2.3.2. Typical values of afterglow for NaI and CsI are 0.3-5%/ms and .1-.8%/6 ms [22].

To obtain good quality data, a number of samples might have to be digitized and averaged at each point to reduce the effect of noise. If the noise performance of the detector is good, this number may not be too high and so we can operate the detector at high speeds. From Figure 2.22 and Figure 2.23, it can be seen that for NaI detector, digitizing and averaging 5000 samples at each point provides a compromise between good quality data and data acquisition time.

2.4.3.6 Dynamic range of the detector The dynamic range of a detector is determined by how wide a range of input signal that the detector can handle and how fine a variation in incident flux that the detector can distinguish. For the detector system developed as part of the project, the input signal range that can be handled is determined by

- The incident flux range that the detector material can convert before it saturates
- The incident light range that the photodiode can convert before it saturates
- The input current range that the instrumentation can handle before it saturates
- The noise characteristics of the detector system

From Figure 2.20, it can be seen that the detector with a collimator of 0.025" diameter and source to detector distance of 48" is capable of measuring incident flux over most of the entire range of the X-ray generator (IRT320 X-ray generator, which has the maximum capacity among the generators that are available at Center for NDE, was used for this test). To modify the performance of the detector in this regard, a number of parameters like the collimator size, source to detector distance, and scale factor resistance value could be

changed to obtain the required performance. As for the total range that the photodiode can convert, we do not have concrete and relevant information. However, the instrumentation can handle an input current range of 100 fA to .13nA before the output saturates. If the same detector needs to be used for measuring higher flux intensities, the scale factor of the entire instrumentation could be decreased so as to handle higher flux intensities.

Table 2.2 shows the statistics of data collected under various conditions. From this table, for unity gain in the software programmable gain amplifier, and 5000 samples averaged with the X-ray generator turned off, and for the output range of 10 V of the detector, the dynamic range of the detector with a confidence level of 3σ is 3333 : 1. This is the best possible range from the detector because, the X-ray generator is turned off and the software programmable gain is unity. With the X-ray generator turned on and a software programmable gain of 8 and 5000 samples averaged per point, the dynamic range with a confidence level of 3σ is 208 : 1. This is the worst dynamic range possible from the detector as the X-ray generator is turned on, and a software programmable gain of 8 is used. This means that the noise will also get multiplied by a factor of 8 and hence the worst case.

With the prototype detector system, the next step is to use the detector in a digital radiography and computed tomography system.

Table 2.2 Estimation of noise for NaI based detector

X-ray Gen.	Software programmable gain	Number of samples averaged	Standard deviation (σ)
OFF	1	1	0.0026
		5000	0.001
	8	1	0.030
		5000	0.010
ON	1	1	0.005
		5000	0.002
	8	1	0.032
		5000	0.016

3. DIGITAL RADIOGRAPHY AND COMPUTED TOMOGRAPHY USING CURRENT MODE DETECTORS

Digital radiography and Computed tomography are two basic inspection techniques followed in the field of X-ray based nondestructive evaluation. As the name suggests, digital radiography is a radiograph of an object (interchangeably called sample in this thesis) in digital form instead of the conventional film radiograph. Computed tomography is also digital, but it provides information about the cross section of the sample. For viewing two dimensional projection image of samples, a digital radiography system is used and for viewing cross sections of samples, a computed tomography system is used.

Tomography refers to the cross-sectional imaging of an object from either transmission or reflection data collected by illuminating the object from many different directions. Fundamentally, tomographic imaging deals with reconstructing an image from its projections. In the strict sense of the word, a projection at a given angle is the integral of the image in the direction specified by that angle, as illustrated by Figure 3.1. However, in a loose sense, projection means the information derived from the transmitted energies, when an object is illuminated from a particular angle. In this project, the current mode point detector described in chapter 2 is used to collect projection data and then the cross section image is reconstructed using the software provided in [24]. Reference [25] provides an indepth discussion about computed tomography and various reconstruction techniques.

The current mode detector that was described in chapter 2 is a point detector. In this chapter, the versatility of the detector described in chapter 2 will be demonstrated by using it

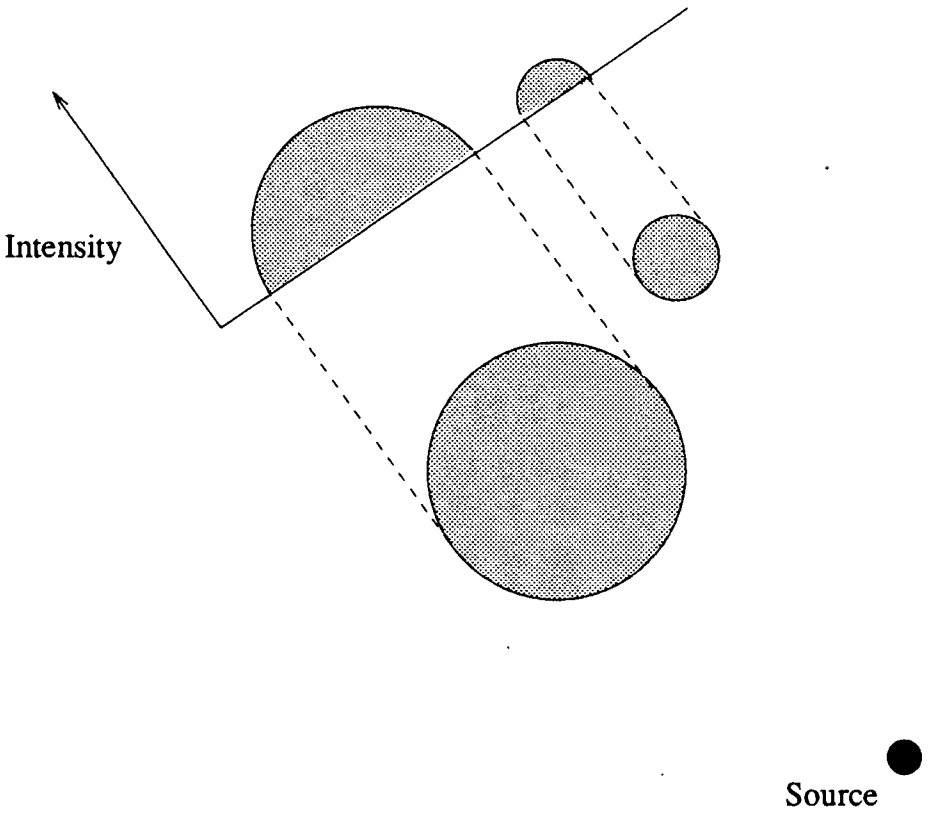

Figure 3.1 One projection of an object consisting of a pair of cylinders

in a digital radiography system and computed tomography system for evaluating samples made of a wide range of materials. The chapter begins with an explanation of the data acquisition system setup used for digital radiography and computed tomography systems. This is followed by a discussion of the performance and results obtained from the digital radiography and computed tomography system.

3.1 System setup

Figure 3.2 shows the block diagram of the system setup for the digital radiography and computed tomography system. The setup for a digital radiography system or a computed tomography system consists of a fixed position X-ray source (IRT320 X-ray generator), and a fixed position point detector (developed as part of this research work) with a pencil beam of X-ray radiation (Refer Figure 1.3). In between the source and the detector is a five-axes sample positioner(From DAEDAL Inc.) which can move the sample through the pencil beam in any of the given five axes. A PC based multifunction data acquisition board (Analogic DAS12/50) is used for data acquisition.

Due to lack of available free slots and also due to the requirements of other projects, the controllers for the five-axes sample positioners are distributed among two PCs. From Figure 3.2, it can be seen that the multifunction data acquisition card and the controllers for the three axes X,Y and Z are installed on PC1. The controllers for the other two axes, θ and ϕ, are installed on PC2. The two PCs are connected to each other and to Internet through ethernet network interface. The PCs run MS-Windows version 3.1 operating system.

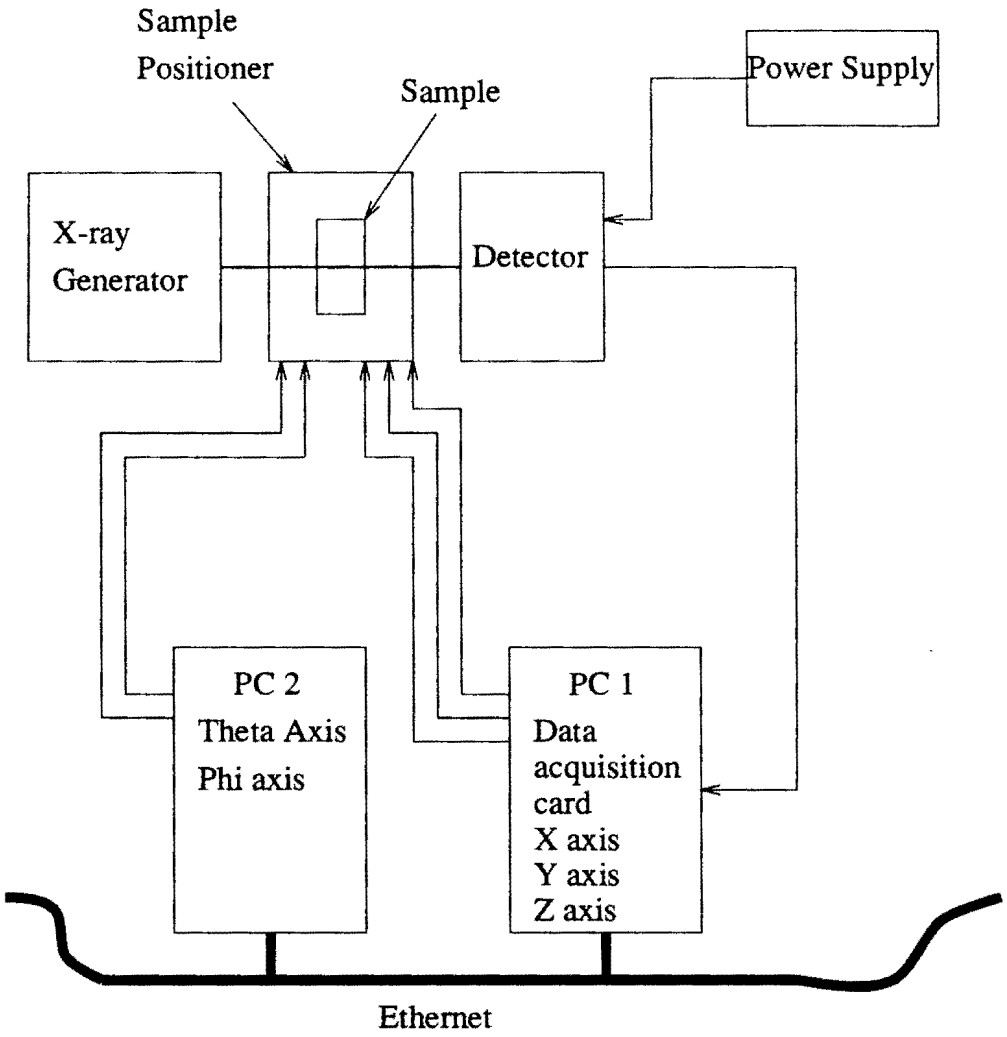

Figure 3.2 System setup for digital radiography and computed tomography

3.1.1 Distributed control for sample positioners

As will be seen subsequently in section 3.4, a digital radiography system will require the movement of the sample in the Y and Z axes. The controllers for Y and Z axes are available on PC1. For a computed tomography system, sample movement is required in Y and θ axes. This requires distributed control of the motion control hardware on PC2 from PC1. To achieve this, a network software was designed and developed based on client server architecture and TCP/IP protocol.

Figure 3.2 shows the two systems connected through an ethernet interface. An iterative server software was designed and developed using Windows Socket Library and the server is run on PC2 (to control θ and ϕ axes). Reference [26] provides complete details about the Windows Socket interface implementation. Figure 3.3 shows the flow chart for the server software and Appendix D provides the source code for the server. A data packet format as shown in Appendix D was decided upon for communication of commands and results between the two PCs. The client software is run on PC1. Whenever the θ or ϕ axes need to be controlled, the client software encodes the command in a packet according to the format defined in Appendix D, and transmits the packet across the network to the server(PC2). The server extracts the command and arguments from the packet, executes the command on the local motion control hardware and sends back the result to the client.

3.1.2 Data acquisition card

The main part of the data acquisition setup is the PC based multifunction data acquisition card. Reference [27] provides a complete description and programming details for the data acquisition card. It consists of analog to digital converters, programmable interval

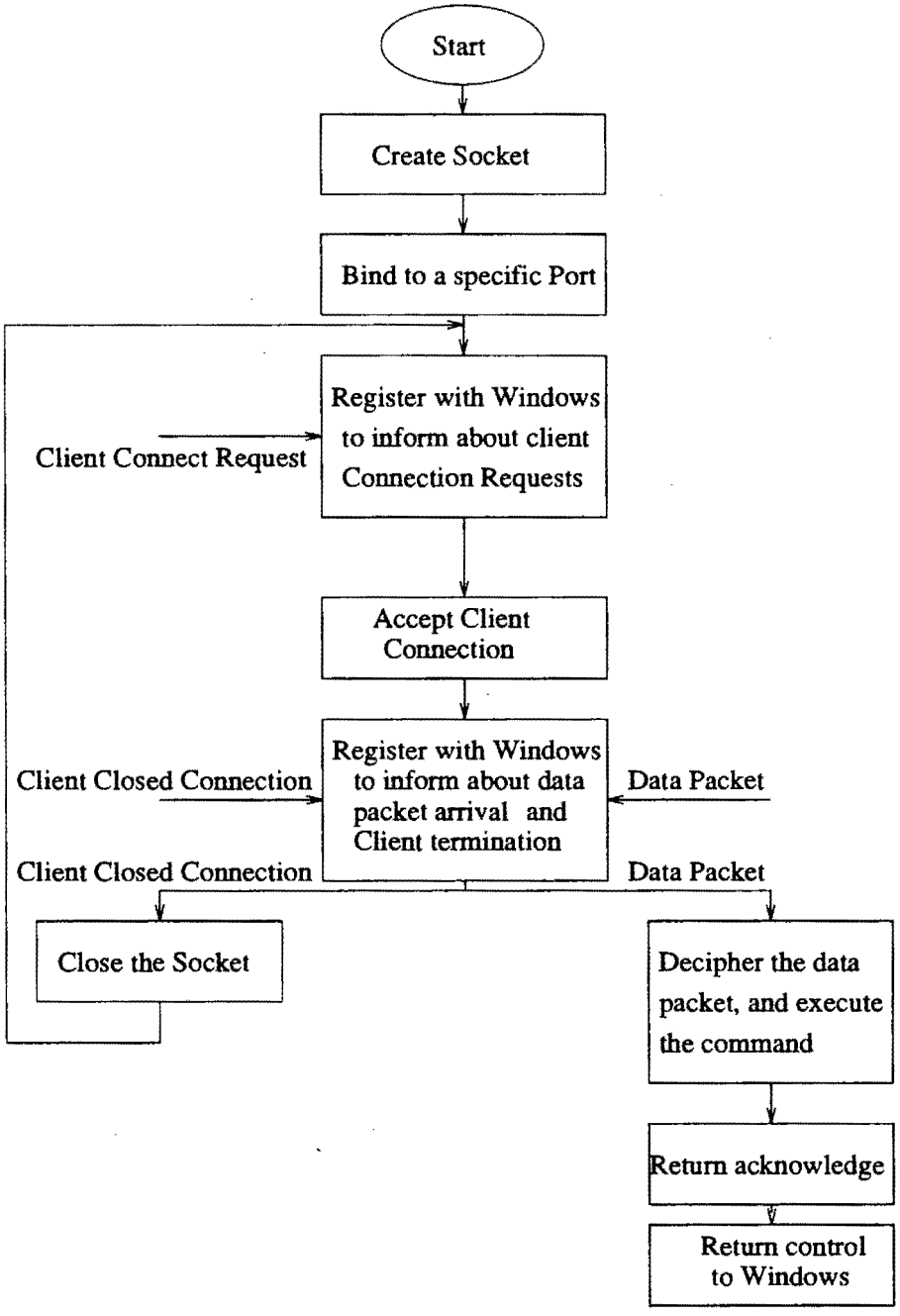

Figure 3.3 Flow chart of a Windows based non blocking server

timers, digital to analog converters, and parallel digital input/output lines. The analog to digital converter has a 12 bit range. The most important specification that is of interest to us is the conversion time of the A/D converter. From [27], it is to be noted that the conversion time of the A/D converter is 20 μs. For acquiring 5000 samples, it will take 100 ms. This value of 5000 samples was decided based on the histograms in Figure 2.22, Figure 2.23, and desired speed of operation of the system.

3.1.2.1 ***Reasons for choosing a 12 bit analog to digital converter*** From Figure 2.21 it can be seen that the peak-to-peak noise voltage at the output is 16 mV. For a 10 V input range and 12 bit digitization, single bit corresponds to 2.44 mV. So the total peak-to-peak noise will correspond to 8 least significant bit errors. For a 10 V input range and 16 bit digitization, each bit will correspond to 0.15 mV and the total peak-to-peak noise will correspond to 131 least significant bit errors. This was the reason for choosing a 12 bit analog to digital converter with an input range of 10 V.

3.2 Scans for digital radiography and computed tomography

There are two types of scans performed in a digital radiography system. They are the one dimensional scan (commonly referred to as 1D scan) and the two dimensional scan (commonly referred to as 2D scan). Appendix E provides the source code listing of the software that was developed for performing 1D, 2D and tomo scan using the current mode detector described in this thesis.

3.2.1 1D scan

Figure 3.4 shows the setup for a 1D, 2D and tomo scan. The one dimensional scan can be performed on any of the available linear axes. The most commonly used axis for one dimensional scan is the Y axis. The procedure for a one dimensional scan is as follows. The sample is set in the desired initial position. Using the detector, data is collected and stored. The sample is moved by one step and the data acquisition is repeated again. This is continued till a given total distance is traversed.

3.2.2 2D scan

The two dimensional scan is similar to one dimensional scan with the addition of one more axis, usually the Z axis. Figure 3.4 shows the setup for a two dimensional scan. The procedure is similar to one dimensional scan in the sense that after a one dimensional scan is performed, the sample is moved in the Z axis and the one dimensional scan is performed again.

3.2.3 Tomo scan

The motion control for tomoscan is the same as a two dimensional scan with the exception that a rotational axis (θ) is used instead of the linear axis (Z). Figure 3.4 shows the setup for a tomoscan. It is common to move the rotational axis through a total of 180° in order to yield a complete set of projection data. Reference [24] provides a reconstruction software that could be used to reconstruct the images from the scan data.

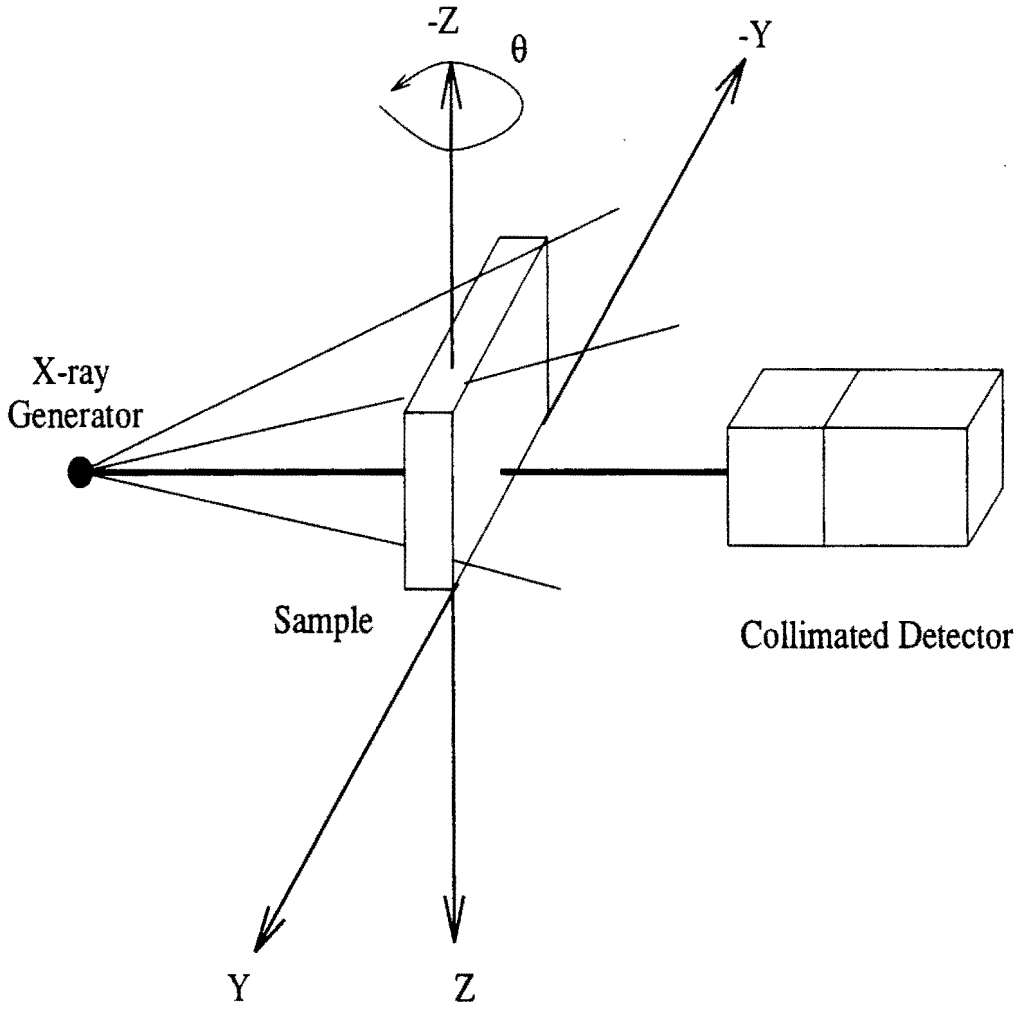

Figure 3.4 Setup for 1D scan, 2D scan, and tomo scan

3.3 Results and performance of digital radiography and computed tomography system

Figures 3.5 to 3.13 show different images obtained using the digital radiography and computed tomography system designed and developed as part of this research work. To evaluate the performance of these systems, a discussion of the following parameters are essential.

- Spatial resolution
- Contrast resolution
- Dynamic range of the system
- Speed of operation

3.3.1 Spatial resolution

Spatial resolution of a system is characterized by how fine a point in the sample can be resolved by the system. This depends primarily on the size of the collimator used. But, the size of the collimator that can be used depends on the detector performance and its noise characteristics. The detector should be capable of producing sufficiently strong signals with a given collimator. The prototype system was evaluated with a .025" (635 micron) diameter collimator. The collimator size can easily be decreased given the range that the detector can handle, but problems of mechanical alignment with the existing setup is a deterring factor.

There are standard samples available in the field of nondestructive evaluation for evaluating the spatial resolution of a system. The resolution gauge is one these. Figure 3.5 shows the two dimensional image of the resolution gauge obtained using the digital radiography system described above. From the figure, it can be noted that up to 2.5 line pairs per

Figure 3.5 Two dimensional image of resolution gauge
(Scan duration = 10.33 hrs)

Figure 3.6 Two dimensional image of 150 micron tungsten wire stuck over 1" titanium block

WAVE 0

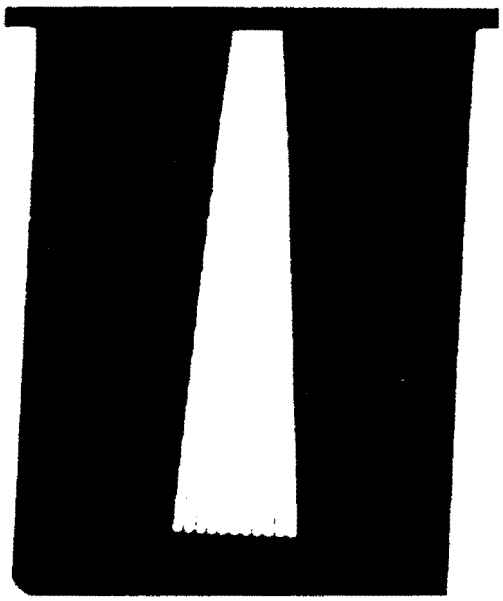

WAVE 1

Figure 3.7 Two dimensional image of 0.02" thick penetrameter
(Scan duration = 4 hrs)

Figure 3.8 Two dimensional image of an aircraft turbine blade
(Scan duration = 4 hrs)

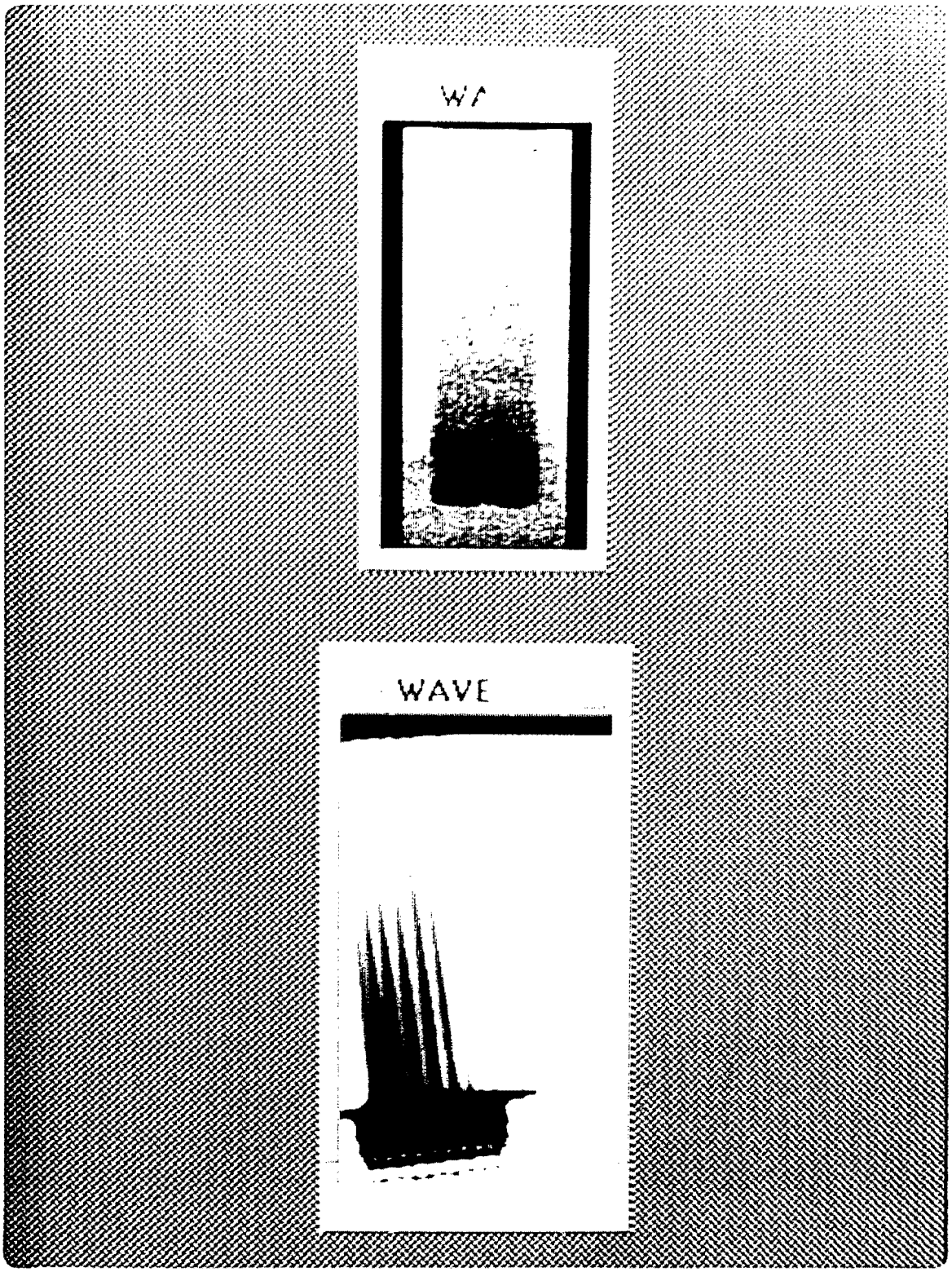
WAVE

Figure 3.9 Tomo scan image of a circular aluminum block of diameter 1", with holes of diameter 4.5 mm, 3mm, and 3mm drilled in it

Figure 3.10 Tomo scan image of a square aluminum block with 1mm holes drilled in it

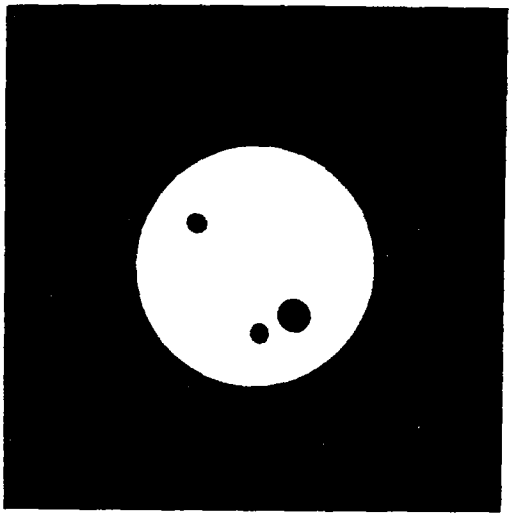

WAVE 2

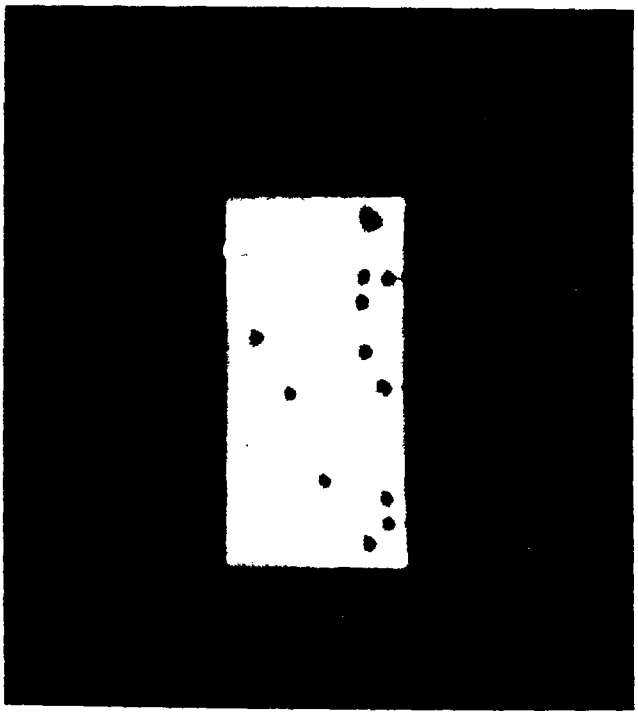

Figure 3.11 Tomo scan image of a piece of rock containing uranium ore

Figure 3.12 Tomo scan image of a vial of diameter 1" containing dirt sample

WAVE 2

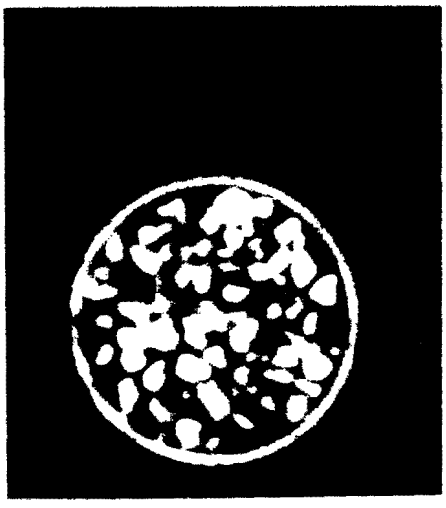

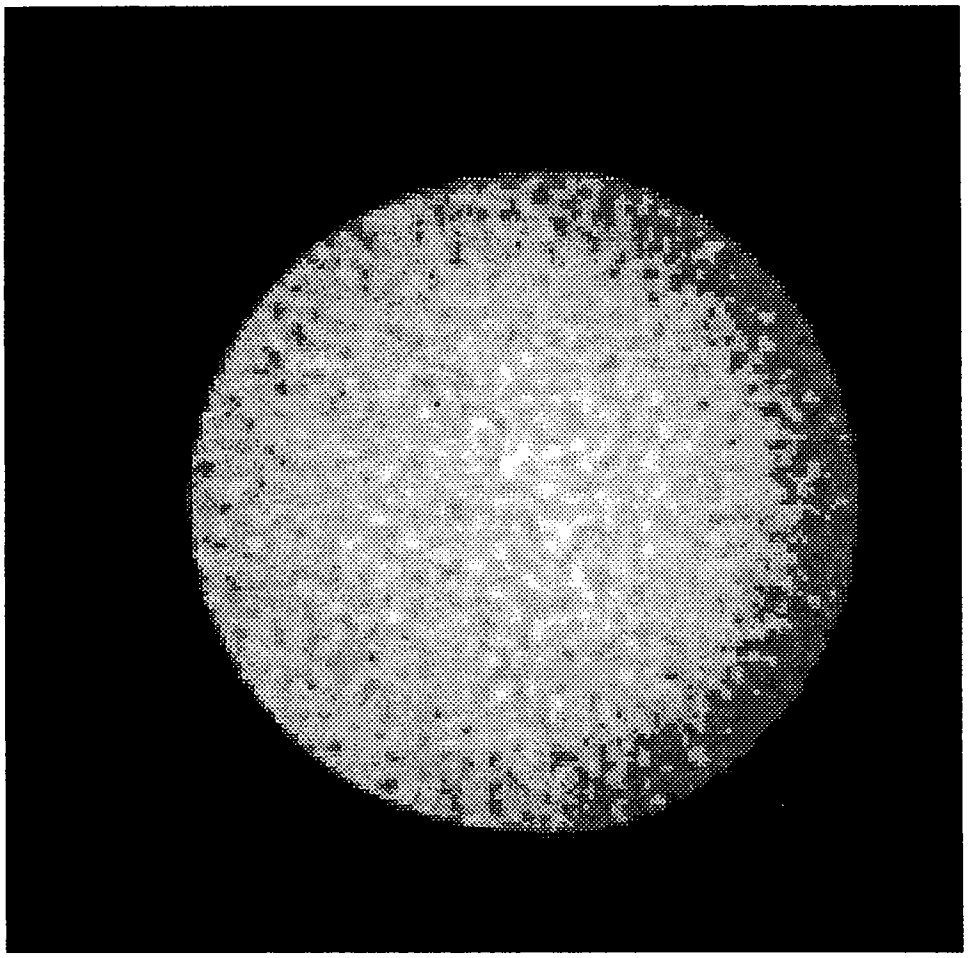

Figure 3.13 Tomo scan image of a ceramic sample demonstrating the density gradient

millimeter can be resolved easily. This will improve further if the collimator size is decreased. Existing digital radiography systems operating using current mode detectors provide a spatial resolution of approximately 1 line pair per millimeter. Thus, we have gained a lot in terms of spatial resolution compared to existing current mode detectors in the industry today.

Figure 3.6 shows the two dimensional image of a piece of tungsten wire of diameter 6 mils (152 microns) stuck over a block of nickel of 1" thickness. The two materials have different densities and as a result, different attenuation coefficients and the detector should have a wide dynamic range to handle such samples. In addition, the thickness of the tungsten wire is so small that the spatial resolution of the system has to be very good to detect the tungsten wire. The scan was performed using a .025" collimator and after aligning the detector with the generator, the alignment was slightly offset to get finer collimation. From Figure 3.6, it can be seen that the detector system is capable of handling such samples and it demonstrates the capabilities of the system in terms of spatial resolution and dynamic range.

3.3.2 Contrast resolution

The contrast resolution of a system is characterized by the percentage size of flaw that can be detected in a homogenous material. There are standard samples available to evaluate the contrast resolution of a system. The two dimensional image of one such sample, called the penetrameter is shown in Figure 3.7. It shows a number 20 penetrameter attached on to an aluminum block of 1" thickness. From the image in Figure 3.7, the penetrameter can be easily seen. This means that the system is able to distinguish a 1.02" thick aluminum from 1" thick aluminum. This corresponds to a contrast resolution of 2%.

3.3.3 Dynamic range of the system

Dynamic range of a system is determined by how wide an input signal swing that can be handled with how fine a step that could be measured. This is determined by the noise characteristics of the system and the data acquisition system. The noise characteristics of the system was discussed in chapter 2. As for the data acquisition system, it is a 12 bit conversion with input ranges of -5 to +5 V or -10 to +10 V. These are user set and this can be changed according to the type of the sample to be evaluated. From Figure 2.20, it can be seen that the detector can handle most of the range of the IRT X-ray generator (maximum of 320 kVp and 10 mA) with a -5V to +5V input range and 12 bit digitization. Figure 3.8 shows the two dimensional scan image of an aircraft turbine blade made of nickel. In order to produce usable signal from the detector when scanning the part of the sample of 0.6" thickness, the X-ray flux intensity has to be high. At the same time, the flux intensity will be very high for other parts of the sample and as a result, the detector will saturate if the dynamic range is not sufficient. In Figure 3.8, the entire sample can be seen easily, demonstrating the wide dynamic range of the system.

3.3.4 Speed of operation

Speed of operation of digital radiography or computed tomography system is one of the benefits gained by the system developed in this research work. The time taken to perform the two dimensional scan on the aircraft turbine blade shown in Figure 3.8 is 2.7 hours and the total number of scan points is 9600 (5000 samples averaged per point). This corresponds to a scan time of about a second per point. For a digital radiography system using a germanium detector in photon counting mode of operation, a scan time of 15 seconds is ob-

served per point. Thus, an improvement of at least 15 times in speed of operation is achieved by the system developed as part of the research work.

The conversion time of the analog to digital converter is 20 μs per sample. To collect 5000 samples, 10ms is spent in data acquisition. From the observation of scan times, it can be easily seen that the remaining 900 ms per point is spent in the movement of the sample. This is due to the finite acceleration and deceleration time of the motors in the sample positioner.

In addition to the performance benefits obtained in terms of speed of operation and spatial resolution, the system developed is compact and costs much less than a germanium detector system. The detector operates at room temperature which is another performance benefit.

3.3.5 Versatility of the detector

Figure 3.9 shows a tomo scan image of a circular aluminum block of diameter 1", with holes of diameters 4.5 mm, 3 mm and 3 mm drilled in it. Figure 3.10 shows the cross sectional image from a tomo scan of a square block of aluminum (1" x 0.5" x 0.5") with one mm diameter holes drilled in it. The white speck at the top left corner of this image is a piece of screw driver bit (higher density and as a result higher attenuation compared to aluminum)that got stuck inside one of the holes. Figure 3.11 shows the cross sectional view of a piece of rock containing uranium ore. The white traces in the image correspond to the uranium ore in the rock. Figure 3.12 shows the tomo scan image of a vial of diameter 1", containing dirt (loosely packed small rock pieces). Figure 3.13 shows the tomo scan image of a ceramic sample which is made of dry pressed alumina. From the figure, a density variation

across the ceramic sample can be easily seen. In addition to the density variation, small white spots are seen throughout the cross section. These could be conglomerates of alumina formed due to some chemical phenomena. The X-ray generator was run at 280 kVp and 4.17 mA for this tomo scan. All these images demonstrate the versatility of the system in evaluating samples made of different materials, dynamic range of the system, its spatial and contrast resolution.

All the tomography images discussed so far, are reconstructed using a back projection reconstruction algorithm provided in reference [24]. A filter is also used to smooth the image and this filter is part of the reconstruction algorithm provided in reference [24].

4. CONCLUSIONS AND FUTURE WORK

The research work described in this thesis was motivated by some of the requirements in the field of X-ray based nondestructive testing and the limitations of existing systems in meeting these requirements.

4.1 Conclusions

As part of this research work, a low noise current sensing instrumentation was designed and developed that could be used in a current mode X-ray detector system. The instrumentation has an observed peak to peak noise of 12 mV (20 Hz bandwidth) at the output and the scale factor of the instrumentation is 10^{11}. The instrumentation was coupled to a CdZnTe crystal for evaluating the performance of the crystal in current mode. Strong dependence of dark current on temperature was observed and an unacceptable level of afterglow made it infeasible to use CdZnTe for our purposes. Detectors based on scintillating crystals like sodium iodide were evaluated. To convert the light output from these crystals into a usable current signal, a photodiode based front end module was developed. The detector has very low dependence of dark current on temperature and extremely low afterglow. The detector assembly based on sodium iodide was used in digital radiography and computed tomography systems. To implement these systems, a networking based software solution for distributed hardware control was proposed and implemented. The prototype system has a spatial resolution of 2.5 lp/mm with a 0.025" diameter collimator. The system is able to resolve at least up to 2 % of contrast sensitivity. It has a maximum output range of -10V to +10V with 12 bit digitization and the system does not saturate for most of the available flux range of the X-ray generator presently available here at CNDE (IRT320 X-ray generator

with a maximum 320kVp and 10 mA). The system has much better dynamic range compared to an image intensifier based (coupled to a CCD camera) system. It is at least 15 times faster in data acquisition as compared to a germanium detector based system (photon counting mode) present here at the center for NDE. The detector assembly is compact and low in cost. The system is versatile in that it was tested with samples made of different materials. The system operates at room temperature.

In toto, the research work encompassed understanding the physical and operational properties of some of the X-ray detecting materials, design of digital radiography and computed tomography systems using these detector materials, engineering and implementing the design, and evaluating the performance of the system that was implemented. The design and development phase consisted of low noise electronic circuits design and development, design, development and implementation of data acquisition software, network based distributed control software and other utility software modules. The engineering phase consisted of integrating the various hardware and software modules together into a working digital radiography and computed tomography system. The evaluation phase concluded the thesis by measuring various performance characteristics of the system.

To conclude, the highlights of the digital radiography and computed tomography system designed and developed as part of this research work are

- Higher spatial resolution compared to existing current mode systems in the industry today.
- Higher speed of operation compared to photon counting mode systems.
- Comparable contrast resolution with existing systems.
- Low cost.

- Compact size.
- Better dynamic range compared to image intensifier based systems.
- Easy adaptability to different kinds of X-ray detecting materials.
- Room temperature operation.

4.2 Future work

The digital radiography and computed tomography system developed in this thesis was based on a point detector. Design and development of an array detector based on the principles discussed in this thesis is a natural follow up of this work. As part of this thesis, the noise characteristics of the instrumentation used for sensing the current signal were discussed and quantified. It was also concluded that the performance of the front end system involved in converting X-rays to current will dominate the noise characteristics of the entire system. It will be interesting to evaluate this factor as this will provide an indication as to where to concentrate during the development of an array detector. It will also quantify the performance limits of the system more accurately.

The prototype system presently available has a limitation in terms of the size of collimator that can be used. This is due to mechanical alignment problems of the generator with the detector collimator. Better techniques for collimating and aligning the detector could be implemented. If the source is also collimated, noise introduced in the image due to scattered X-rays from other parts of the sample could be reduced.

For digital radiography and computed tomography, the point detector has to be moved across the sample and data collected. There is a possibility of the X-ray beam inten-

sity varying with time and this will introduce error in the data collected. This could be corrected by using a "beam monitor" (another detector assembly to monitor the beam fluctuations).

From an observation of the scans performed using this system, it was noted that about 800 ms of time is spent in moving the sample from one point to another. This is due to the finite acceleration and deceleration time of the motors in the sample positioner. To avoid this and to improve the speed of the system, a real-time continuous scan technique could be used. In this, the sample should not be stopped at each point for data acquisition. Instead, it should be moved in a continuous fashion at a constant velocity, with data collection triggered by real-time interrupts. This is based on the fact that precise points in time will correspond to precise points in space, if the velocity of movement is constant. But such a system will introduce a blur in the image due to linear motion. So, the images have to be deblurred.

BIBLIOGRAPHY

1. Review of progress in Quantitative Nondestructive Evaluation, Series, Edited by Donald O. Thompson and Dale E. Chimenti, Plenum press, New York

2. Nondestructive Testing Handbook - Volume 3, Radiography and Radiation testing, American Society for Nondestructive Testing , U.S.A. (1985)

3. W. Bencivelli, et al., Evaluation of elemental and compound semiconductors for X-ray digital radiography, Nuclear Instruments and Methods in Physics Research, A310 (1991), 210-214

4. R.L Heath, R. Hofstadter and E.B. Hughes, Inorganic Scintillators. A ,Review of Techniques and Applications, Nuclear Instruments and Methods 162 (1979), 431-476

5. Engineering staff of Analog Devices, Inc., Analog-Digital conversion Handbook, Third edition, Prentice Hall, Englewood Cliffs, NJ (1986)

6. 1992 Amplifier Reference Manual, Analog Devices, Norwood, MA (1992)

7. Jack F. Butler et al., Gamma and X-ray detectors manufactured from Cd1-xZnxTe grown by a high pressure Bridgman method, Aurora Technologies Corp., San Diego, CA

8. J.F. Butler, F.P. Doty and C. Lingren, Recent developments in CdZnTe gamma ray detector technology, SPIE 1992 International Symposium, July 1992, San Diego, California

9. J.F. Butler, C.L. Lingren and F.P. Doty, $Cd_{1-x}Zn_xTe$ gamma ray detectors, Proceedings SPIE 1734, (1992), 131

10. G. Baldazzi et al., An evaluation of the possible use of CdTe microdetectors for astrophysical, biomedical and industrial imaging, Nuclear Instruments and Methods in Physics Research A322 (1992) 644-650

11. J.F. Butler et al, Progress in $Cd_{1-x}Zn_xTe$ radiation detectors, Preprint, MRS-93 conference, April 12-16 (1993), San Fransisco, CA

12. Raulf Polichar, Richard Schirato, and John Reed, Applications of monolithic CdZnTe linear solid state ionization detectors for X-ray imaging, X-ray Detector Physics and Applications (1992) SPIE Vol. 1736, 43-53

13. G. Entine, M.R. Squillante, H.B. Serreze, Fast, High flux, Photovoltaic CdTe Detector, IEEE Transactions on Nuclear Science, Vol. NS-28, No. 1, Feb 1981,

558-562

14. M. Cuzin et al., Applications of CdTe detectors in X-ray imaging and metrology, X-ray Detector Physics and Applications II (1993) SPIE Vol. 2009, 192-202

15. W.J. McGann et al, A new solid-state detector for radiation-therapy imaging, Nuclear Instruments and Methods in Physics Research A299 (1990) 172-175

16. R.J. Fox and D.C Agouridis, CdTe photovoltaic gamma-ray dosimeter, Nuclear Instruments and Methods 157 (1978) 65-69

17. P.A. Glasow et al, Aspects of semiconductor current mode detectors for X-ray computed tomography, IEEE Transactions on Nuclear Science, Vol. NS-28, No. 1, Feb. (1981), 563-570

18. B.Jaduszliwer and C.M. Kahla, Current to Voltage amplifier with a high voltage isolated input, Rev. Sci. Instrum., Vol. 60, No. 6, (1989), 1197-1199

19. 1992 Amplifier Applications Guide, Analog Devices Inc., Norwood, MA (1992)

20. Harshaw/Filtrol Scintillation Phospor catalog, Harshaw Radiation Detectors, Harshaw/Filtrol partnership, Solon, Ohio (1984)

21. Elements of scintillation detection, Harshaw/Filtrol partnership, Solon, Ohio (1984)

22. Scintillation detectors: A reference guide, Harshaw scintillation detectors, Harshaw/Filtrol partnership, Solon, Ohio (1984)

23. 1990-91 Photodiodes Catalog, Hamamatsu, Bridgewater, NJ (1990-91)

24. Kini Vivekanand, M.S. Thesis, Iowa State University, Ames, (1994)

25. Avinash C. Kak, Malcolm Slaney, Principles of Computerized Tomographic Imaging, IEEE Press, New York, (1988)

26. Windows Sockets, Version 1.1, FTP Software, Inc., North Andover, MA (1993)

27. Analogic - DAS12/50 User's manual, Industrial Computer Source, San Diego, CA (1993)

28. Ralph Morrison, Grounding and Shielding Techniques in Instrumentation, Second edition, Wiley - Interscience Publication, New York, (1977)

29. Ralph Morrison, Instrumentation Fundamentals and Applications, Wiley - Interscience Publication, New York, (1984)

30. Edward F. Vance, Coupling to Shielded Cables, Wiley - Interscience Publication, New York, (1978)

31. Ralph Morrison, Noise and other Interferring Signals, Wiley - Interscience Publication, New York, (1992)

32. Wade D. Peterson, The VMEbus Handbook, VFEA International Trade Association, Scottsdale, AZ (1993)

33. Getting Started with your VME-AT2000 Software for MS-DOS, National Instruments, Austin TX (1993)

34. NI-VXI DOS reference manual, National Instruments, Austin, TX 78730, (1993)

35. NI-VXI C software reference manual for VME, National Instruments, Austin, TX , (1991)

36. IP-Precision ADC User manual, GreenSpring Computers, Menlo Park, CA (1993)

APPENDIX A. DEFINITION OF SPECIFICATIONS AND COMMONLY USED TERMS

The following provides an explanation of some of the more commonly used terms and specifications in this thesis. Reference [6] provides a complete explanation and further details of the following.

Common mode rejection

An ideal operational amplifier responds only to the difference voltage between inputs (e+ - e-) and produces no output for a common mode voltage, that is when both the inputs are at the same potential. However, due to slightly different gains between the inverting and non inverting inputs, there might be an output voltage even when both the inputs are at the same potential. If the output error voltage, due to a known magnitude of common mode voltage, is referred to the input (dividing by the closed loop gain), it reflects the equivalent common mode error voltage between the inputs. Common mode rejection ratio (CMRR) is defined as the ratio of common mode voltage to the resulting common mode error voltage. Common mode rejection is usually expressed logarithmically:

$$\text{CMR (in dB)} = 20 \log 10 \text{ (CMRR)}$$

Initial bias current

Bias current is defined as the current required at either input of an amplifier for infinite source impedance to drive the output to zero (assuming zero common mode voltage). For differential amplifiers, bias current is present at both the negative and positive input. All the specifications provided by Analog Devices as well as the bias current specification used

in this thesis pertain to the larger of the two, not the average.

Input impedance

Differential input impedance of voltage input amplifiers is defined as the impedance between the two input terminals at 25^{O} C, assuming that the error voltage is nulled or very near zero volts. Common mode impedance is defined as the impedance between each input and the power supply common, specified at 25^{O}C.

Input offset voltage

Offset voltage is defined as the voltage required at the input from zero source impedance to drive the output to zero; its magnitude is measured by closing the loop to establish a large fixed gain, measuring the amplified error at the output and dividing the measured value by the gain.

Input noise

Input voltage and current noise characteristics can be specified and analyzed the same way as offset voltage and bias current characteristics. In evaluating noise performance, bandwidth or period must be considered. Also, rms noise from different sources is summed as root of squares, rather than linear, addition. Depending on the amplifier design, noise may have differing characteristics as a function of frequency, being dominated by "1/f noise", resistor noise or junction noise, at various frequencies.

APPENDIX B. PRINCIPLES AND TECHNIQUES FOLLOWED IN THE DEVELOPMENT OF INSTRUMENTATION

Instrumentation development

In section 2.2.2, the design of instrumentation for very low current measurements was discussed. Although the design of the instrumentation and the circuit looks deceptively simple, development of this instrumentation and making it operational is very complicated. In the following, the various factors that need to be considered for the successful development and operation of the instrumentation are discussed. This is followed by the actual details that were followed in the development of prototype detector circuits.

The following section on development considerations is a summary of details provided in [6], [19], and [28-31].

Development considerations

There are a number of factors that need to be considered in the development of a low current measurement circuit. They are:

Layout and connection considerations The development of a very high impedance measurement system like the one discussed in this thesis, introduces a new level of problem associated with the reduction of leakage paths and noise pickup.

A primary consideration in high impedance system design and development is to place the amplifier as close to the signal as possible. This will minimize current leakage paths, noise pickup and capacitive loading.

The use of guarding techniques is essential to realizing the capability of the instrumentation in measuring ultra-low currents. Guarding is achieved by applying a low impedance bootstrap potential to the outside of the insulation material surrounding the signal line. This bootstrap potential is held at the same level as that of the high impedance line; therefore there is no voltage drop across the insulation and, hence, no leakage. The guard will also act as a shield to reduce noise pickup and serves an additional function of reducing the effective capacitance to the input line.

Printed circuit board layout and construction is critical for achieving the ultimate in low leakage performance of the instrumentation. The best performance can be realized by using a teflon IC socket for the operational amplifier; but at least a teflon standoff should be used for the high impedance, low current lead. If this is not feasible, the input guarding scheme will minimize leakage as much as possible; the guard ring must be applied to both sides of the board. The guard ring is connected to a low impedance potential at the same level as the inputs. Circuit boards which are sufficiently sensitive to require guard rings should not contain plated through holes (unless the PCB is made of teflon), because the bulk resistivity of the PCB material is less than the surface resistivity.

Just as conductors are improperly viewed as superconductors (i.e., zero resistance), so are insulators often mistakenly treated as perfect insulators, rather than very high resistances, which is the more accurate model when we are considering low current and high impedance circuits. Most printed circuit board materials are very good insulators, but they are not perfect, and inadequately cleaned PCB material may be quite a poor insulator. Another important concern for achieving and maintaining low leakage currents is complete cleanli-

ness of circuit boards and components. Completed assemblies should be washed thoroughly in a high residue solvent like TMC Freon or high purity methanol followed by a rinse with deionized water and nitrogen drying.

Passive components selection Selection of passive components employed in high impedance situations is critical. High value resistors should be of carbon film or deposited ceramic oxide type to obtain the best in low noise and high stability performance. The best packaging for these resistors is a glass body sprayed with silicone varnish to minimize humidity effects. These resistors must be handled very carefully to prevent surface contamination. Capacitors for any high impedance or long term integration situation should be of polystyrene formulation for optimum performance.

Power supply bypassing, Active decoupling and instrumentation amplifier stability issues

Power supply decoupling is an important issue in any electronic design. Normally, bypass capacitors (values of 0.01 μf are typical) are connected between the power supply pins of each integrated circuit and ground. While usually adequate, this practice can be ineffective or even create worse transients than no bypassing at all. It is important to consider where the circuit's currents originate, where they will return, and by what path. Once this has been established, these currents can be bypassed around ground and other signal paths. In general, most instrumentation amplifiers (such as AD524C) have their integrators referenced to the negative supply and should be decoupled with respect to the output reference terminal. This means that, for each chip, a bypass capacitor should be connected between each power supply pin and the point on the board where the instrumentation amplifier's reference terminal is connected.

Power supply requirements Error signal and noise can enter the signal path from every node in the circuit and this includes the power supplies. The effect is complicated because the power supply is apt to connect to many circuits at the same time. The important entry point is the input circuit as this is where the effect is most felt. The circuits used at the input are usually differential in character to avoid any sensitivity to power supply change. Most commercially available ICs or operational amplifiers are designed with well balanced differential input stages and meet this criteria. In very sensitive electronic circuits like the one discussed in this thesis, switching mode power supplies should not be used for the following reason. A serious problem posed by switching regulators is the flow of high frequency switching current in the grounding system. If the line filters and power supply filters are referenced to various grounds, significant amount of interference currents can flow. This current has content at the harmonics of the switching frequency and this content cannot be easily isolated by shielding. In addition to all these requirements, the power supply chosen should be capable of delivering the required voltage and current for the entire instrumentation with very high degree of stability.

Grounding, signal routing At a glance, grounding and shielding are two simple concepts. Any point that needs to be grounded is to be connected to the power supply ground. Any circuit that needs to be shielded is to be enclosed in a metal box and the box grounded. But there is a lot more to it than these simple concepts.

Kirchoff's law states that at any point in the circuit, the algebraic sum of the currents is zero. (Refer Figure B.1) This means that all currents flow in circles and, particularly, that the return current must always be considered when designing and developing a circuit.

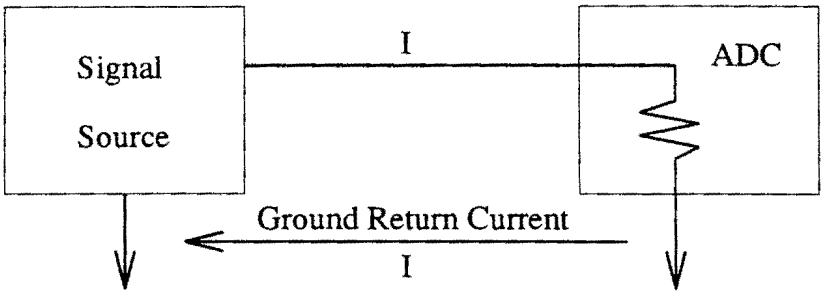

Figure B.1 Kirchoff's law

When designing and developing a single ended circuit where a signal is referenced to "ground", it is common to assume that all the points on the circuit diagram where the ground symbol is to be found are at the same potential. This is incorrect.

A more realistic model of ground is one in which there are complex impedances in the ground path. Not only do the ground currents flow in the complex impedances which exist between the two "ground" points giving rise to a voltage drop in the total signal path, but external currents may also flow in the same path, generating uncorrelated noise voltages that are seen by the ADC.

It is evident, of course, that other currents can flow only in the ground impedance if there is a current path for them. Figure B.2 shows such a path at ground potential, which is the notorious "ground loop", but equally severe problems could be caused by a circuit

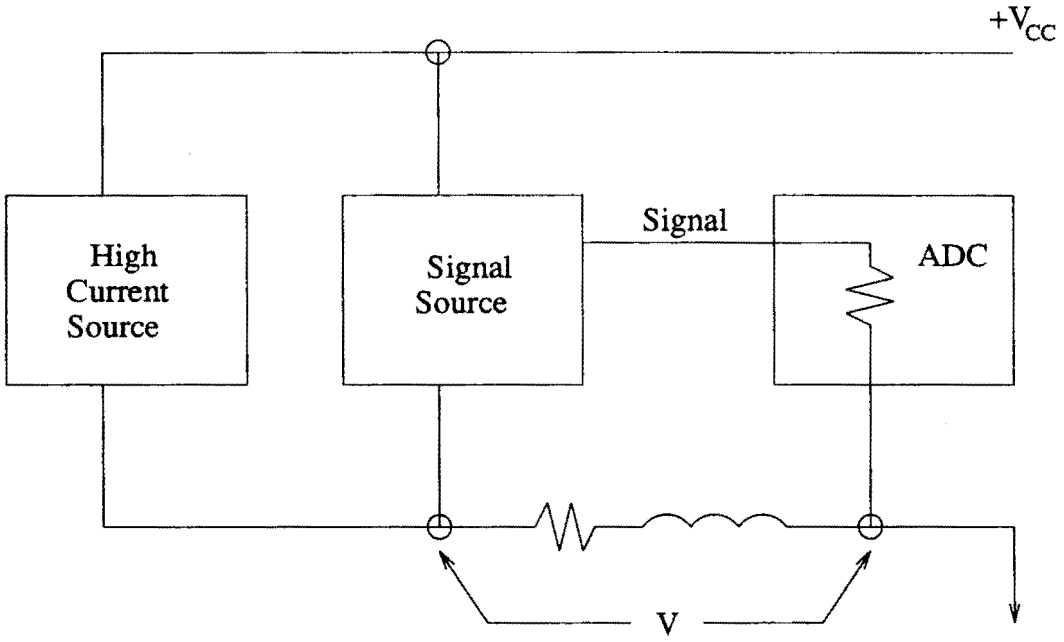

Figure B.2 Noise due to current flowing in common ground

sharing an unlooped ground return with the signal source but drawing a large and varying current from its supply and ground return. There are a number of possible ways of attacking the problem of ground noise, apart from the (presently) impracticable one of using superconducting grounds. One such scheme, the "star" ground philosophy, is discussed below.

The "star" ground builds on the theory that there is a single point in the circuit to which all voltages are referred. This is known as the star point. In mixed signal applications, it is typical to have separate power supplies for the analog and digital parts, with separate analog and digital grounds joined at the star point.

Digital circuitry is noisy. Saturating logic draws large fast current spikes from its power supply during switching and, having noise immunity of hundreds of millivolts or more, has little need of high levels of supply decoupling.

Analog circuitry, on the other hand, is very vulnerable to noise in power supplies or grounds. It is therefore sensible to separate analog and digital circuitry to prevent digital noise from corrupting analog performance. This will involve separation of both power supplies and grounds, which may be inconvenient in a mixed signal system. Nevertheless, if a system is to give the full performance of which it is capable, it is often essential to have separate analog and digital grounds and power supplies. The fact that some analog circuitry will operate from a single +5V power supply does not mean that it may be safely operated from the same noisy +5V supply as the microprocessor and the dynamic RAM, the electric fan, and a solenoid jackhammer!

However, analog and digital ground in a system must be joined at some point to allow signals to be referred to a common potential. This star point, or analog/digital common

point is chosen so that it does not introduce digital currents into the analog part of the system - it is often convenient to make this connection at the power supplies.

Signal routing It is evident from the above discussion that we can minimize noise by paying attention to the system layout and preventing different signals from interfering with each other. High level analog signals must be separated from low level analog signals, and both must be kept away from digital signals. All sensitive areas are to be isolated from each other and signal paths should be kept as short as possible. Lots of ground plane use is recommended for proper isolation.

Shielding principles

Electrostatic shielding The word shield is a common place in electronics. The idea is deceptively simple and yet is a source of much difficulty. The idea takes on the form of shielded wires, shield plates, shield boxes, metal screens, etc. This business of shielding is based on the concept of mutual capacitance.

The concept of mutual capacitance can be made clearer by considering the system of conductors shown in Figure B.3. The mutual capacitance c_{12} is the ratio of induced charge Q_1 to the potential V_2. If conductor 1 has a charge Q_1 then conductor 2, which surrounds 1, must have a charge $-Q_1$ because all the flux from 1 must terminate on 2. The external field about conductors 2 and 3 is zero; therefore Q_3 equals zero. The ratio of $Q_3/V_1 = c_{31} = 0$. Conductor 1 is said to be completely screened. It is very commonplace to talk about grounding the shield. It is correct to say that a shield can be at any potential and still provide shielding. This statement is true in the sense that relative changes in the conductor potentials within the shield have no influence on conductors outside of the shield. Also, changes in the

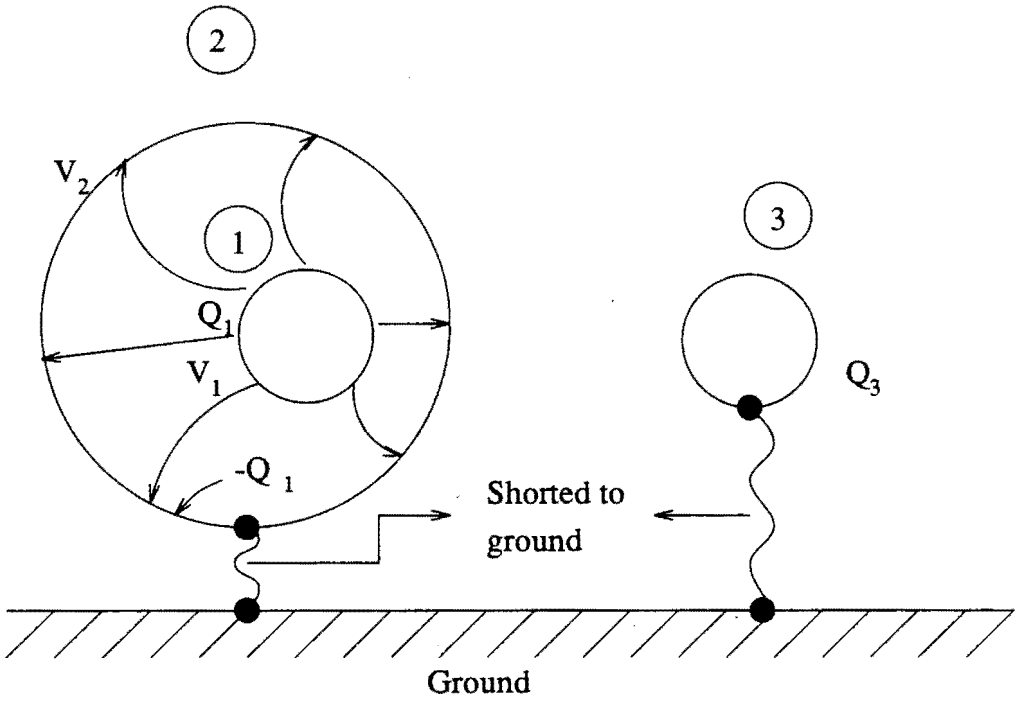

Figure B.3 A system with electric screening of conductor 2

potentials of the conductors outside of the shield have no effect on the relative potential of the conductors within the shield. These statements do not require that the shield be earthed or defined in any way. The only requirement is that the conductors under discussion be fully surrounded by a conducting surface.

Development details

Circuit description Figure 2.7 shows the complete circuit diagram that was developed as a prototype for the instrumentation. It has a current to voltage converter stage built using AD515AL FET input operational amplifier. A scale factor resistor of 1 GΩ is used as this is a prudent choice considering the cost, size, minimum gain required in this stage, and not amplifying the dark current so as to saturate the amplifier. Two .01 microfarad capacitors are mounted between the power supply pins and ground for effective filtering of noise and power supply decoupling. The output from the current to voltage converter is fed to the non inverting input of the AD524C instrumentation amplifier. A gain of 100 is preset by connecting the appropriate gain selection pin of AD524C to pin RG1. Two capacitors of .01 microfarads are connected between the power supply pins and output reference pin for power supply decoupling. The sense pin of AD524 is shorted to the output pin. An anti-aliasing passive first order low pass filter with a cut off frequency of 20 Hz is connected to the output of the instrumentation amplifier for effective filtering of noise from the signal and to avoid aliasing effects.

Circuit board development The main consideration in the development of the circuit board is the total size of the circuit board and cleanliness. Utmost importance was given in the design and development of the PCB to maintain the length of the tracks as small as

possible and the total size as small as possible. The circuit board was developed locally in the laboratory using photosensitive PCB material. As mentioned in the section on layout considerations, a guard ring was used on the PCB on both sides around the input pins of the current to voltage converter. Although this is a overkill in terms of having a teflon standoff and a guard ring, this arrangement was chosen to reduce the effects of leakage current. The AD515AL was mounted on a teflon socket with all the pins of the teflon socket soldered to the circuit board except the two input pins, which were soldered directly to the teflon stand-offs. Figure B.4 shows the mounting arrangement followed in the development of the instrumentation.

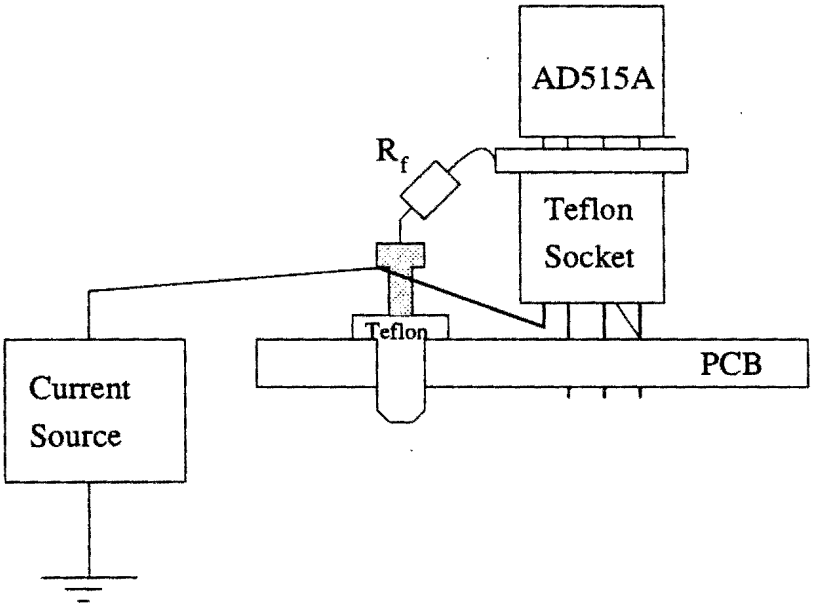

Figure B.4 Mounting arrangement

Grounding, shielding, cabling and power supply Shielding is an important factor in the development of this instrumentation. To give a feel of the effect of shielding on this circuit, the output of the current to voltage converter saturates (goes to +13V or -13V) , if the top cover of the enclosure is opened with the circuit powered and input signal being zero. This means that the noise picked up is amplified to such high levels, that the instrumentation is practically useless unless it is shielded. Figure B.5 shows the complete detector setup with the shield, cables and power supply connected. An aluminum box is used to enclose the circuit. The shield is connected through the shield of the multiconductor shielded twisted cable used for power supply and signals to the ground of the power supply.

Because of the sensitivity of the instrumentation to noise, a star connected ground system was used. Figure B.5 shows the various ground reference wires that were brought out and connected to the star point at the power supply ground. To carry signals out of the instrumentation and power into the instrumentation, a six core (3 pair) shielded twisted pair cable was used.

A dedicated power supply with an output of +15 V and -15 V DC was built for the detector. There is a single cable carrying DC power, detector output signal and various grounds that comes out of the detector and plugs into the power supply box. The detector output signal is directed on to another connector from which it is connected to the digitizing circuitry. A shielded enclosure is built inside the power supply box in order to shield the detector output from noise inside the power supply box.

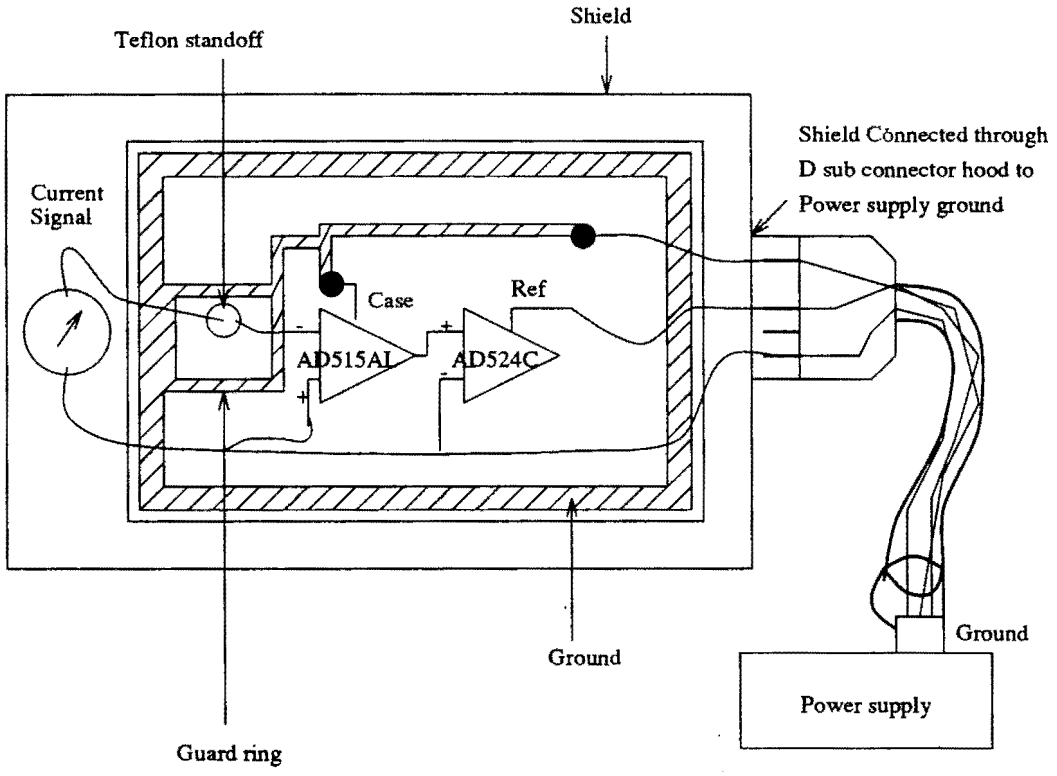

Figure B.5 Grounding and shielding scheme adapted in the prototype instrumentation

APPENDIX C. VME BUS BASED DATA ACQUISITION SYSTEM

During the development phase of the detector system, a VMEbus based data acquisition system was used to perform all the bench top tests. There is no specific reason for using a VME bus based system for this purpose except for the fact that it was available. In this appendix, an explanation of the system setup is presented.

System setup

Figure D.1 shows the system setup of the VME bus based data acquisition system. The system is of the external CPU configuration type, which means that the CPU controlling the VME system is external to the VME bus. The complete system setup consists of a 80486DX (66 Mhz) based PC hosting a VME MXI interface card. The VME MXI card is connected through a MXI bus to the extended controller present on the VME bus. The entire VME system is controlled from the PC using the NIVXI software library from National Instruments. In addition to the extended controller, the VME system presently hosts a VIPC (Very Intelligent Processor Card from Green Spring Inc.) which in turn controls a set of digital I/O lines, programmable interval timers, analog to digital converters, digital to analog converters (all of these are from Green Spring Inc.). Out of these, only the analog to digital converters are used for the research work described in this thesis. Reference [32] provides a detailed description of the principle of operation of VME bus. Reference [33-35] provides the necessary details for programming the VME based data acquisition system. Reference [36] provides various details about the analog to digital converters used for data acquisition using the VMEbus system.

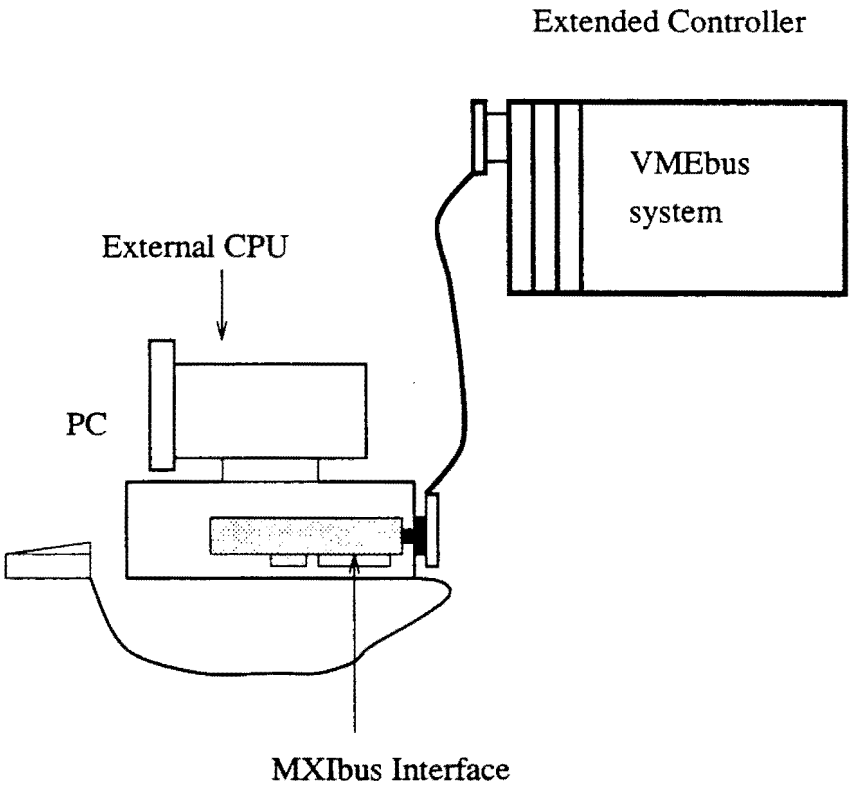

Figure D.1 VMEbus based data acquisition system setup

APPENDIX D. DATA PACKET FORMAT FOR NETWORK TRANSFER AND SOURCE CODE FOR SERVER SOFTWARE

The following is the data packet format for sending the remote command for controlling the θ and ϕ axes motors. The packet format has been designed keeping in mind the changes that might be needed to accomodate other hardware in addition to motor controllers.

```
packet    {
              int       device_id;
              int       command;
              char      parameters[100];
              char      returnval[100];
              int       ack;
              char      buf[100];
};
```

The same packet format is used for transmitting the commands from the client as well as the results from the server. The packet format is explained below.

Since there are a number of hardware devices available on the PCs at the center for NDE (X-ray group), and each of these devices have a number of commands, the packet format was designed to encode the commands for these devices. A device id is assigned to each hardware device and each command is defined in the header file. Instead of transmitting the entire command as a string, the device ids and commands are coded into the packet and transmitted. The parameters for the commands are filled in the parameters field of the packet. The returnval field is used to return results and ack field is set to TRUE for a successful acknowledge and FALSE for negative acknowledge. The field buffer is provided for future use. The source code of the server software is provided below.

server.cpp

```
/* SERVER.CPP -- Server program.(Interprets Motor commands)

 COMMENTS: In this program, the motor control related parts are taken from the motor
control library software available at the center for NDE, Ames, Iowa
 */

#define WINDOWS
#include <windows.h>
#include "winsock.h"
#include <dos.h>
#include <stdio.h>
#include <string.h>
#include <windowsx.h>
#include <alloc.h>
#include "server.h"
#include "network.h"
#include "motion.h"
#define OK 1
#define NOT_OK        2
// Declaring a local motor theta, that will be accessed across the network.
 Motor motor_theta("Mtheta",512,1,MY_TRUE);
 Motor *motor_ptr;
// Data packet definition given in network.h
packet rpacket; char FAR * rpacket_ptr;
// Function declarations
sendack(SOCKET);
long FAR PASCAL _export WndProc (HWND, UINT, UINT, LONG) ;
// Windows related routines
```

```
int PASCAL WinMain (HANDLE hInstance, HANDLE hPrevInstance, LPSTR lpszCmd-
Param, int nCmdShow)
{
   static char szAppName[] = "Server" ;
   HWND hwnd ;
   MSG    msg ;
   WNDCLASS wndclass ;
   if (!hPrevInstance)  {
      wndclass.style = CS_HREDRAW | CS_VREDRAW ;
      wndclass.lpfnWndProc = WndProc ;
      wndclass.cbClsExtra = 0 ;
      wndclass.cbWndExtra = 0 ;
      wndclass.hInstance = hInstance ;
      wndclass.hIcon = LoadIcon (hInstance,szAppName) ;
      wndclass.hCursor = LoadCursor (NULL, IDC_ARROW) ;
      wndclass.hbrBackground = GetStockObject (WHITE_BRUSH) ;
      wndclass.lpszMenuName = szAppName ;
      wndclass.lpszClassName = szAppName ;
      RegisterClass (&wndclass) ;
   }
   hwnd = CreateWindow (szAppName, // window class name
                        "Network Server", // window caption
                        WS_OVERLAPPEDWINDOW, // window style
                        CW_USEDEFAULT, // initial x position
                        CW_USEDEFAULT, // initial y position
                        250,
                        100,
                        NULL,    // parent window handle
                        NULL,    // window menu handle
                        hInstance, // program instance handle
                        NULL) ;                  // creation parameters

   ShowWindow (hwnd, nCmdShow) ;
   UpdateWindow (hwnd) ;
```

```
    while (GetMessage (&msg, NULL, 0, 0))    {
        TranslateMessage (&msg) ;
        DispatchMessage (&msg) ;
    }
    return msg.wParam ;

}

long FAR PASCAL _export WndProc (HWND hwnd, UINT message, UINT wParam,
LONG lParam)
{

    HDC     hdc ;
    PAINTSTRUCT ps ;
    RECT    rect ;
    WORD wVersionRequested;
    WSADATA wsaData;
    static int err,n,len;
    HMENU hMenu;
    static char server_address[20];
    static char client_address[20];
    const char FAR * server_addr_ptr;
    const char FAR * client_addr_ptr;
    char dummy[256];

    static SOCKET s1;
    static SOCKET newsockfd;
    static SOCKADDR_IN server_addr, client_addr;
    static SOCKADDR_IN FAR * serv_addr_ptr;
    static SOCKADDR_IN FAR * clien_addr_ptr;
    static int length,i,k;
    static int FAR * length_ptr;
    static unsigned short server_port;
    static int command;
    static int device_id;
```

```
static int local_command;

switch (message)     {
   case WM_COMMAND:
      hMenu = GetMenu(hwnd);

      switch (wParam)   {
         case IDM_QUIT:
            SendMessage(hwnd,WM_DESTROY,0,0L);
            return 0;

      }
   return 0;

   case WM_CREATE:
      motor_theta.setwindow_handle(hwnd,"Server");
      length_ptr = &length;
      length = sizeof(client_addr);
      serv_addr_ptr = &server_addr;
      clien_addr_ptr = &client_addr;
      server_addr_ptr = server_address;
      client_addr_ptr = client_address;
      rpacket_ptr = (char FAR *)&rpacket;

      //Network related code

      server_port = 4000;
      sprintf(server_address,"%s","129.186.202.97");
      sprintf(client_address,"%s","129.186.202.45");

      // Initialization of Windows socket library
      wVersionRequested = 0x0101;
```

```
err = WSAStartup(wVersionRequested,&wsaData);
    if (err != 0) {
        MessageBox(hwnd,"WSASTARTUPERROR"," ",MB_OK);
        return 0;

    }

// Open a connection oriented socket
s1 = socket(PF_INET,SOCK_STREAM,0);
    if (s1 == INVALID_SOCKET) {
        MessageBox(hwnd,"INVALID SOCKET s1"," ",MB_OK);
        exit(1);

    }

// Initializing the server address
server_addr.sin_family = PF_INET;
server_addr.sin_addr.s_addr = htonl(INADDR_ANY);

server_addr.sin_port = htons(server_port);

client_addr.sin_family = PF_INET;
client_addr.sin_addr.s_addr = htonl(INADDR_ANY);
client_addr.sin_port = htons(0);

    if(bind(s1,(LPSOCKADDR) serv_addr_ptr,sizeof(server_addr)) !=0) {
        err = WSAGetLastError();
        sprintf(dummy,"BIND ERROR : %d",err);
        MessageBox(hwnd,dummy," ",MB_OK);
    }

// listening on socket s1 port 4000 for a connection

err = listen(s1,5);
```

```
        if (err == SOCKET_ERROR) {
            err = WSAGetLastError();
            sprintf(dummy,"LISTEN ERROR: %d",err);
            MessageBox(hwnd,dummy," ",MB_OK);
        }

    // Register with Windows through a select call to inform
    // when there is a client connect request.
    err = WSAAsyncSelect(s1,hwnd,wMsg1,FD_ACCEPT);
        if (err == SOCKET_ERROR) {
            err = WSAGetLastError();
             sprintf(dummy,"WSAAsyncSelect ERROR: %d",err);
             MessageBox(hwnd,dummy," ",MB_OK);
        }

return 0;

// When there is a client connect request, Windows sends

// a message with wMsg1 in the message.
case wMsg1:
    k = LOWORD(lParam);
    switch(k) {
        case FD_ACCEPT:
            newsockfd = accept(s1,(LPSOCKADDR) clien_addr_ptr,length_ptr);
                if (newsockfd < 0) {
                    err = WSAGetLastError();
                    sprintf(dummy,"ACCEPT ERROR MESSAGE : %d",err);
                     MessageBox(hwnd,dummy," ",MB_OK);
                }
             err = WSAAsyncSelect(newsockfd,hwnd,wMsg1,FD_READ|FD_CLOSE);
                if (err == SOCKET_ERROR) {
```

```
            err = WSAGetLastError();
            sprintf(dummy,"WSAAsyncSelect ERROR: %d",err);
            MessageBox(hwnd,dummy," ",MB_OK);
        }
        MessageBox(hwnd,"After 2 select"," ",MB_OK);
return 0;

case FD_READ:
    n = recv(newsockfd,rpacket_ptr,sizeof(packet),0);
        if(n == SOCKET_ERROR) {
            err = WSAGetLastError();
            if ((err == WSAECONNABORTED) || (err == WSAENOTCONN))
                return 0;
            sprintf(dummy,"RECEIVE ERROR : %d",err);
            MessageBox(hwnd,dummy," ",MB_OK);
        }
        else if(n == sizeof(packet)) {
            device_id = 0;
            command = 0;
            device_id = rpacket.device_id;
            command = rpacket.command;
            switch (device_id) {
                case MOTOR_THETA: {
                    local_command = MOTOR;
                    motor_ptr = &motor_theta;
                break;
                }

                default:
                    local_command = INVALID;
                break;
```

```
}

switch (local_command) {
    case MOTOR:
        switch (command) {
            case SETMODE_CONTINUOUS: {
                motor_ptr->setmode_continuous();
                sendack(newsockfd);
            break;
            }

            case SETMODE_NORMAL: {
                motor_ptr->setmode_normal();
                sendack(newsockfd);
            break;
            }

            case SETPOSITION_ABSOLUTE: {
                motor_ptr->setposition_absolute();
                sendack(newsockfd);
            break;
            }

            case SETPOSITION_INCREMENTAL: {
                motor_ptr->setposition_incremental();
                sendack(newsockfd);
            break;
            }

            case SETDIRECTION_CW: {
                motor_ptr->setdirection_cw();
                sendack(newsockfd);
```

```
break;
}

case SETDIRECTION_CCW: {
   motor_ptr->setdirection_ccw();
    sendack(newsockfd);
break;
}

case CHANGE_DIRECTION: {
    motor_ptr->change_direction();
     sendack(newsockfd);
break;
}

 case SETPOSITION_ZERO: {
     motor_ptr->setposition_zero();
      sendack(newsockfd);
 break;
 }

 case SETVELOCITY: {
     float velocity;
     sscanf(rpacket.parameters,"%f",&velocity);
     motor_ptr->setvelocity(velocity);
     sendack(newsockfd);
 break;
 }

 case SETACCELERATION: {
     float accelaration;
     sscanf(rpacket.parameters,"%f",&accelaration);
```

```
    motor_ptr->setacceleration(accelaration);
    sendack(newsockfd);
break;
}

case SETLIMIT_ACCELERATION: {
    float accelaration;
    sscanf(rpacket.parameters,"%f",&accelaration);
    motor_ptr->setlimit_acceleration(accelaration);
    sendack(newsockfd);
break;
}

case SETGOHOME_ACCELERATION: {
    float accelaration;
    sscanf(rpacket.parameters,"%f",&accelaration);
    motor_ptr->setgohome_acceleration(accelaration);
    sendack(newsockfd);
break;
}

case SETBACKUPTO_HOME: {
    BooLean backupto_home;
    sscanf(rpacket.parameters,"%d",&backupto_home);
    motor_ptr->setbackupto_home(backupto_home);
    sendack(newsockfd);
break;
}

case SETACTIVEHOME_STATE: {
    BooLean active_state;
    sscanf(rpacket.parameters,"%d",&active_state);
```

```
            motor_ptr->setactivehome_state(active_state);
            sendack(newsockfd);
        break;
        }

        case SETFINALGOHOME_DIRECTION: {
            BooLean finalgohome_direction;
scanf(rpacket.parameters,"%d",&finalgohome_direction);
motor_ptr>setfinalgohome_direction(finalgohome_direction);
            sendack(newsockfd);
        break;
        }

        case SETHOMEDGE_REFERENCE: {
            BooLean homeedge_reference;
      sscanf(rpacket.parameters,"%d",&homeedge_reference);
      motor_ptr->sethomedge_reference(homeedge_reference);
            sendack(newsockfd);
        break;
        }

        case MOVE_LONG: {
            long int absolute_steps;
            sscanf(rpacket.parameters,"%ld",&absolute_steps);
            motor_ptr->move(absolute_steps);
            sendack(newsockfd);
        break;
        }

        case MOVE_INCH: {
            float absolute_inches;
            sscanf(rpacket.parameters,"%f",&absolute_inches);
```

```
    motor_ptr->move_inch(absolute_inches);
    sendack(newsockfd);
break;
}

case MOVE_DEGREE: {
    float absolute_degrees;
    sscanf(rpacket.parameters,"%f", &absolute_degrees);
    motor_ptr->move_degree(absolute_degrees);
    sendack(newsockfd);
break;
}

case MOVE: {
    motor_ptr->move();
    sendack(newsockfd);
break;
}

case LIMIT_ENABLE: {
    motor_ptr->limit_enable();
    sendack(newsockfd);
break;
}

case LIMIT_DISABLE: {
    motor_ptr->limit_disable();
    sendack(newsockfd);
break;
}

case REPORT_LIMIT: {
```

```
    BooLean ret_val;
    ret_val = motor_ptr->report_limit();
    sendack(newsockfd);
break;
}

case PAUSE_MOTION: {
    motor_ptr->pause_motion();
    sendack(newsockfd);
break;
}

case CONTINUE_MOTION: {
    motor_ptr->continue_motion();
    sendack(newsockfd);
break;
}

case STOP_MOTION: {
    motor_ptr->stop_motion();
    sendack(newsockfd);
break;
}

case KILL_MOTION: {
    motor_ptr->kill_motion();
    sendack(newsockfd);
break;
}

case SHUTDOWN: {
    motor_ptr->shutdown();
```

```
    sendack(newsockfd);
break;
}

case GOHOME: {
    float velocity;
    sscanf(rpacket.parameters,"%f",&velocity);
    motor_ptr->gohome(velocity);
    sendack(newsockfd);
break;
}

case CHECKMOTION: {
    BooLean ret_val;
    ret_val = motor_ptr->checkmotion();
    sendack(newsockfd);
break;
}

case GETPOSITION_AB: {
    long ret_val;
    ret_val = motor_ptr->getposition_ab();
    sprintf(rpacket.returnval," %ld ",ret_val);
    sendack(newsockfd);
break;
}

case GETPOSITION_REL: {
    long ret_val;
    ret_val = motor_ptr->getposition_rel();
    sprintf(rpacket.returnval," %ld ",ret_val);
    sendack(newsockfd);
```

```
break;
}

case GETADDRESS: {
    int ret_val;
    ret_val = motor_ptr->getaddress();
    sprintf(rpacket.returnval," %d ",ret_val);
    sendack(newsockfd);
break;
}

case GETNUMBER: {
    int ret_val;
    ret_val = motor_ptr->getnumber();
    sprintf(rpacket.returnval," %d ",ret_val);
    sendack(newsockfd);
break;
}

case SETMESSAGE_FLAG: {
    BooLean c_message_flag;
    sscanf(rpacket.parameters,"%d",&c_message_flag);
    motor_ptr->setmessage_flag(c_message_flag);
    sendack(newsockfd);
break;
}

case INITIALIZE: {
    BooLean pc23_initialize_flag;
 sscanf(rpacket.parameters, "%d",&pc23_initialize_flag);
    motor_ptr->initialize(pc23_initialize_flag);
    sendack(newsockfd);
```

```
                    break;
                    }
                }
                break;

                case INVALID: {
                    printf("INVALID DEVICE ID : %d\n",device_id);
                break;
                }

                case GENERATOR:{
                    printf("PRESENTLY NOT IMPLEMENTED\n");
                break;
                }
        }
}
return 0;

case FD_CLOSE:
   // MessageBox(hwnd,"CLOSING NEWSOCK CORRECTLY"," ",MB_OK);
   n = closesocket(newsockfd);
      if ( n == SOCKET_ERROR) {
         err = WSAGetLastError();
         sprintf(dummy,"CLOSE SOCKET newsockfd ERROR %d",err);
         MessageBox(hwnd,dummy," ",MB_OK);
       }
      err = WSAAsyncSelect(s1,hwnd,wMsg1,FD_ACCEPT);
           if (err == SOCKET_ERROR) {
              err = WSAGetLastError();
              sprintf(dummy,"WSAAsyncSelect ERROR: %d",err);
              MessageBox(hwnd,dummy," ",MB_OK);
```

```
                    }
                }
                return 0;

                case WM_DESTROY:
                  n = closesocket(s1);
                     if ( n == SOCKET_ERROR)  {
                        err = WSAGetLastError();
                        sprintf(dummy,"CLOSE SOCKET s1 ERROR %d",err);
                        MessageBox(hwnd,dummy," ",MB_OK);
                      }

                   n = closesocket(newsockfd);
                      if ( n == SOCKET_ERROR)  {
                        err = WSAGetLastError();
                        sprintf(dummy,"CLOSE SOCKET newsockfd ERROR %d",err);
                        MessageBox(hwnd,dummy," ",MB_OK);
                      }
                 WSACleanup();
                  PostQuitMessage (0) ;
               return 0 ;
               }

return DefWindowProc (hwnd, message, wParam, lParam) ;

}

sendack(SOCKET i)

{
               int n;
                while(motor_theta.checkmotion() == MY_TRUE);
                rpacket.ack = MY_TRUE;
```

APPENDIX E. SOFTWARE FOR 1D, 2D AND TOMO SCAN

scan.cpp

```
/*
 This program executes the various scans that can be performed using the
 current mode x-ray detector. It consistes of a text oriented user
 interface, a network based sample positioning, and DAS12/50 based
 data acquisition code. The motor control library is taken from the
 motion control library available at the Center for NDE, Ames.
 */

// Header files
#define WINDOWS
#include <windows.h>
#include "winsock.h"
#include <dos.h>
#include <stdio.h>
#include <string.h>
#include <windowsx.h>
#include <alloc.h>
#include "server.h"
#include "motion.h"
#include "rmotion.h"
#define OK              1
#define NOT_OK          2

 int choice;
 char filename[100];
 float x_distance;
```

```
float y_distance;
float z_distance;
int theta_degrees;
int no_samples;
float x_step_sixe;
float y_step_size;
float z_step_size;
int theta_step_size;
int gain;
FILE *fp1;
FILE *fp2;
FILE *fp3;
char answer;
char disp;
float data_arr[1000];


// Initialization of local motors for X, Y and Z  axes.
Motor motor_x("MX", 768, 1, MY_TRUE);
Motor motor_y("MY", 768, 2);
Motor motor_z("MZ", 768, 3);
// Initialization of remote motor theta
RMotor motor_theta("MTH", MOTOR_THETA);
// Socket declaration
static SOCKET sid;

// Function to send a packet across the network
int sfn(char far *buf)
{
        int n, err;
```

```
        n = send(sid, buf, sizeof(packet), 0);
        if(n == SOCKET_ERROR) {
                err = WSAGetLastError();
                printf("SEND ERROR: %d",err);
        }
    return n;
}

// Function to receive a packet across the network.
int rfn(char far *buf)
{
        int n, err;

        n = recv(sid, buf, sizeof(packet), 0);
        if(n == SOCKET_ERROR) {
                err = WSAGetLastError();
                printf("SEND ERROR: %d",err);
        }
    return n;
}

void user_interface (int);
void move_and_collect(int);
void store_data(int);
void x_move(float);
void y_move(float);
void z_move(float);
void theta_move(float);
void collect_data(int);
```

```
void dataacq_init();
void set_gain (int);
void convert_to_grd();
// Main program
void main()
{
 WORD wVersionRequested;
 WSADATA wsaData;
 static int err,n,len;
 static unsigned int k;
 char  server_address[20];
 char  client_address[20];
 const char FAR * server_addr_ptr;
 const char FAR * client_addr_ptr;
 char  dummy[40];
 static SOCKADDR_IN  server_addr;
 static SOCKADDR_IN client_addr;
 static SOCKADDR_IN FAR * serv_addr_ptr = &server_addr;
 static SOCKADDR_IN FAR * clien_addr_ptr = &client_addr;
 static unsigned short server_port;

 server_addr_ptr = server_address;
 client_addr_ptr = client_address;
 server_port = 4000;
 sprintf(server_address,"%s","129.186.202.97");
 sprintf(client_address,"%s","129.186.202.45");

 // Initializing Windows socket library
 wVersionRequested = 0x0101;
 err = WSAStartup(wVersionRequested,&wsaData);
```

```
if (err != 0) {
   printf("ERROR: startup\n");
   exit(1);
}

// Create a socket
sid = socket(PF_INET,SOCK_STREAM,0);
if (sid == INVALID_SOCKET) {
   printf("ERROR: INVALID SOCKET\n");
   exit(1);
}

// Initializing the socket data structure with addresses
server_addr.sin_family = PF_INET;
server_addr.sin_addr.s_addr = inet_addr(server_addr_ptr);
server_addr.sin_port = htons(server_port);

client_addr.sin_family = PF_INET;
client_addr.sin_addr.s_addr = htonl(INADDR_ANY);
client_addr.sin_port = htons(0);

/*
 n = connect(sid,(struct sockaddr FAR *) serv_addr_ptr,sizeof(server_addr));
 if (n == SOCKET_ERROR) {
    err = WSAGetLastError();
    printf("CONNECT ERROR: %d\n",err);
    exit(1);
 }
*/
choice = 0;
```

```
dataacq_init();
while ((choice > 0) || (choice < 6)) {
   printf("WELCOME TO THE WORLD OF HIGH SPEED DETECTORS\n");
   printf("1. SAMPLE POSITIONING\n");
   printf("2. 1D SCAN\n");
   printf("3. 2D SCAN\n");
   printf("4. TOMO SCAN\n");
   printf("5. Quit\n");
   printf("Enter your choice:");
   scanf("%d",&choice);
   switch (choice) {
      case 1:
         user_interface(1);
      break;

      case 2:
         user_interface(2);
            if (answer == 'y') {
               if ((fp1 = fopen(filename,"w+")) == NULL) {
                  printf("Error in opening file : %s\n",filename);
                  exit(1);
               }
            move_and_collect(2);
            }
         printf("END OF SCAN\n");
      break;

      case 3:
        user_interface(3);
           if (answer == 'y') {
```

```
                if ((fp1 = fopen(filename,"w+")) == NULL)  {
                    printf("Error in opening file : %s\n",filename);
                    exit(1);
                }
              move_and_collect(3);
              }
           printf("END OF SCAN\n");
        break;

        case 4:
           user_interface(4);
              if (answer == 'y')  {
                 if ((fp1 = fopen("temp.dat","w+")) == NULL)  {
                    printf("Error in opening file : %s\n",filename);
                    exit(1);
                  }
              move_and_collect(4);
              convert_to_grd();
              }
        break;

         case 5:
            printf("Quitting the program.....\n");
            exit(0);
         break;
printf("END OF SCAN\n");
}
}}

void user_interface (int vari)  {
```

```
int dummy = 1;

x_distance = 0.0;
y_distance = 0.0;
z_distance = 0.0;

answer = 'n';
switch (vari)  {
        case 1:
           printf("SAMPLE POSITIONING\n");
        break;
        case 2:
           printf("1D SCAN\n");
        break;
        case 3:
           printf("2D SCAN\n");
        break;
        case  4:
           printf("TOMO SCAN\n");
        break;
}
printf("ALL DISTANCES IN INCHES PLEASE\n");
switch(vari)  {
        case 1:  {
           while ((dummy >0) || (dummy < 7))  {
            printf("1. MOVE ALONG X-AXIS\n");
            printf("2. MOVE ALONG Y-AXIS\n");
            printf("3. MOVE ALONG Z-AXIS\n");
            printf("4. MOVE ALONG THETA-AXIS\n");
            printf("5. DETECTOR OUTPUT\n");
```

```
printf("6. QUIT THIS MENU\n");
printf("ENTER CHOICE:");
scanf("%d",&dummy);
   switch(dummy) {
      case 1:
         printf("Enter distance to be moved in X:");
         scanf("%f",&x_distance);
         x_move(x_distance);
      break;

      case 2:
         printf("Enter distance to be moved in Y:");
         scanf("%f",&y_distance);
         y_move(y_distance);
      break;

      case 3:
         printf("Enter distance to be moved in Z:");
         scanf("%f",&z_distance);
         z_move(z_distance);
       break;

        case 4:
           printf("Enter degrees to be moved in theta:");
           scanf("%f",&theta_degrees);
           theta_move(theta_degrees);
         break;

         case 5:
            printf("Enter number of samples to average per point:");
```

```
                    scanf("%d",&no_samples);
                    printf("Enter software gain (1,4,8):");
                    scanf("%d",&gain);
                     set_gain(gain);
                    collect_data(1);
                     printf("DETECTOR OUTPUT IS %f\n",data_arr[1]);
                  break;

                  case 6:
                      return;
                  break;
               }
          }
         return;
      }
case 2:
   printf("Enter step size:");
   scanf("%f",&y_step_size);
   printf("Enter the distance to be scanned:");
   scanf("%f",&y_distance);
 break;

 case 3:
    printf("Enter step size in Y axis:");
    scanf("%f",&y_step_size);
    printf("Enter Scan distance in Y axis:");
    scanf("%f",&y_distance);
    printf("Enter step size in Z axis:");
    scanf("%f",&z_step_size);
    printf("Enter Scan distance in Z axis:");
```

```
        scanf("%f",&z_distance);
      break;

      case 4:
        printf("Enter Scan distance in Y axis:");
        scanf("%f",&y_distance);
        printf("Enter Scan distance in Y axis:");
        scanf("%f",&y_distance);
        printf("Enter Total angle of rotation in theta axis:");
         scanf("%d",&theta_degrees);
         printf("Enter step size in theta axis in degrees:");
         scanf("%d",&theta_step_size);
         break;
    }
    printf("Enter the name of the file to store data:");
    scanf("%s",filename);
    printf("Enter the number of samples to be averaged per point:");
    scanf("%d",&no_samples);
    printf("Enter the software programmable gain:");
    scanf("%d",&gain);
    printf("IS THE X_RAY GENERATOR ON? (y or n):");
    scanf("%s",&answer);
}


void move_and_collect(int number)
{

float n1;
int no_y_iteration;
```

```
int no_z_iteration;
int no_theta_iteration;
int i,k;

 switch(number)  {
  case 2:
            printf("STARTING SCAN\n");
            printf("Would you like to display the detector output on the screen? (y or n):");
            scanf("%s",&disp);
            set_gain(gain);
            no_y_iteration = y_distance/y_step_size;
            motor_y.setvelocity(0.25);
            motor_y.setacceleration(1.0);
            for (i = 0; i <= no_y_iteration; i++)  {
                y_move(i * y_step_size);
                collect_data(i);
            }
            store_data(2);
            y_move(0.0);
            fclose(fp1);
  break;

  case 3:
   printf("STARTING SCAN\n");
            printf("Would you like to display the detector output on the screen? (y or n):");
            scanf("%s",&disp);
            set_gain(gain);
            no_y_iteration = y_distance/y_step_size;
            no_z_iteration = z_distance/z_step_size;
            motor_y.setvelocity(0.25);
```

```
        motor_y.setacceleration(1.0);
        motor_z.setvelocity(0.25);
        motor_z.setacceleration(1.0);
        for (k = 0; k <= no_z_iteration; k++)  {
            z_move(k * z_step_size);
            if ((k % 2) == 0)  {
               for (i = 0; i <= no_y_iteration; i++)  {
                  y_move(i * y_step_size);
                  collect_data(i);
                }
             }
             else {
               for (i = no_y_iteration; i >= 0; i--)  {
                  y_move(i * y_step_size);
                  collect_data(i);
                }
              }
         store_data(3);
        }
        fclose(fp1);
        y_move(0.0);
        z_move(0.0);
break;

case 4:
        printf("STARTING SCAN\n");
        printf("Would you like to display the detector output on the screen? (y or n):");
        scanf("%s",&disp);
        set_gain(gain);
        no_y_iteration = y_distance/y_step_size;
```

```
            no_theta_iteration = theta_degrees/theta_step_size;
            motor_theta.register_sendfn(sfn);
            motor_theta.register_recvfn(rfn);
            motor_theta.setvelocity(0.25);
            motor_theta.setacceleration(1.0);
            motor_theta.setvelocity(0.25);
            motor_theta.setacceleration(1.0);
            for (k = 0; k <= no_theta_iteration; k++)  {
                theta_move(k * theta_step_size);
                if ((k % 2) == 0)  {
                   for (i = 0; i <= no_y_iteration; i++)  {
                      y_move(i * y_step_size);
                      collect_data(i);
                    }
                }
                else {
                    for (i = no_y_iteration; i >= 0; i--)  {
                       y_move(i * y_step_size);
                       collect_data(i);
                     }
                }
                store_data(3);
            }
            fclose(fp1);
   break;
  }
}


void store_data(int scan_type)
```

```
{
int j;

 switch (scan_type)  {
   case 2:
      for (j = (y_distance/y_step_size); j >= 0; j--)
              fprintf(fp1,"%f          %f\n",(j * y_step_size), data_arr[j]);
   break;

   case 3:
              for (j = (y_distance/y_step_size); j >= 0; j--)
                 fprintf(fp1,"%f ", data_arr[j]);
                 fprintf(fp1,"\n");
   break;
 }
}


void x_move(float dist)
{  int i;
  motor_x.move_inch(dist);
  while (motor_x.checkmotion() == MY_FALSE);
  while(motor_x.checkmotion() == MY_TRUE);
}

void y_move(float dist)
{
  motor_y.move_inch(dist);
  while(motor_y.checkmotion() == MY_FALSE);
  while(motor_y.checkmotion() == MY_TRUE);
```

```
}

void z_move(float dist)
{
  motor_z.move_inch(dist);
  while(motor_z.checkmotion() == MY_FALSE);
  while(motor_z.checkmotion() == MY_TRUE);
}

void theta_move(float degrees)
{
  motor_theta.move_degree(degrees);
}

void dataacq_init()
{
outport(544,9217);
outport(546,0);
outport(548,55);
outport(544,41985);
}

void set_gain(int hell)
{
  switch (hell)  {
    case 1:
            outport(548,55);
    break;

    case 4:
```

```
            outport(548,55);
    break;

    case 8:
            outport(548,247);
    break;

    default:
     printf("Wrong gain value given. Setting to unity value\n");
            outport(548,55);
    break;
  }
}

void collect_data(int i)
{
 int value;
 unsigned int check = 8;
 unsigned int stat;
 int j = 0;
 float value2 = 0.0;
 float value1 = 0.0;
 int flag = 1;
while(j != no_samples)  {
    if (flag == 1)  {
        outport(550,0);
        flag = 0;
     }
  stat = inport(558);
  stat = stat & check;
```

```
    if (stat == 8)  {
        value = inport(550);
        value = value & 4095;
        value1  = value * 2.44E-03;
        value1 -= 5.0;
        value2 += value1;
        flag = 1;
        j++;
      }
   }
   value2 = value2/no_samples;
   data_arr[i] = value2;
   i++;
   if (disp == 'y')
      printf("value is %d %e\n",i,value2);
}

void convert_to_grd()
{
  int i,m;
  float j,k;
  float min,max;
  float offset;
  float zero_line[1000];
  float final_line[1000];

  if ((fp1 = fopen("temp.dat","w+")) == NULL)  {
      printf("Error in opening file : %s\n",filename);
      exit(1);
  }
```

```
if ((fp2 = fopen(filename,"w+")) == NULL)  {
    printf("Error in opening file : %s\n",filename);
    exit(1);
}
min = 0.0;
max = 0.0;

fscanf(fp1,"%f",&j);
min = j;
max = j;
while (!feof(fp1))  {
    fscanf(fp1,"%f",&j);
    if (j < min)
       min = j;
    if (j > max)
       max = j;
}
offset = 0.0;
if (min < 0.0)  {
   offset = -(min);
   min += offset;
   max += offset;
}

fprintf(fp2,"DSAA\n");
fprintf(fp2,"%d%d\n",(int)(y_distance/y_step_size),(int)(theta_degrees/theta_step_size));
fprintf(fp2,"%f        %f\n",0.0,y_distance);
fprintf(fp2,"%d        %d\n",0,(int)theta_degrees);
fprintf(fp2,"%f        %f\n",min,max);
```

```
rewind(fp1);
for (m = 0; m < 90; m++)  {
    for (i = 0; i <= (y_distance/y_step_size); i++)  {
      fscanf(fp1,"%f", &j);
      j += offset;
      fprintf(fp2,"%f ",j);
      if (m == 0)
            zero_line[i] = j;
      if (m = 89)
            final_line[i] = j;
     }
    fprintf(fp2,"\n");
}
fprintf(fp2,"COR_NOT_FOUND\n");
for (i = 0; i <= (y_distance/y_step_size); i++)  {
    fprintf(fp2,"%f ",zero_line[i]);
}
fprintf(fp2,"\n");
for (i = 0; i <= (y_distance/y_step_size); i++)  {
    fprintf(fp2,"%f ",final_line[i]);
}
fprintf(fp2,"\n");
fclose(fp2);
fclose(fp1);
}
```